

THEMS



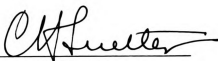
This is to certify that the
thesis entitled

STUDIES ON THE MECHANISM OF TRYPTOPHANASE
CATALYSIS

presented by
DAVID SHERIDAN JUNE

has been accepted towards fulfillment
of the requirements for

PH.D. degree in BIOCHEMISTRY


Major professor

Date 8-30-79



OVERDUE FINES ARE 25¢ PER DAY
PER ITEM

Return to book drop to remove
this checkout from your record.

--	--

STUDIES ON THE MECHANISM OF TRYPTOPHANASE CATALYSIS

By

David S. June

A DISSERTATION

Submitted to

Michigan State University

in partial fulfillment of the requirements

for the degree of

DOCTOR OF PHILOSOPHY

Department of Biochemistry

1979

ABSTRACT

STUDIES ON THE MECHANISM OF TRYPTOPHANASE CATALYSIS

By

David S. June

In an attempt to gain insight into the mechanism of tryptophanase catalysis and to further elucidate the role of monovalent cations in the catalytic process, equilibrium and kinetic studies were performed in the presence and absence of substrates and inhibitors under a variety of experimental conditions. Experimentally, this research was divided into three parts, each dealing with separate but interrelated characteristics of the enzyme. The results of these investigations were integrated into a simple model of tryptophanase catalysis and monovalent cation activation.

The first part of this research deals with the effects of pH and monovalent cations on the spectral and kinetic properties of tryptophanase. The apparent pKa value for the spectral interconversion of the 420 nm and 337 nm forms of the enzyme as a function of pH was determined in saturating concentrations of NH_4^+ , K^+ , Rb^+ , Cs^+ , and Li^+ . The apparent pKa for this spectrophotometric titration was found to be inversely proportional to the V_{max} obtained in the various cations using S-orthonitrothiophenyl-L-cysteine (SOPC) as

the substrate. A simple mechanism was proposed to explain the simultaneous increase in pK_a' and decrease in V_{max} in poor cation activators.

Values of K_m and V_{max} for the degradation of SOPC and K_D for the binding of L-alanine to tryptophanase were determined over the range of enzyme stability. The results were consistent with the interpretation that a zwitterionic amino acid binds to an enzyme molecule following deprotonation of a functional group on the protein with an apparent pK_a in the range 8.2 - 8.5. V_{max} was independent of pH in both K^+ and Li^+ over the range of pH studied.

The second part of this research deals with scanning stopped flow studies on the kinetics and mechanism of the pH-dependent interconversion of the spectral forms of tryptophanase. These studies, which involved incremental pH jumps and drops over the range of enzyme stability, demonstrated that the spectral forms of tryptophanase interconvert in a complex fashion on the stopped flow time scale following a rapid change in pH. These spectral changes were analyzed in terms of three distinct phases: 1) an abrupt phase, which is complete in less than 5 msec, 2) a fast first order interconversion of 420 nm and 337 nm absorbance, and 3) a slow first order process involving growth at 355 nm coupled to two decays centered at 325 nm and 430 nm in the incremental pH jumps; and decay at 355 nm with concomitant growth

at 430 nm and 290 nm in the case of the incremental pH drop experiments. Major features of the data were interpreted in terms of a simple model including kinetic constants and postulated structures.

The final section of this thesis covers scanning stopped flow studies on the mechanism of quinonoid formation with tryptophanase using the competitive inhibitors L-alanine and L-ethionine. The effects of pH, concentration of inhibitor, differing monovalent cations, and substitution of deuterium at the α -position of alanine on this reaction were examined. These results were integrated with the findings of the earlier studies into a simple mechanism of tryptophanase catalysis up to and including α -proton abstraction.

DEDICATION

To Jennifer and Meredith

ACKNOWLEDGEMENTS

I would like to express my sincere appreciation to Dr. Clarence H. Suelter for being a friend as well as an excellent thesis advisor. Thanks also to Dr. James L. Dye for his sagacious advice and guidance. Financial support by the National Institute of Health and the National Science Foundation is also acknowledged.

I am grateful to Ann Aust, Mark Brody, David Husic, Gerard Oakley, Mary Pearce, Debra Thompson and Shyun Long-Yun; some fine people who helped make my stay at MSU more pleasant and productive. My parents, whose unquestioning support helped me more than they know, deserve special thanks. And finally, to my wife Jennifer, thank you for making these four years meaningful.

TABLE OF CONTENTS

	Page
List of Tables	vi
List of Figures	viii
List of Abbreviations	xi
Organization	xii
I. Introduction	1
A Brief Overview of Pyridoxal-P Catalysis	1
Literature Survey	4
References	14
II. Effects of pH and Monovalent Cations on the Spectral Characteristics and Kinetic Properties of Tryptophanase	
Introduction	16
Materials and Methods	16
Results	21
Discussion	46
References	53
III. Studies on the Kinetics and Mechanism of the pH-dependent Interconversion of the Spectral Forms of Tryptophanase	
Introduction	54
Materials and Methods	55
Results	57
Interpretation of Experimental Results and Discussion	91
References	107

Table of Contents - continued

	Page
IV. Scanning Stopped Flow Studies on the Mechanism of Quinonoid Formation with Tryptophanase using Competitive Inhibitors	
Introduction	109
Materials and Methods	110
Results	114
Discussion	146
References	153
Appendix A	155
Appendix B	161

LIST OF TABLES

Table		Page
	Section I	
I.	Activating constants for Monovalent cations	7
	Section II	
I.	The effect of monovalent cations on the apparent pKa for the interconversion of the 420 nm and 337 nm forms of tryptophanase.	32
II.	Kinetic parameters for the degradation of SOPC and the formation of the quinonoid with L-alanine as a function of pH.	47
	Section III	
I.	Kinetic parameters for the fast first order interconversion of 420 nm and 337 nm absorbances in the pH jump and drop experiments.	79
II.	Kinetic parameters for the slow first order process in the incremental pH jump experiments.	88
III.	The percentages of total enzyme that exist in each of the four forms H^+E_β , E_β , H^+E_γ and E_γ at various pH values.	97
	Section IV	
I.	Kinetic parameters for the biphasic growth of quinonoid as a function of ethionine concentration.	123
II.	Kinetic parameters for biphasic quinonoid growth at three concentrations of alanine.	127

List of Tables - continued

Table		Page
III.	Kinetic parameters for the absorbance changes at 337 nm, 420 nm and 508 nm which occur when tryptophanase is mixed with ethionine.	134
IV.	Kinetic parameters for the triphasic growth of quinonoid at pH values 7.2, 8.0 and 8.7.	138
V.	Kinetic parameters for the biphasic growth of quinonoid observed when a tryptophanase-ethionine complex is mixed with monovalent cations.	142

LIST OF FIGURES

Figure		Page
Section II		
1	Effect of various buffers on tryptophanase activity.	23
2	Plots of the absorbance of tryptophanase at 420 nm and 337 nm measured as a function of pH.	25
3	Relationship between V_{max} for the degradation of SOPC and pK_a' for the interconversion of the 420 nm and 337 nm forms of tryptophanase.	36
4	The pH dependence of the dissociation constant, K_D , for L-alanine.	39
5	Variation of the affinity of tryptophanase for SOPC and the maximal velocity with SOPC.	42
Section III		
1	Absorbance spectrum of tryptophanase at low and high pH values and absorbance difference - wavelength - time surface observed in a pH drop experiment.	59
2	Abrupt difference spectra obtained in the incremental pH jump and drop experiments.	63
3	The change in absorbance at 295 nm as a function of pH for the abrupt spectral changes observed in the incremental pH jump and drop experiments.	69
4	Spectral changes occurring during the fast first order interconversion of 420 nm and 337 nm absorptions.	73

List of Figures - continued

Figure		Page
5	The changes in absorbance at 337 nm and 420 nm observed in the incremental pH jump and drop experiments as a function of pH.	77
6	Changes in absorbance at 295 nm, 337 nm and 420 nm as a function of time during the fast first order conversion of 420 nm to 337 nm absorbance following a jump in pH from 7.00 to 9.33.	81
7	Spectral changes occurring during the slow first order process following a rapid change in pH.	86
8	The change in absorbance at 355 nm as a function of pH observed in the slow first order process in the incremental pH jump experiments.	90
9	Variation of the apparent first order rate constant for the fast first order interconversion of 420 nm and 337 nm absorptions in the incremental pH jump and drop experiments.	96
10	Absorption spectra of various ionic forms of pyridoxal-P. H ₂ PL (0), HPL (Δ), PL (+).	100
11	Difference spectrum obtained by subtracting the H ₂ PL spectrum in Figure 10 from the HPL spectrum.	102

List of Figures - continued

Figure		Page
	Section IV	
1	Tryptophanase spectra collected as a function of time after mixing with ethionine.	116
2	Tryptophanase spectra collected as a function of time after mixing with alanine.	119
3	The biphasic growth in absorbance at 508 nm after mixing tryptophanase with ethionine.	121
4	The variation of the apparent first order rate constants, k_1' and k_2' for the fast and slow phases, respectively, of the biphasic growth of quinonoid with ethionine concentration.	126
5	The changes in the tryptophanase absorption spectrum at 337 nm and 420 nm as a function of time after mixing with ethionine.	130
6	The rate and extent of quinonoid formation as a function of pH.	136
7	The rate and extent of quinonoid formation in the presence of various monovalent cations.	141
8	The effect of deuterium substitution at the α -position of alanine on the rate and extent of quinonoid formation with tryptophanase.	145

LIST OF ABBREVIATIONS

Bicine	N,N-bis (2-hydroxyethyl) glycine
EDTA	ethylenediaminetetraacetic acid
Epps	N-2-hydroxyethylpiperazine propane sulfonic acid
Mes	2 (N-morpholino)ethane sulfonic acid
pKa'	apparent pKa
pyridoxal-P	pyridoxal-5'-phosphate
SOPC	S-orthonitrothiophenyl- -cysteine
Tes	N-tris(hydroxymethyl)methyl-2- aminoethane sulfonic acid

ORGANIZATION

This dissertation is divided into four sections. The first section is composed of a brief description of aspects of pyridoxal-P catalysis pertinent to this thesis and a literature survey on tryptophanase from *Escherichia coli* B/1t7-A. The next three sections contain the results of investigations into the mechanism of tryptophanase catalysis and activation by monovalent cations. These three sections are presented in a form similar to that required for publication in most scientific journals. An appendix containing the derivations of equations used in the computer-assisted fitting of experimental data is included at the end of the text.

Section I

INTRODUCTION

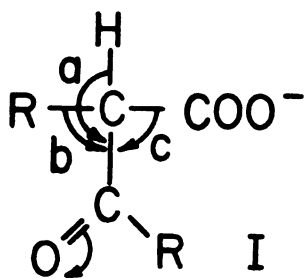
INTRODUCTION

A Brief Overview of Pyridoxal-Phosphate Catalysis:

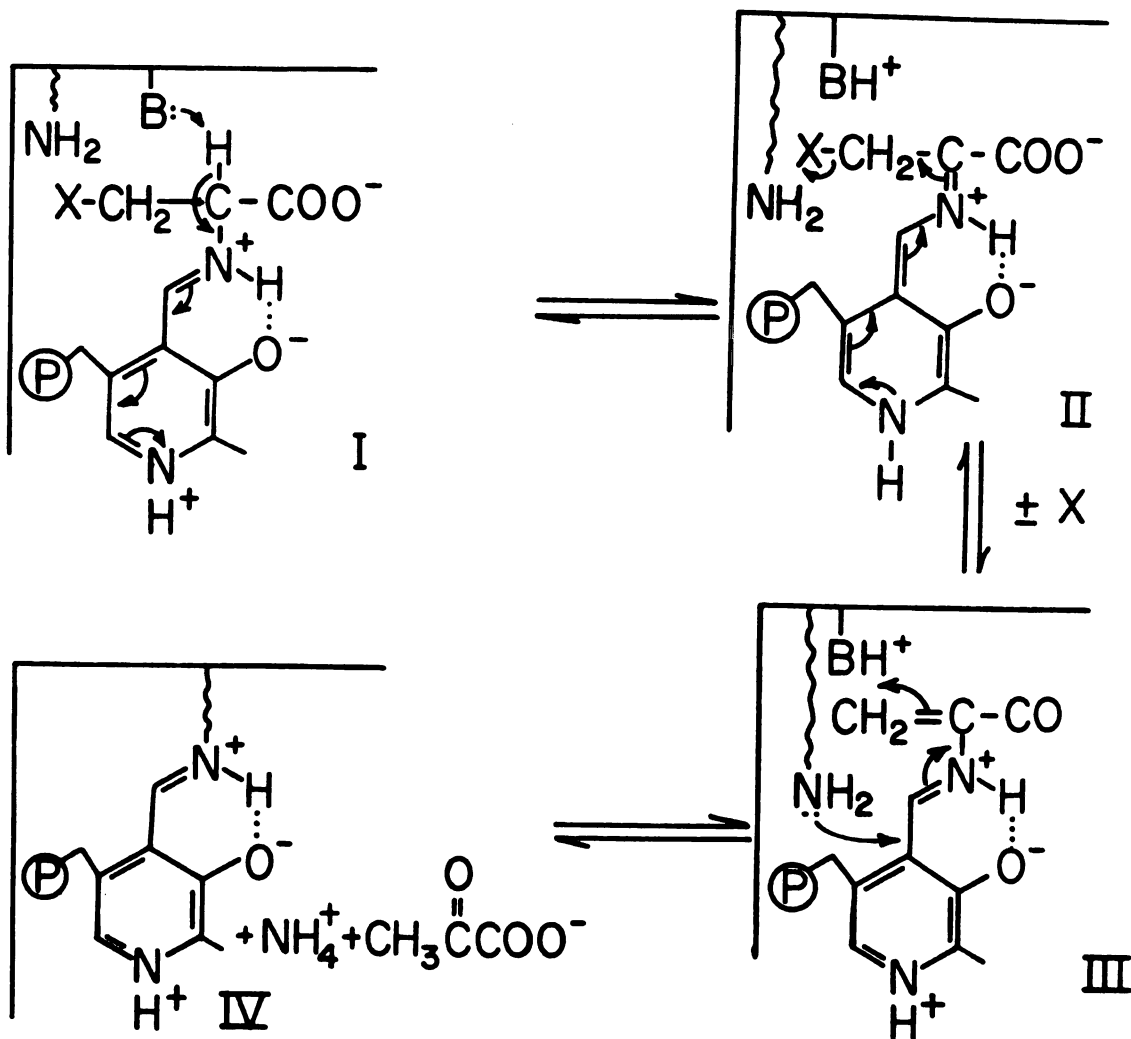
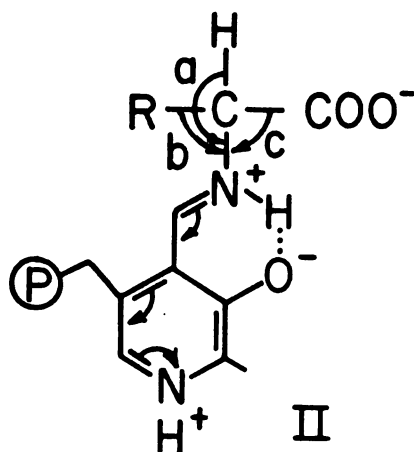
The reaction of pyridoxal-P with amino acids is used today as a model system by students interested in the mechanism of enzyme catalysis. Pyridoxal-P achieved recognition as an important biological catalyst when the first mechanistic hypotheses regarding the chemistry of this compound were advanced by Snell (1) and Braunstein (2) in 1958. Since that time, pyridoxal-P has been shown to function as a coenzyme for a large number of enzymes. In addition, pyridoxal and pyridoxal-P, in the complete absence of enzymes, were shown to catalyze α,β -elimination reactions of amino acid substrates as well as various other reactions such as transamination, decarboxylation, and racemization carried out by enzymes which require this cofactor (3).

The mode of action of pyridoxal-P can be most easily visualized if one assumes that the coenzyme replaces the α -amino group of amino acid substrates with a group which is electronically the equivalent of an adjacent carbonyl (4). This configuration allows for electron withdrawal from the α -carbon toward the carbonyl group, in the case of model structure I as shown in Scheme I, or, in the case of pyridoxal-P, toward the electronegative pyridinium nitrogen as outlined in Scheme I, structure II.

Pyridoxal-P generally participates in reactions by promoting electron withdrawal from the α -carbon of the bound amino acid leading to the cleavage of the bonds designated a, b, and c in structure II. The role of the enzyme molecule, then, is to enhance the rate and to confer specificity to ensure that a single set of products is made instead of the several possible sets which can form in the absence of protein. As an example of pyridoxal-P catalysis, let us consider an α,β -elimination reaction. In this case, an amino acid substrate with a leaving group, X, on the β -carbon interacts to form a Schiff's base with the coenzyme via a transaldimination reaction with the pyridoxal-P bound to an enzyme through an ϵ -amino group of lysine. (structure I, Scheme II). Loss of the α -proton, presumably assisted by a basic group at the enzyme active site, leads to a quinonoid intermediate II which characteristically absorbs at around 500 nm. This intermediate can then lose X as shown in Scheme II to form a bound α -amino-acrylate complex, III. The reaction is completed following a second transaldimination reaction, this time with the ϵ -amino group of lysine acting as a nucleophile at the carbonyl carbon of the imine, to release the imino acid (5) which subsequently undergoes non-enzymatic hydrolysis.

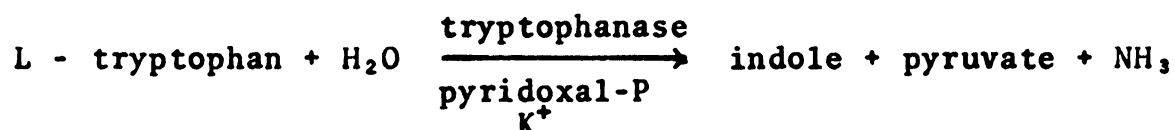


SCHEME I



SCHEME II

A. Introduction - Tryptophanase was first recognized by Happold and Hoyle in 1935 (6) as the enzyme responsible for the production of indole in bacterial cultures. Subsequently, Happold and Struyvenberg (7) demonstrated the requirement for NH_4^+ , K^+ or Rb^+ for enzymatic activity and that Na^+ and Li^+ were apparently inhibitory. Wood, Gunsalus and Umbreit (8) discovered that tryptophanase required the coenzyme pyridoxal-P and that pyruvate, indole and ammonia were formed in stoichiometric amounts from tryptophan. These and other investigations led to the formulation of the basic reaction catalyzed by tryptophanase:



A recent review by Snell (9) effectively summarizes most of what was known about the enzyme up to 1975 and reviews by Happold (10) and Wada (11) cover early aspects of these studies.

B. Source of the enzyme - Tryptophanase is induced in a wide variety of bacteria (9) where it apparently plays a role in the catabolism of tryptophan. However, the enzyme is formed in variable amounts and differs in physical and catalytic properties depending on the bacterial source (9).

In order to consistently obtain high yields of tryptophanase Newton and Snell (12) developed a constitutive strain of *Escherichia coli* called B/1t7-A. Since this mutant lacks

the genes for tryptophan synthetase (13) tryptophan for protein synthesis must be obtained by reversal of reaction 1. This undoubtedly contributes to the high yield of tryptophanase obtained (up to 10% of the soluble protein) when these cells are cultured in the presence of indole.

C. Structural properties - Tryptophanase from *E. coli* B/1t7-A has a molecular weight of 220,000 and is composed of four identical subunits (14). It is a pyridoxal-P dependent enzyme with one coenzyme moiety bound per subunit in an azomethine linkage to an ϵ -amino group of a lysine residue at the active site. As with other pyridoxal-P enzymes, the coenzyme can be resolved from tryptophanase to give apoenzyme by the addition of reagents such as penicillamine or cysteine which form thiazolidine derivatives with pyridoxal-P.

Snell and coworkers (14) carried out extensive ultracentrifugation studies on both apo- and holoenzyme and showed that the conversion of apo- to holoenzyme is accompanied by a large conformational change. This conformational change resulted in a more compact structure which may account for the greater stability of holoenzyme to denaturation by sodium dodecyl sulfate (14), heat (15) and changes in pH. These studies also revealed that the apoenzyme in the presence of Na^+ or K^+ but not imidazole undergoes a concentration-dependent dissociation into dimers as the temperature is decreased below 20°C (14). In his review article (9), Snell points out that since Na^+ and K^+ behave in a similar fashion

with respect to dissociation of the apoenzyme, it is unlikely that this effect is related to the large difference in the ability of these cations to activate tryptophanase catalytically. In contrast to apoenzyme, tetrameric holoenzyme remained intact throughout the entire temperature range 3 - 25°C.

Toraya *et al.* (16) compared by gel filtration studies the effect of various monovalent cations on the binding of the coenzyme and their effectiveness as activators. They found that NH_4^+ , K^+ and Rb^+ , which are good activators, enhanced the binding constant for coenzyme. Enzyme in the presence of the poor activators Cs^+ , Na^+ and Li^+ demonstrated a lower affinity for pyridoxal-P. The dissociation constant was 31 μM and 1.8 μM in the presence of Na^+ and K^+ , respectively.

A possible criticism of this study is that the concentrations of cations used (0.1 M) may not have been saturating. Suelter *et al.* (17) have shown that the activation constants for the various cations vary from 54 mM in the case of Li^+ to 0.23 mM for NH_4^+ (Table I). The failure to observe activity in these studies may be partially attributable to low cation concentrations rather than to intrinsic differences in pyridoxal-P binding.

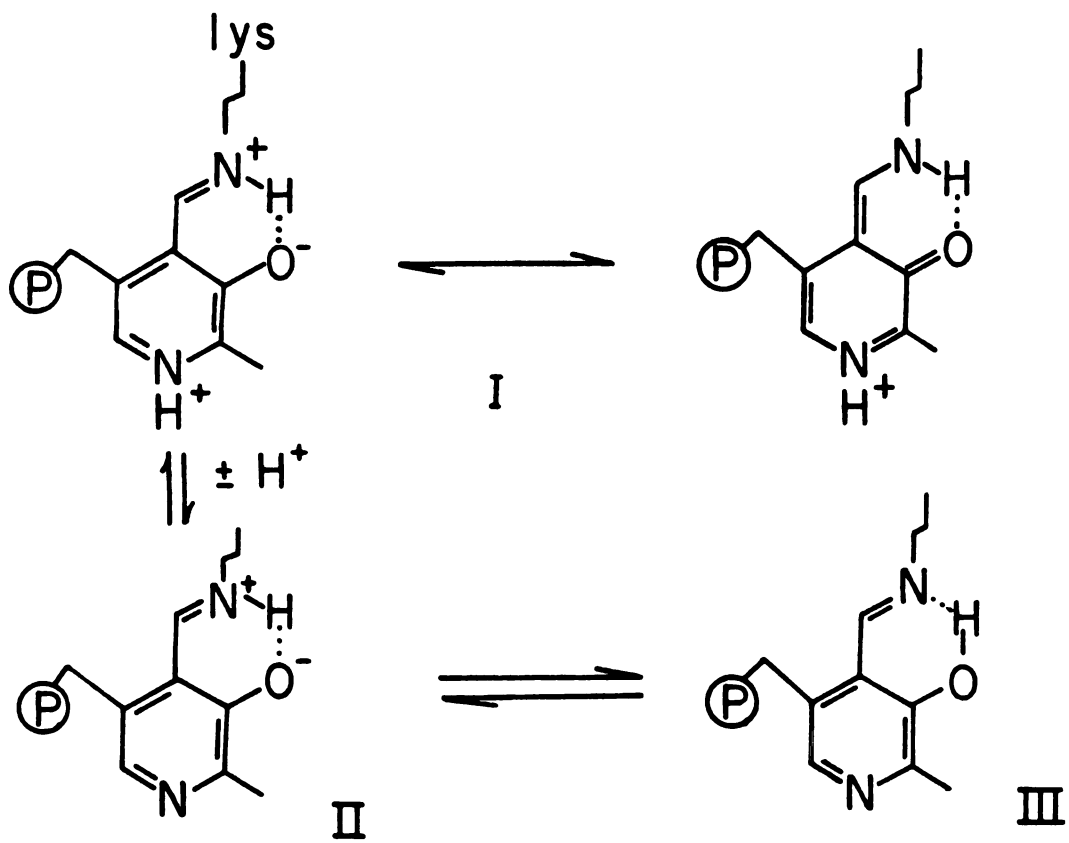
Table I

Activating Constants for Monovalent Cations

CATION	K_D (mM)
Lithium	54 ± 11.6
Sodium	40 ± 0.06
Potassium	1.44 ± 0.06
Thallium (I)	0.95 ± 0.1
Ammonium	0.23 ± 0.01
Rubidium	3.5 ± 0.3
Cesium	14.6 ± 2.6

D. Spectral properties - Holotryptophanase exhibits three absorption maxima centered at 278 nm, 337 nm and 420 nm. The peak at 278 nm is due to protein while the peaks at 337 nm and 420 nm are contributed by the bound coenzyme. On the basis of model studies (18) pyridoxal-P aldimines absorbing in the wavelength range 410 nm - 430 nm are usually associated with the resonance forms identified as I in Scheme III. Since changes in the state of protonation at the pyridinium nitrogen give rise to only small changes in absorbance and positions of absorbance maxima (19) the state of protonation at the pyridinium nitrogen for most enzymes is unclear. Form II may exist in some cases. The coenzyme structure giving rise to the 337 nm band in tryptophanase is probably III as suggested by Davis and Metzler (20) and Snell (9).

Morino and Snell (21) demonstrated that the relative intensities of the interconvertible 337 nm and 420 nm bands of tryptophanase depended on both pH and the nature of the monovalent cation in the medium. At low pH values the 420 nm form of the enzyme predominated. As the pH was increased, absorbance at 337 nm increased at the expense of 420 nm absorbance. According to Morino and Snell (21) the change in 337 nm and 420 nm absorbances as a function of pH describe a single titration curve with an apparent pKa of 7.2 indicative of a single proton process. These



SCHEME III

authors also showed that in the absence of monovalent cations, that is, in imidazole-HCl buffer, the bound coenzyme was entirely in a form which absorbed at 420 nm. The addition of 0.1 M Na^+ caused an increase at 420 nm which may be attributable to increased binding of pyridoxal-P. Neither of these spectra changed significantly between pH 7.0 and 9.0. When 0.1 M K^+ replaced Na^+ as the cation at pH 8.0, a dramatic change was observed in the spectrum in which the 337 nm form of the enzyme became the dominant species. They associated the 337 nm form of tryptophanase with activity because this was the form that predominated at pH values above 8.0 where the enzyme exhibited its greatest apparent activity. The observation that effective monovalent cation activators promoted the formation of the 337 nm form, while a poor activator, Na^+ , did not, also appeared to be consistent with this interpretation.

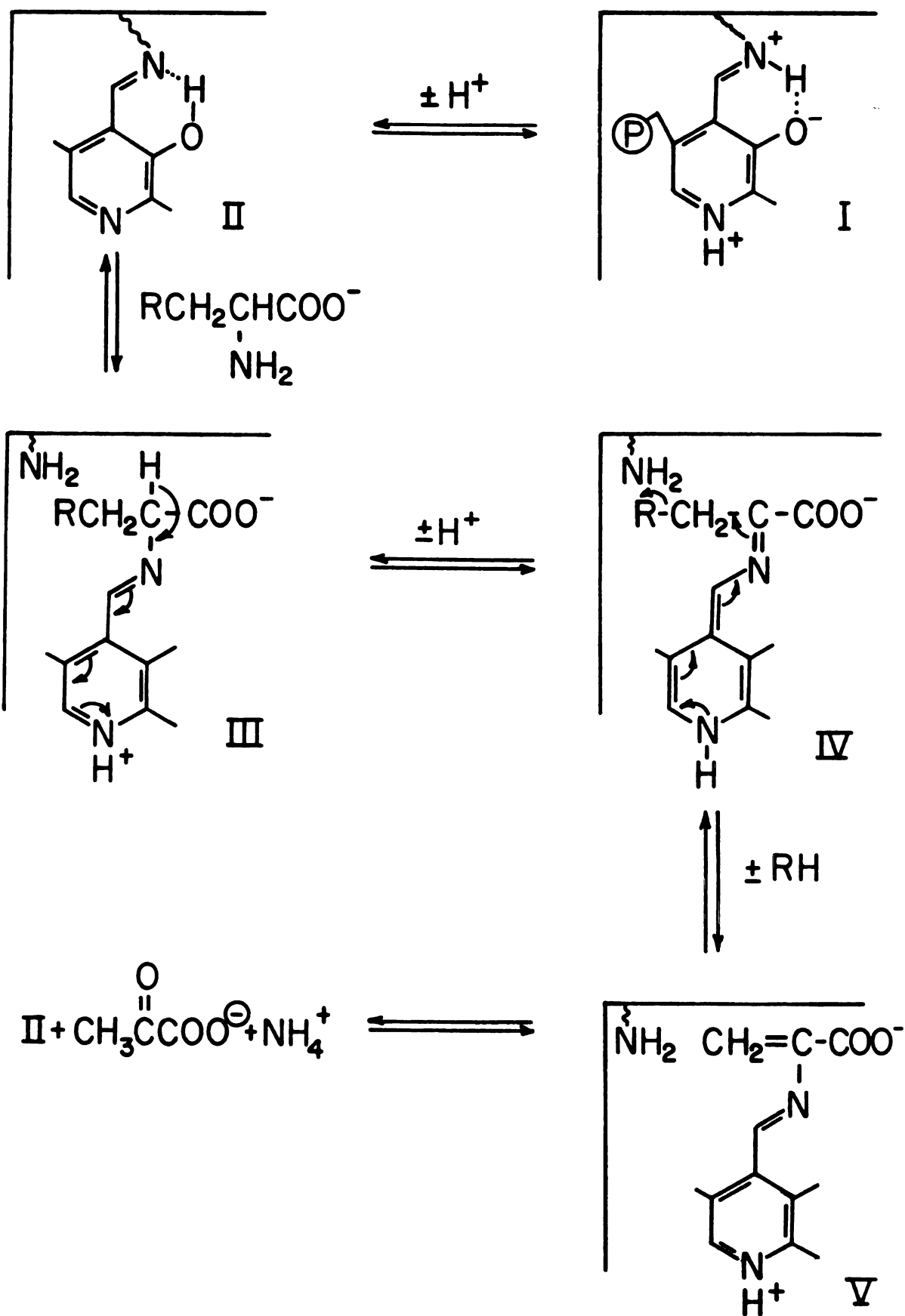
Although other coenzyme structures could give rise to absorbance at 337 nm, Davis and Metzler (20) argue that Scheme III serves to explain the effects of pH and monovalent cations on the absorption spectrum of tryptophanase observed by Morino and Snell (21), if it is assumed that dissociation of a proton from I, with an apparent pKa of 7.2, ultimately gives structure III. The structures II and III would be favored at high pH values and in a hydrophobic environment. The increased amount of 337 nm absorbance in the presence

of effective monovalent cation activators is consistent with the data of Toraya *et al.* (16) showing that the coenzyme is bound more tightly, and presumably in a less polar environment, in the presence of these cations.

E. Mechanism of tryptophanase catalysis - A mechanism of tryptophanase catalysis consistent with the available data was outlined by Snell (9) in his review article. This mechanism is highly schematic in the sense that several intermediates (e.g. those which occur during the transaldimination reactions) are not shown. Likewise, Snell mentions that the exact ionic forms of the coenzyme involved at each step are not known.

The first step in this proposed reaction sequence involves the conversion of inactive enzyme, represented by structure I in Scheme IV, absorbing at 420 nm, to an active form of the enzyme (II) which absorbs at 337 nm. As mentioned, Morino and Snell (21) obtained an apparent pKa value of 7.2 for this process in the presence of potassium.

The second step involves the formation of the Michaelis complex between the enzyme and a suitable amino acid substrate or inhibitor via a transaldimination reaction. The third step is the loss of the α -proton from the bound amino acid to form the quinonoid intermediate IV which characteristically exhibits intense absorption at approximately 500 nm (21). The reaction with dead-end inhibitors stops



SCHEME IV

at this point. In the case of substrates, that is amino acids with labilizable β -substituents, this absorption band disappears as substrate is depleted. Experiments in $^2\text{H}_2\text{O}$ and $^3\text{H}_2\text{O}$ (21) in the presence of the inhibitor L-alanine or substrates confirmed that the α -proton of alanine is labilized during quinonoid formation and that α -proton loss occurs at a rate faster than elimination of the β -substituent when substrates other than S-orthonitrophenyl-L-cysteine (SOPC) (21) are used. Suelter and Snell (17) demonstrated that no tritium was incorporated into unreacted SOPC and concluded from this that loss of the α -proton was rate-limiting for the reaction with this artificial substrate.

The fourth and fifth steps in Scheme IV represent the loss of the β -substituent of the substrate, the ultimate regeneration of the active enzyme and product formation. Based on their results, Hillebrand *et al.* (5) suggested that α -aminoacrylate was released from the active site either as α -iminopropionate or the carbinolamine of pyruvate when SOPC was the substrate.

It is clear from this summary of the mechanism of tryptophanase catalysis that much work remains to be done in elucidating the forms of pyridoxal-P which participate in the catalytic process and the effects of monovalent cations on the spectral and kinetic properties of the enzyme.

REFERENCES

1. Snell, E. E. (1958) Vitamins and Hormones, 16, 77-125.
2. Braunstein, A. E. (1960) in The Enzymes (Boyer, P. D., Lardy, H., and Myrback, K., eds.) Vol. 2, pp. 113-184, Academic Press, New York.
3. Metzler, D. E. and Snell, E. E. (1952) J. Biol. Chem. 198, 363-373.
4. Metzler, D. E., (1977) Biochemistry; The Chemical Reactions of Living Cells, Academic Press, New York.
5. Hillebrand, G. G., Dye, J. L., and Suelter, C. H. (1979) Biochem. 18, 1751-1755.
6. Happold, F. C., and Hoyle, L. (1935) Biochem. J. 29, 1918-1926.
7. Happold, F. C., and Struyvenberg, A. (1954) Biochem. J. 58, 379-382.
8. Wood, W. A., Gunsalus, I. C., and Umbreit, W. W. (1947) J. Biol. Chem. 170, 313-321.
9. Snell, E. E. (1975) Adv. Enzymol. Relat. Areas Mol. Biol. 42, 287-333.
10. Happold, F. C. (1950) Adv. Enzymol. Relat. Subj. Biochem. 10, 51-82.
11. Wada, H. (1964) Tryptophan Metabolism Vol. 1, Sekai Hoken Tsushinsha, Ltd., Osaka, Japan, 77-92.
12. Newton, W. A., and Snell, E. E. (1962) Proc. Nat. Acad. Sci. U.S.A., 48, 1431-1439.
13. Yanofsky, C., and Crawford, I. P. (1959) Proc. Nat. Acad. Sci. U.S.A., 45, 1016-1026.
14. Morino, Y., and Snell, E. E. (1967) J. Biol. Chem., 242 5591-5601.
15. Raibaud, O., and Goldberg, M. E. (1973) J. Biol. Chem. 248, 3451-3455.
16. Toraya, T., Nihira, T., and Fukui, S. (1976) Eur. J. Biochem. 69, 411-419.

References - continued

17. Suelter, C. H., and Snell, E. E. (1977) J. Biol. Chem. 252, 1852-1857.
18. Heinert, D., and Martell, A. E. (1962) J. Amer. Chem. Soc. 84, 3257-3263.
19. Johnson, R. J., and Metzler, D. E. (1970) Methods Enzymol. 18A, 433-471.
20. Davis, L., and Metzler, D. E. (1972) in The Enzymes (Boyer, P. D. ed.) Vol. 7, pp. 33-74.
21. Morino, Y., and Snell E. E., (1967) J. Biol. Chem. 242, 2800-2809.
22. Suelter, C. H., Wang, J., and Snell, E. E. (1976) FEBS Lett. 66, 230-232.

SECTION II

EFFECTS OF pH AND MONOVALENT CATIONS ON THE
SPECTRAL AND KINETIC PROPERTIES OF TRYPTOPHANASE

Tryptophanase (E.C. 4.1.99.1) from *Escherichia coli* B/1t7-A is a member of a group of pyridoxal-P dependent enzymes catalyzing α,β -elimination reactions of amino acid substrates (1). As with other members of this group, tryptophanase requires the presence of monovalent cations for optimum catalytic activity (2,3,4). The enzyme is sensitive to the nature and concentration of the monovalent cation and the pH of the environment (4,5). This sensitivity is manifested in marked changes in the absorption spectrum and alterations in kinetic behavior. This paper presents studies on the effects of pH and monovalent cations on tryptophanase in the presence and absence of substrates and inhibitors which were undertaken in an attempt to gain insight into the role of monovalent cations in this reaction and the functions of ionizable groups on the enzyme and/or pyridoxal-P involved in substrate binding and turnover.

A simple model is presented which suggests that monovalent cations may activate tryptophanase by altering the equilibrium between a catalytically inactive conformation, and a catalytically active conformation.

EXPERIMENTAL PROCEDURES

Materials.- RbCl, CsCl and LiCl were obtained from Ventron, Danvers, Mass. as ultrapure products. NH_4Cl and KCl were Mallinckrodt, analytical reagents. Pyridoxal-5'-phosphate, N-2-hydroxyethylpiperazine propane sulfonic

acid (Epps), N-tris(Hydroxymethyl)methyl-2-aminoethane sulfonic acid (Tes), N,N-bis(2-hydroxyethyl)glycine (Bicine) and 2(N-Morpholino)ethane sulfonic acid (Mes) were obtained from Sigma Chemical Co. 1,3-bis[tris-(hydroxymethyl)methyl-amino]propane (Bis-tris-propane) was from Cal Biochem. $(\text{CH}_3)_4\text{NCL}$ from Aldrich Chemical Company was recrystallized from N-propyl alcohol before use. $(\text{CH}_3)_4\text{NOH}$ was prepared fresh before use by passage of recrystallized $(\text{CH}_3)_4\text{NCL}$ over Dowex-1-OH.

Tryptophanase - Tryptophanase from *Escherichia coli* B/1t7-A was prepared as described by Watanabe and Snell (6) including the modifications of Suelter *et al.* (7). Protein was judged to be greater than 95% tryptophanase by polyacrylamide gel electrophoresis. Holoenzyme was prepared from stock apoenzyme by incubation in 0.1 M potassium phosphate, pH 8.0, 7% $(\text{NH}_4)_2\text{SO}_4$, 1 mM EDTA, 0.2 mM pyridoxal-P, 20 mM dithiothreitol (DTT) for 1 hour at 37°C. Occasionally, activation was achieved in the same buffer at 50°C for 15 min as suggested by Högberg-Raibaud *et al.* (8). The enzyme had a specific activity of 40 - 50 $\mu\text{mol}\cdot\text{min}^{-1}\cdot\text{mg}^{-1}$ when assayed with 0.6 mM S-orthonitrophenyl-L-cysteine (SOPC) in 50 mM potassium phosphate, pH 8.0, 50 mM KCl, at 30°C (9). Activating monovalent cations were removed from enzyme solutions by extensive dialysis. Protein concentration was determined spectrophotometrically using $\epsilon_{278}=0.795 \text{ ml mg}^{-1} \text{ cm}^{-1}$ (4).

Kinetics - Kinetic constants obtained in the presence of 0.5 M KCl and 0.85 M LiCl at various pH values were determined from initial velocities at five SOPC concentrations ranging from 0.056 mM to 0.604 mM in 25 mM (CH₃)₄N-Tes or (CH₃)₄N-Bicine, 0.1 mM pyridoxal-P and 2 mM [(CH₃)₄N]₂-EDTA. Values for K_m and V_{max} as a function of pH in 0.2 M KCl were obtained by analysis of complete reaction progress curves. Absorbance versus time data were fit to the Michaelis-Menten equation with the nonlinear curve fitting program KINFIT (10). The following initial concentrations of SOPC were used: 1.35 mM for pH values 6.60, 6.76; 7.00 and 7.23; 1.10 mM for pH 7.40 and 0.42 mM for all other pH values. The remainder of the assay mix consisted of .025 M (CH₃)₄N-Mes or (CH₃)₄N-Epps, 0.2 M KCl, 20 μM pyridoxal-P and 2 mM EDTA.

Anion Inhibition - Tryptophanase was dialyzed against 5 mM K-Epps, pH 8.0, 40 mM KCl, 1 mM EDTA, 0.1 mM pyridoxal-P and 0.2 mM DTT. Five μl of this enzyme solution (1.5 mg ml⁻¹) was added to a 1 ml assay consisting of 0.6 mM SOPC, 25 mM K-Epps, pH 8.0, 1 mM EDTA and the indicated potassium salt at a concentration of 0.2 M. All assays were carried out at 30°C. K_m and V_{max} were obtained by analysis of complete reaction progress curves.

Spectral Titrations - Dissociation constants for the conversion of the 420 nm form to the 337 nm form of tryptophanase in the presence of various monovalent cations were obtained after extensive dialysis at 4°C against 5 mM

(CH₃)₄N-Epps, pH 8.0 containing the indicated concentration of monovalent cation, 0.1 mM pyridoxal-P, 1.0 mM [(CH₃)₄N]₂-EDTA, and 0.2 mM DTT was added to nine tenths ml of .025 M (CH₃)₄N-Epps, pHi, 0.1 mM pyridoxal-P and 1.0 mM [(CH₃)₄N]₂-EDTA. The final pH value of each protein solution was measured at 30°C on a Sargent-Welch digital pH meter subsequent to measuring the absorbances at 337 nm and 420 nm. The composition of the reference was identical to the sample with the exception that one-tenth ml of a dialysate was substituted for the tryptophanase solution. Absorbance measurements were made at 30°C with a Beckman DU spectrophotometer equipped with a thermostated cell compartment.

pH Stability of the Enzyme in the Presence of Various Monovalent Cations - Tryptophanase at 2 mg ml⁻¹ was incubated at 30°C for a period of 10 minutes in 0.025 M (CH₃)₄N-Epps, in the pH range 6 - 10, containing either 0.1 M KCl, 0.5 M RbCl, 0.5 M CsCl or 0.6 M LiCl, 0.1 mM pyridoxal-P, 1 mM [(CH₃)₄N]₂-EDTA and 0.02 mM DTT. Aliquots were then removed and assayed at 30° C in the standard SOPC reaction mixture.

Titration of tryptophanase with L-alanine as a function of pH - One tenth ml of tryptophanase (approximately 25 mg ml⁻¹) in 1 mM (CH₃)₄N-Epps, pH 8.0, 0.2 M KCl, 1 mM EDTA, 0.1 mM pyridoxal-P, 0.2 mM DTT was added to nine tenths ml of 0.025 M (CH₃)₄N-Epps, pHi, 0.2 M KCl, 1 mM EDTA, 0.1 mM pyridoxal-P in a quartz cuvet. The composition of the reference was identical to the sample with the exception that one

tenth ml of the dialysate was substituted for the tryptophanase solution. Aliquots of 1.1 M L-alanine, 0.1 mM pyridoxal-P, 0.2 M KCl, 1 mM EDTA at pHi, were added to each cuvet and the absorbance was measured at 502 nm. The final pH of each titration mixture was measured subsequent to addition of the last aliquot of alanine.

Treatment of Data - All kinetic and titration data were fitted to the appropriate mathematical function with the non-linear curve fitting program KINFIT (10).

RESULTS

Buffer Effects and Stability - To rule out spurious buffer effects in these pH studies, the initial velocities of tryptophanase in several overlapping buffer systems were investigated (Figure 1). The initial velocities in the overlapping pH regions of Mes, Tes, Bicine and Epps were similar and gave an apparent pH optimum of 8.3 under these conditions. Bis-tris-propane tended to inhibit at low pH values.

From results not shown it was found that tryptophanase under conditions described in Materials and Methods lost less than 5% of its activity when incubated with KCl or RbCl over the pH range 6.2 - 9.5. Enzyme in 0.5 M CsCl or 0.6 M LiCl retained the same stability over a smaller range of pH 6.5 - 9.0.

Spectral Titrations of Tryptophanase in the Presence of Various Monovalent Cations - Previous studies by Morino and Snell (4) showed a pH dependent interconversion of the 420 nm and 337 nm bands of tryptophanase. These studies were extended to determine whether the monovalent cations, NH_4^+ , K^+ , Rb^+ , Cs^+ and Li^+ affected the pK_a' for this interconversion (Figure 2 and Table I). Complete titration curves for Cs^+ and Li^+ could not be obtained since the enzyme was not stable for sufficient time at the extreme pH values. Consequently, the pK_a' values given for Cs^+ and Li^+ in Table I are approximations.

Figure 1. Effect of various buffers on tryptophanase activity. A 1 ml assay consisted of 0.6 mM S-orthonitrophenyl-L-cysteine, 0.025 mM buffer at pHi, 0.2 m KCl, 10 μ M pyridoxal-P, 1 mM EDTA and 5 μ g of purified tryptophanase. Assays were carried out at 30° C in Mes (O), Tes (Δ), Epps (+), Bicine (\diamond), and Bis-tris propane (X).

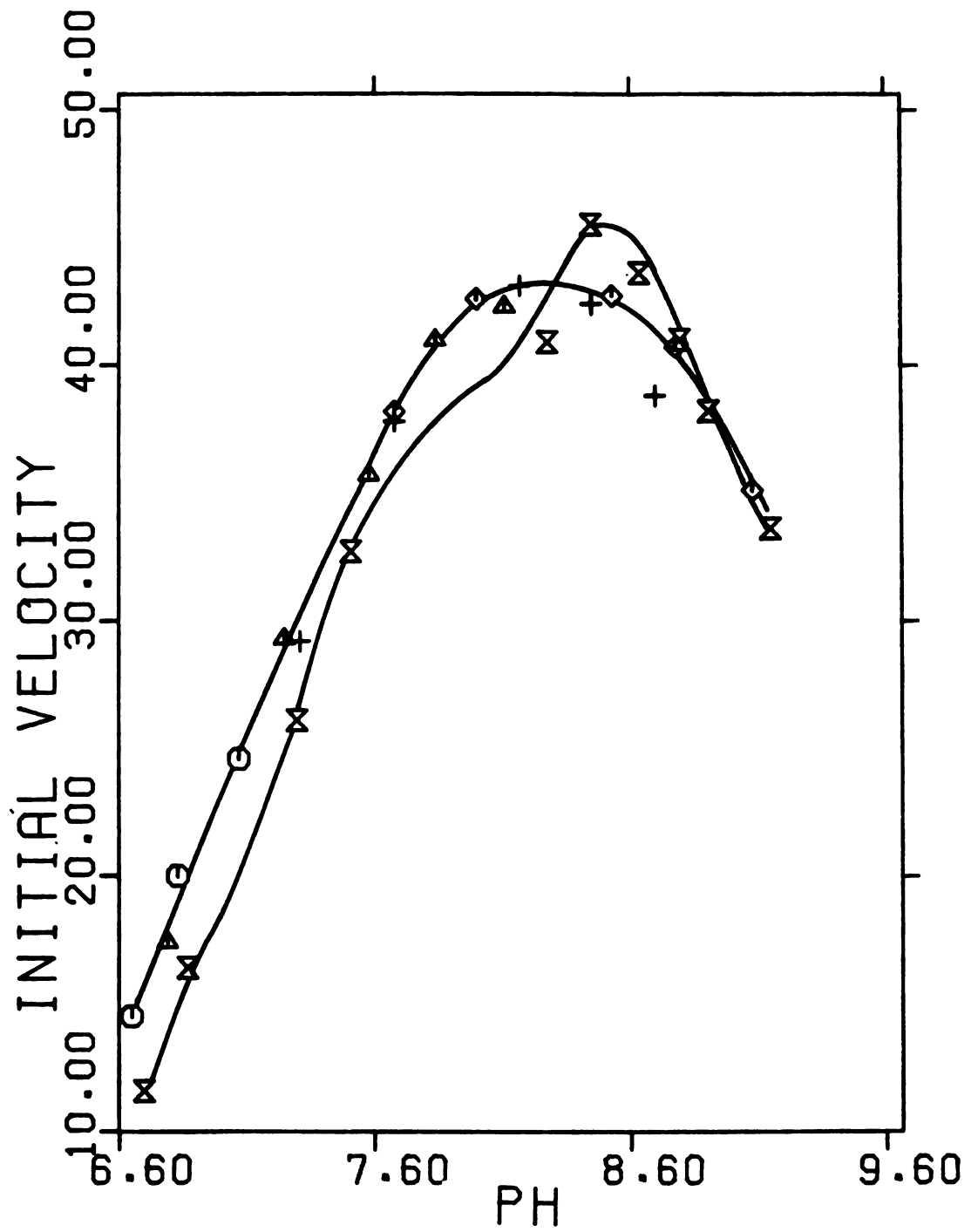


FIGURE 1

Figure 2. Plots of the absorbance of tryptophanase at 420 nm (O) and 337 nm (Δ) measured as a function of pH as described in Materials and Methods. A) 0.025 M NH_4Cl ; B) 0.1 M KCl ; C) 0.2 M KCl ; D) 0.5 M KCl ; E) 0.5 M RbCl ; F) 0.5 M CsCl ; G) 0.6 M LiCl . The solid lines in each graph were calculated using equation 1 with the parameters listed in Table I.

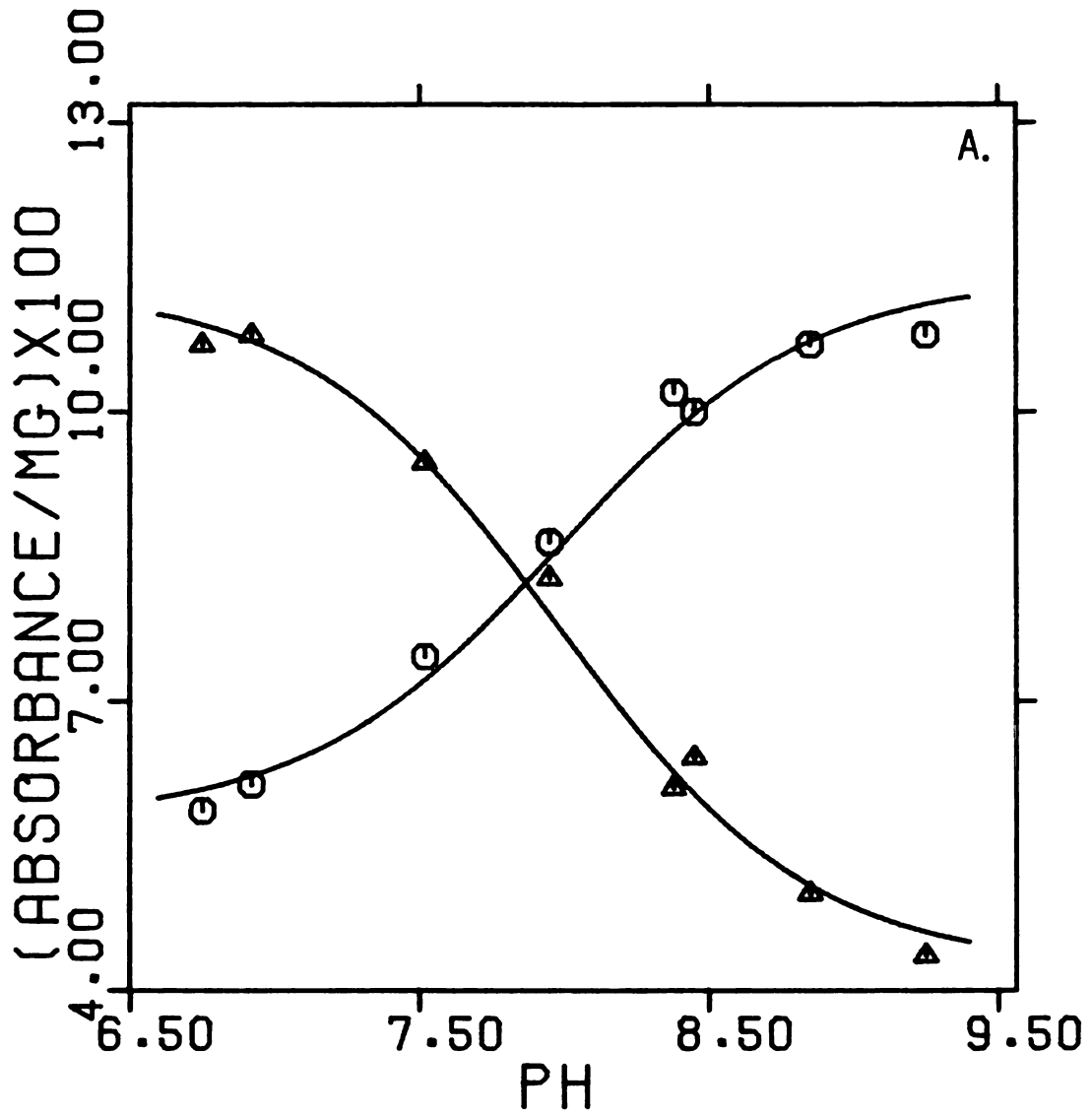


FIGURE 2A

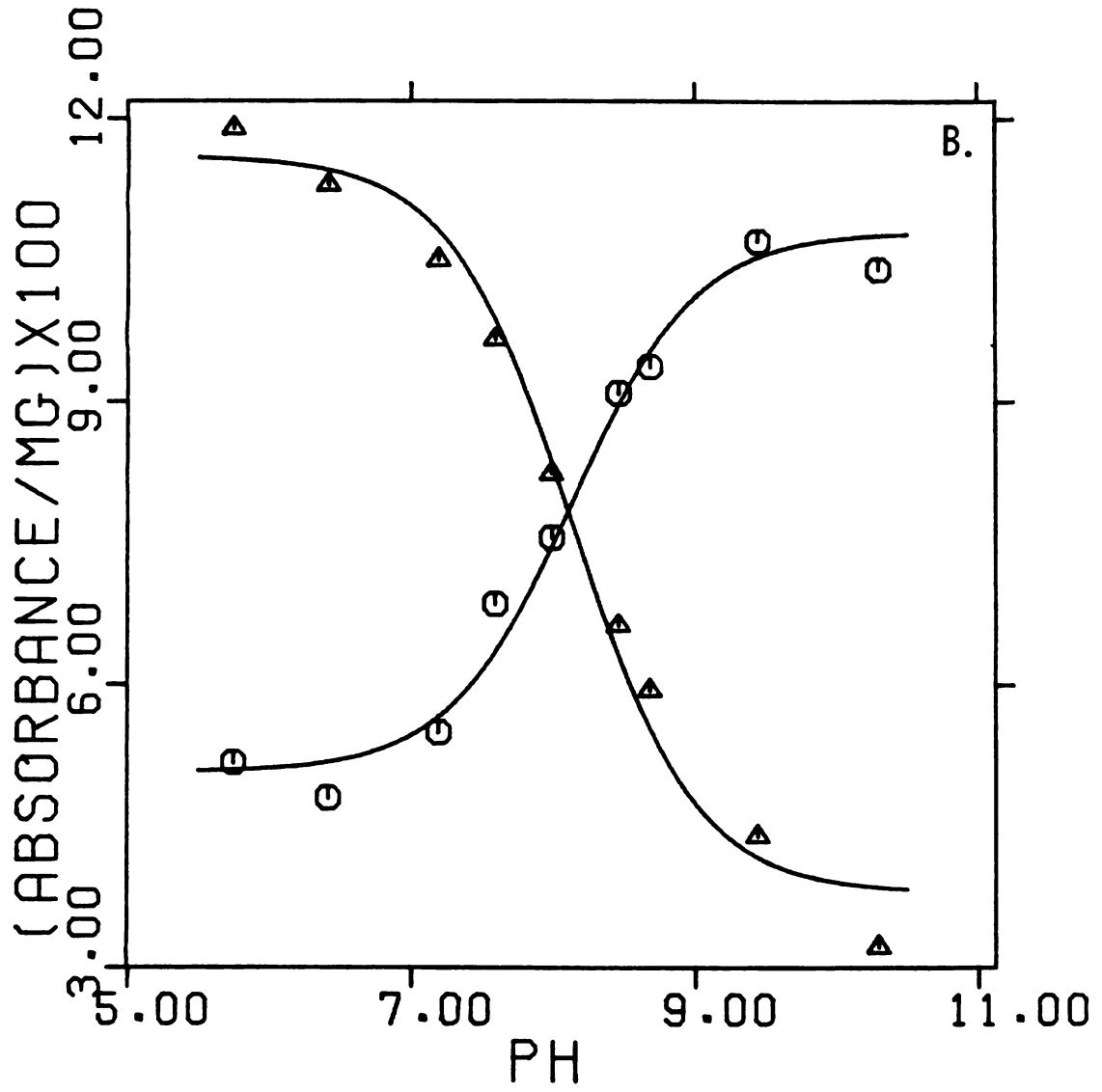


FIGURE 2B

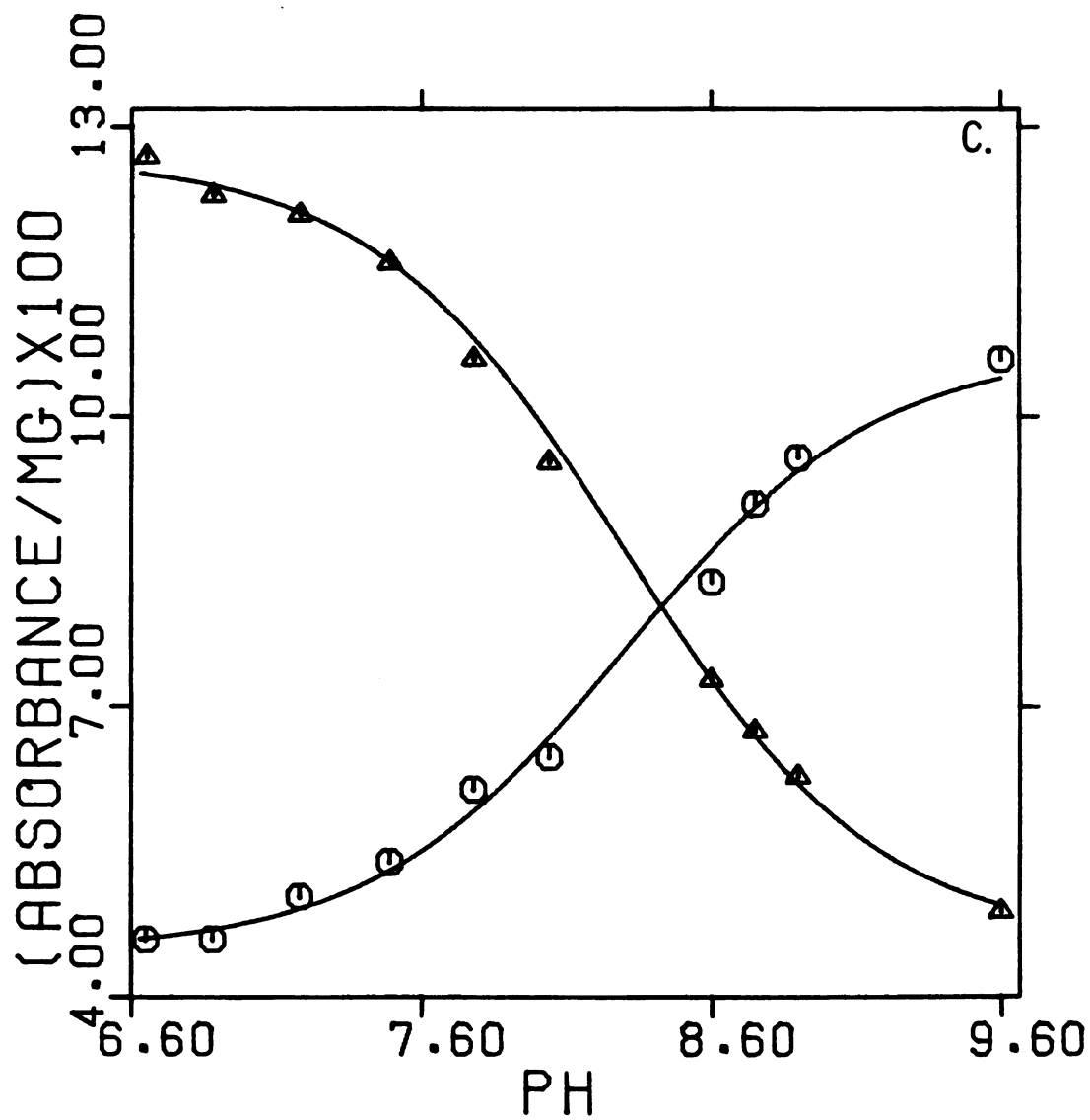


FIGURE 2C

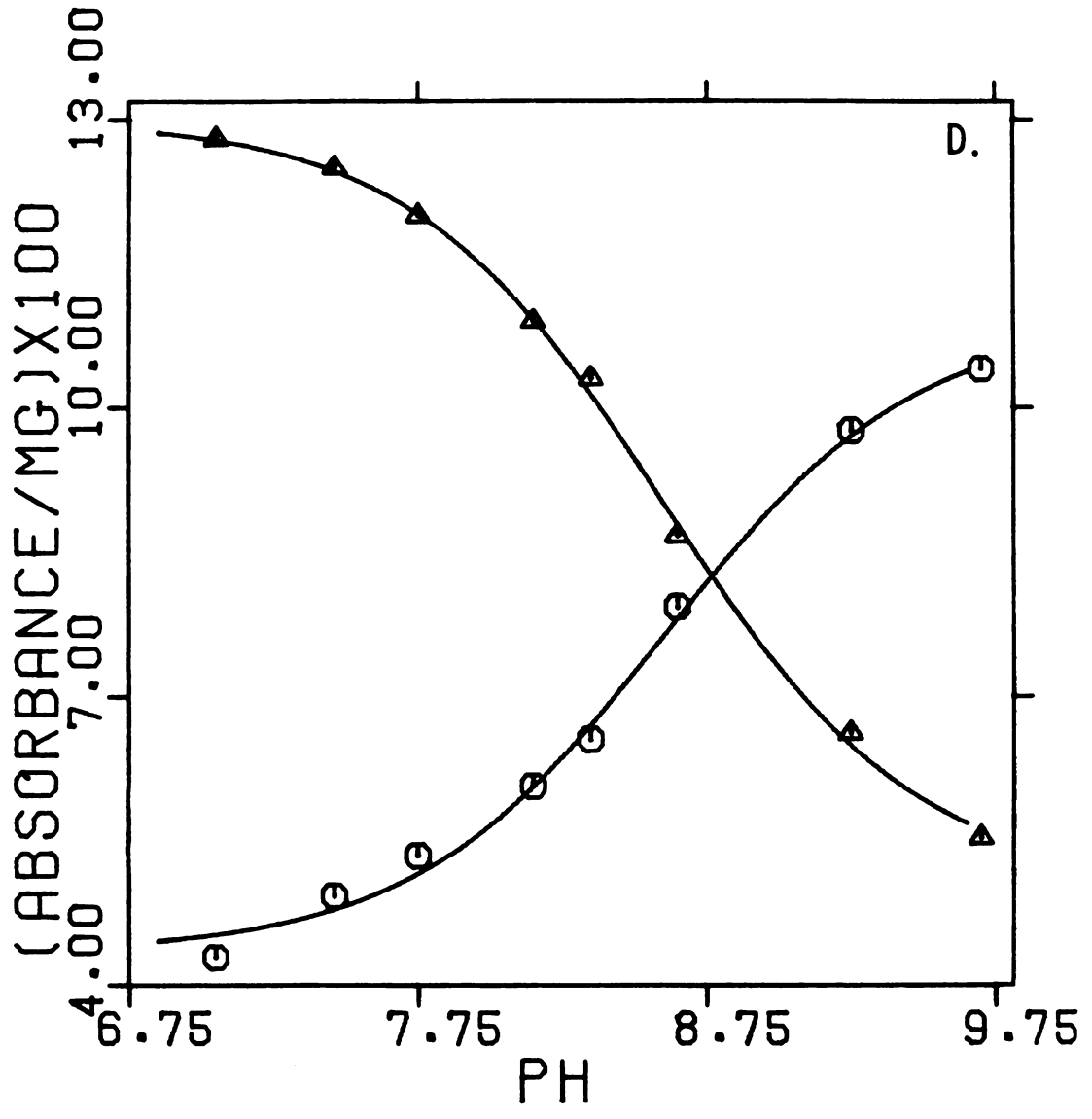


FIGURE 2D

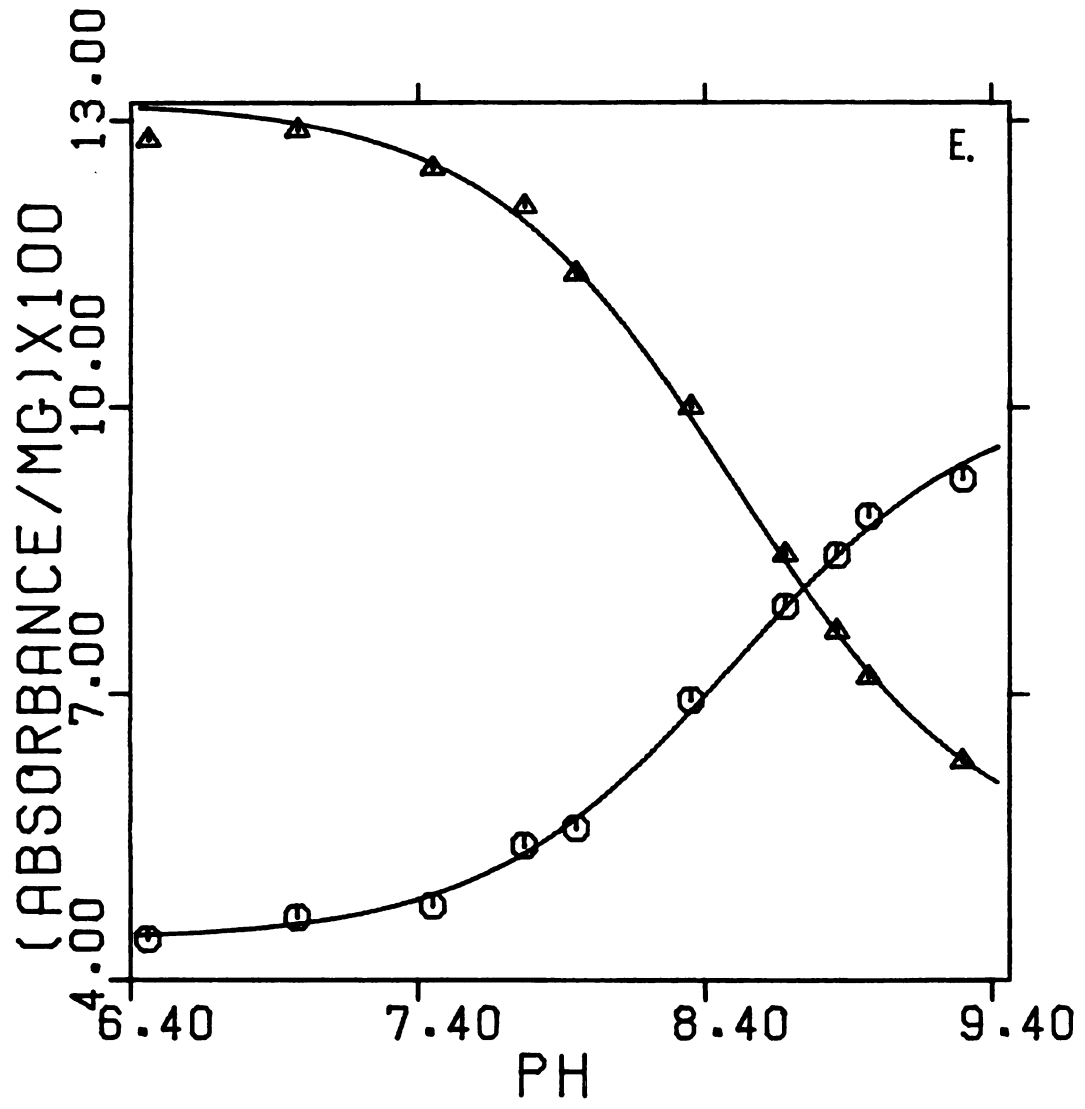


FIGURE 2E

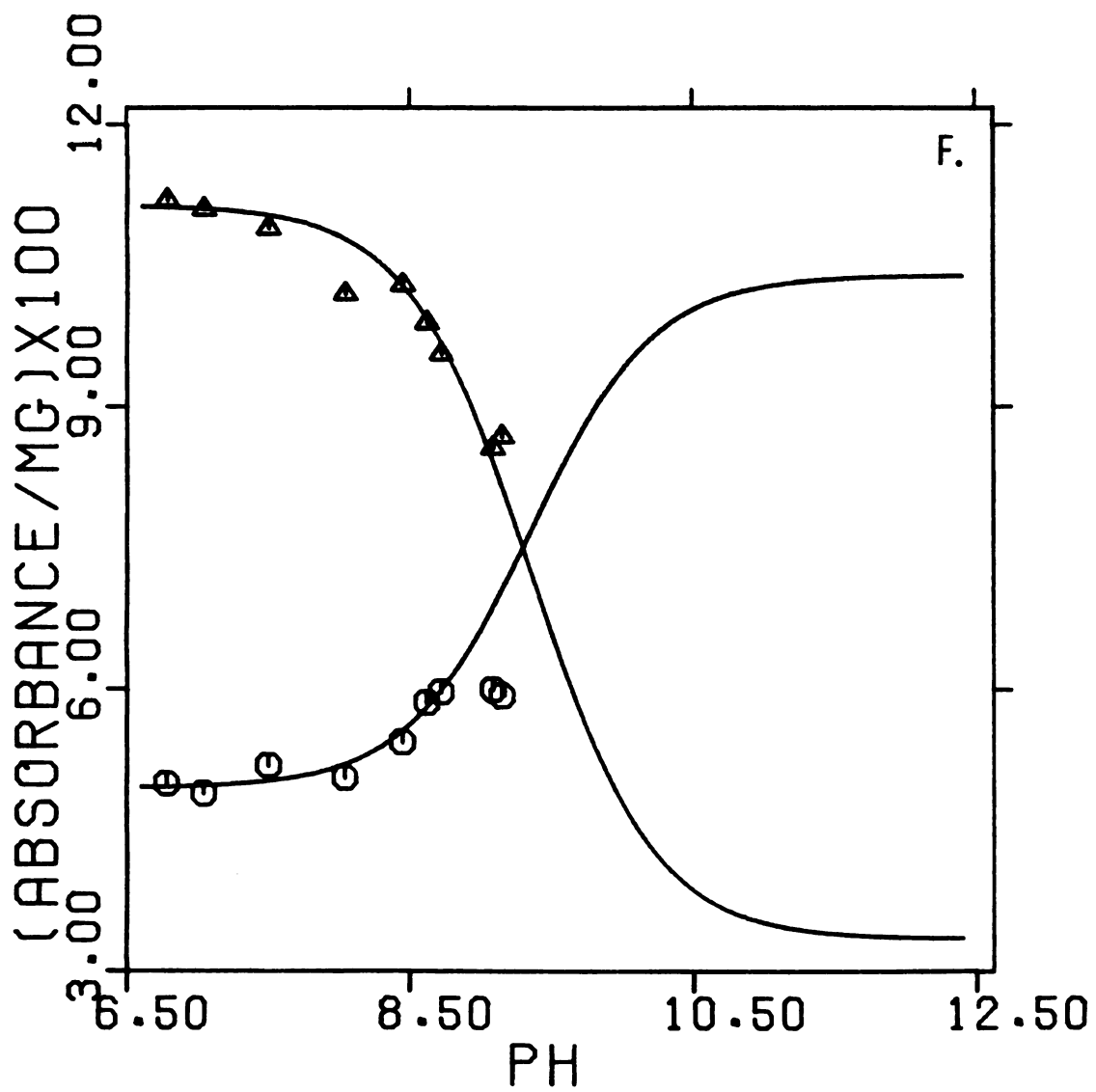


FIGURE 2F

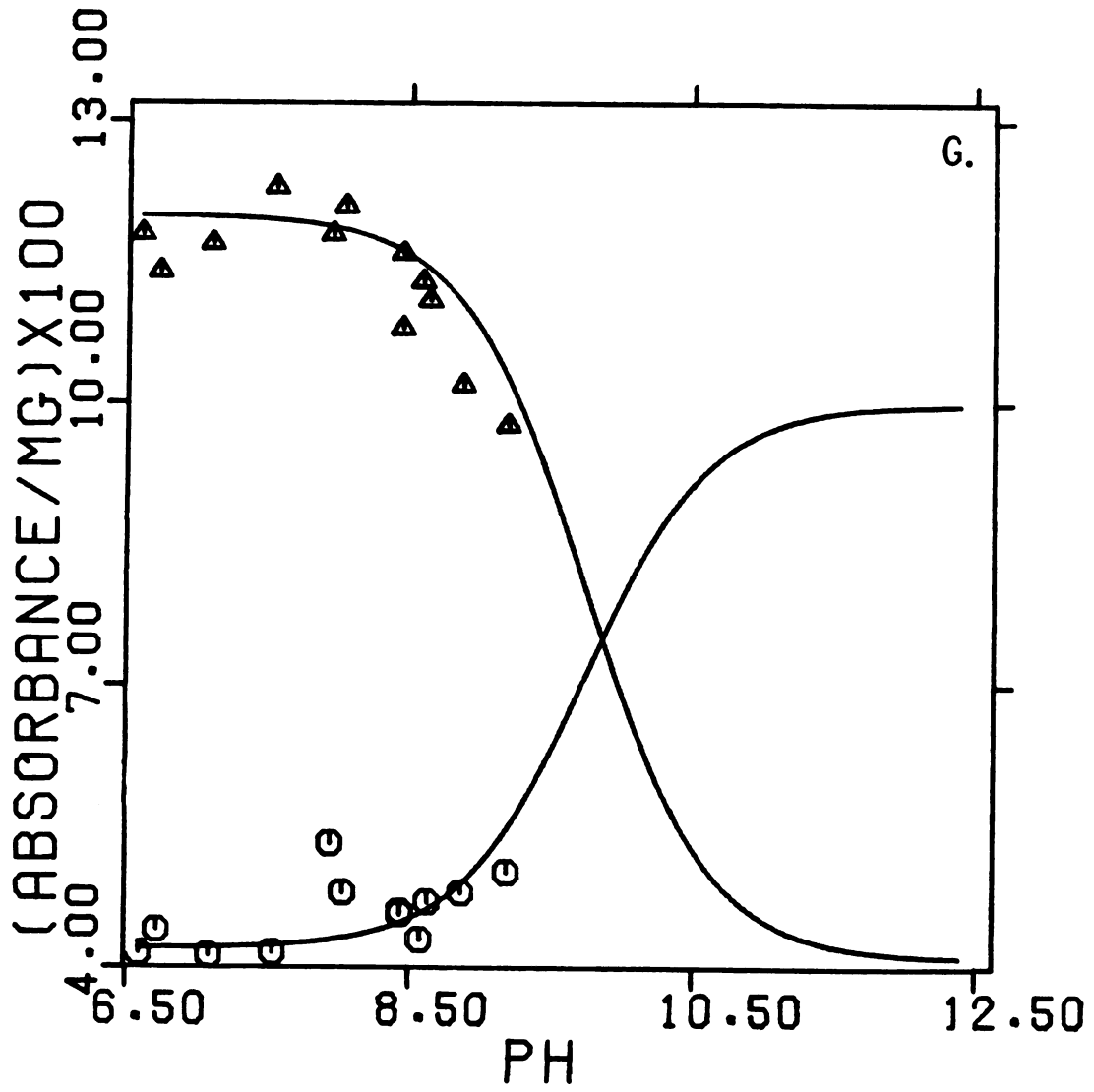


FIGURE 2G

Table I: The effect of monovalent cations on the apparent pKa for the interconversion of the 420 nm and 337 nm forms of tryptophanase.

CATION	Concentration (M)	SA ^a	pKa'	ϵ_{AH}^{420}	ϵ_A^{420}	ϵ_{AH}^{337}	ϵ_A^{337}
NH ₄ ⁺	0.025	44	7.98 ± 0.06	6230 ± 119	2335 ± 127	3174 ± 112	6278 ± 116
K ⁺	0.1	50	8.14 ± 0.06	6369 ± 117	2090 ± 134	2794 ± 111	5918 ± 125
K ⁺	0.2	54	8.30 ± 0.03	6957 ± 54	2510 ± 84	2457 ± 50	5896 ± 75
K ⁺	0.5	54	8.60 ± 0.03	7166 ± 52	2766 ± 75	2391 ± 49	6010 ± 70
Rb ⁺	0.5	50	8.47 ± 0.05	6484 ± 89	2721 ± 88	2755 ± 85	5492 ± 79
	0.5	56	8.50 ± 0.02	7271 ± 32	2865 ± 70	2431 ± 29	5608 ± 57
Cs ⁺	0.5	37	9.35	6105	b	2722	b
Li ⁺	0.6	45	9.75	6600	b	2310	b

a. Specific activity in 0.6 mM SOPC, 50 mM KCl, 50 mM potassium phosphate pH 8, of each enzyme preparation after extensive dialysis against each cation as outlined in Materials and Methods.

b. Because of the instability of the enzyme above pH 9, data sufficient to calculate these extinction coefficients were not possible to obtain.

The titration curves for each cation, NH_4^+ , K^+ and Rb^+ , described by the decrease in absorbance at 420 nm and the increase in absorbance at 337 nm were fitted by the nonlinear curve fitting program KINFIT, as a multiple-data-set* to equation 1, previously given by Johnson and Metzler (11),

$$\epsilon_{\text{obs}} = \frac{\epsilon_A [10^{(\text{pH}-\text{pK})}] + \epsilon_{\text{HA}}}{[1 + 10^{(\text{pH}-\text{pK})}]} \quad (1)$$

where ϵ_A = calculated molar absorption coefficients at 337 nm or 420 nm at infinite pH, ϵ_{HA} = calculated molar absorption coefficients at 337 nm or 420 nm at zero pH, and ϵ_{obs} = observed molar absorption coefficients at 337 nm or 420 nm. Thus, five parameters, $\epsilon_{\text{AH}}^{337}$, ϵ_A^{337} , $\epsilon_{\text{AH}}^{420}$, ϵ_A^{420} and the common parameter for both sets of curves, pKa' , were adjusted to obtain the best fit of the data for each cation.

The data in Table I show that pKa' depends both on the cation and on the ionic strength. If one were to assume that pKa' for NH_4^+ would be higher if the ionic strength were increased, as was observed with K^+ , then the pKa' values obtained in NH_4^+ , K^+ , and Rb^+ are essentially identical but different from those observed with Cs^+ and Li^+ . Although the data presented here have been analyzed in terms of a single ionizing group, it should be pointed out that recent kinetic

* When two or more sets of data, each being fitted to a separate function, share at least one adjustable parameter, the data may be fitted simultaneously with KINFIT as a so-called multiple-data-set.

data has shown this interconversion to be a more complex process (12). On the other hand, it is clear that the pK_a' value for the 337 nm - 420 nm interconversion depends on the monovalent cation, that is, the more effective the cation is as an activator, the lower the observed pK_a' . The calculated extinction coefficients at 337 nm and 420 nm of the enzyme at high and low pH values were essentially the same in NH_4^+ , K^+ and Rb^+ . The data with Cs^+ and Li^+ are not as complete but the extinction coefficients at 337 nm and 420 nm at low pH values are comparable to those observed with NH_4^+ , K^+ , and Rb^+ . The observed variation in the extinction coefficients can be accounted for in terms of the specific activity of each enzyme preparation after the extensive dialysis used to exchange the cations. Generally, the higher the specific activity the higher the ϵ_{AH}^{420} and ϵ_A^{420} and the lower the ϵ_{AH}^{337} and ϵ_A^{337} . On the other hand, the values observed for $[(\epsilon_{AH}^{420} - \epsilon_A^{420})/\text{specific activity}]$ and $[(\epsilon_{AH}^{337} - \epsilon_A^{337})/\text{specific activity}]$ are constant, being 82 ± 5 and 63 ± 6 , respectively.

As indicated in Figure 3, V_{max} , using SOPC as a substrate, decreases as the pK_a' of the 420 nm - 337 nm spectral transition is increased. It is intriguing to note that 0.5 M KCl causes an increase of 0.35 units in pK_a as compared to 0.1 M KCl and a 20% decrease in V_{max} .

Figure 3. Relationship between V_{max} for the degradation of SOPC and pK_a' for the interconversion of the 420 nm and 337 nm forms of tryptophanase.

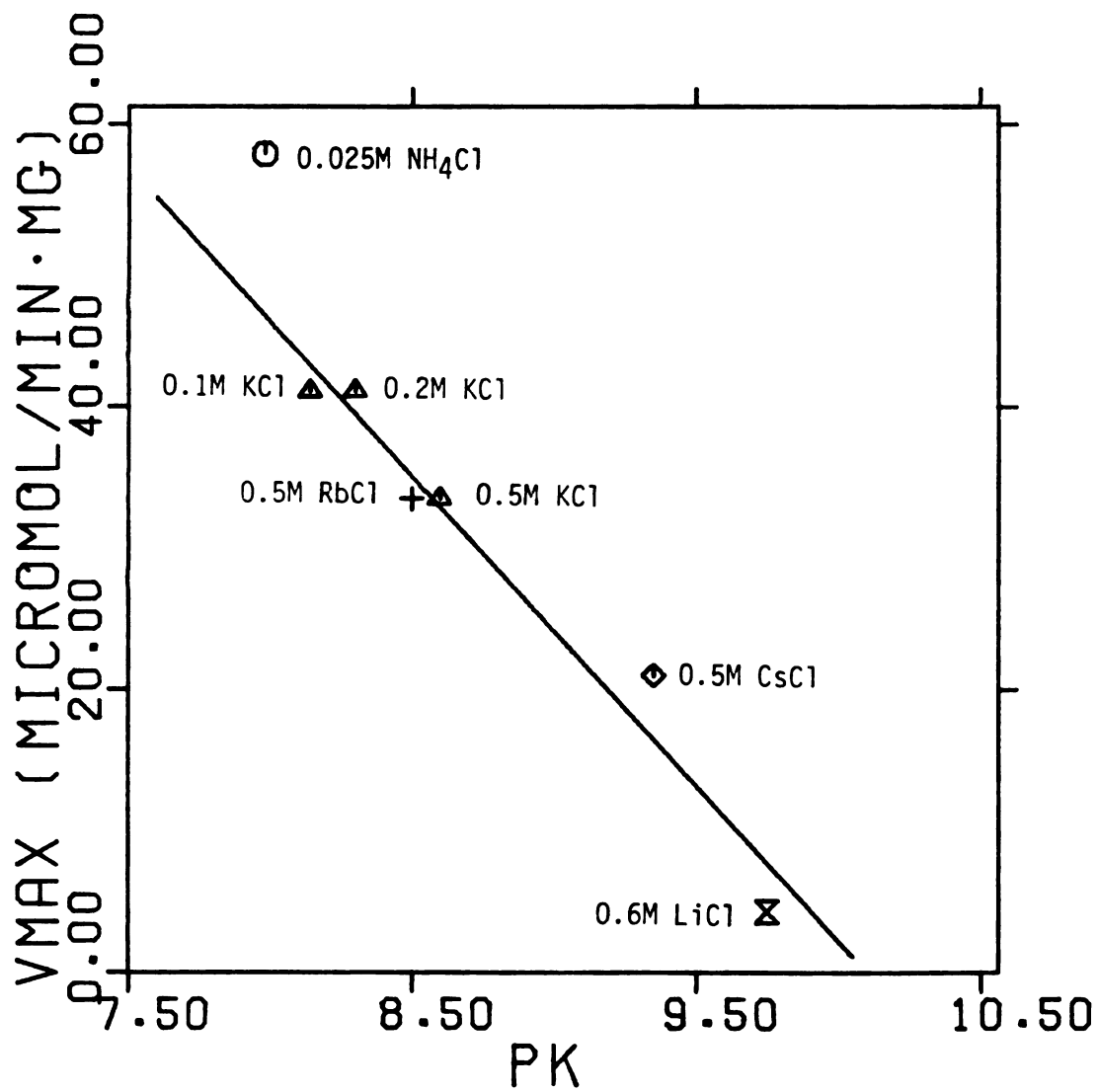


FIGURE 3

Anion Inhibition of TPase - To determine if the inhibition by high concentrations of KCl was due to the presence of an anion binding site on the enzyme as is the case with serine transhydroxymethylase (13), K_m and V_{max} were determined in 0.2 M KCl, K-acetate, KBr, KF and KNO_3 . Only KNO_3 appeared to inhibit, acting in a competitive manner with substrate. K_m was increased from 0.13 mM to 0.47 mM. Fluoride, which might be expected to bind strongly to an anion binding site tended to decrease both K_m and V_{max} , but by less than 10%.

pH Dependence of the Interaction of L-Alanine with Tryptophanase - L-alanine, a competitive inhibitor of tryptophanase, interacts with bound pyridoxal-P to form a quinonoid absorbing maximally at 502 nm (4). The dissociation constant, K_D , for this interaction was examined over the range pH 6.5 - 9.0 (Figure 4). The data were analyzed in terms of Scheme I which describes the binding of a competitive inhibitor which has no dissociable group in the pH range of interest with enzyme which has a dissociable group in this pH range.

Scheme I

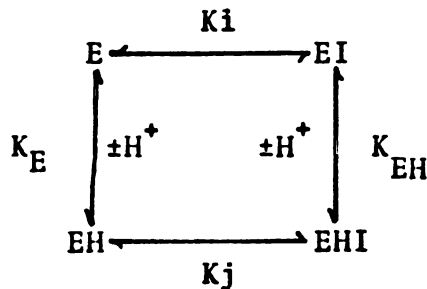


Figure 4. The pH dependence of the dissociation constant, K_D , for L-alanine. The line was calculated with equation 2 of text using the parameters given for alanine in Table II.

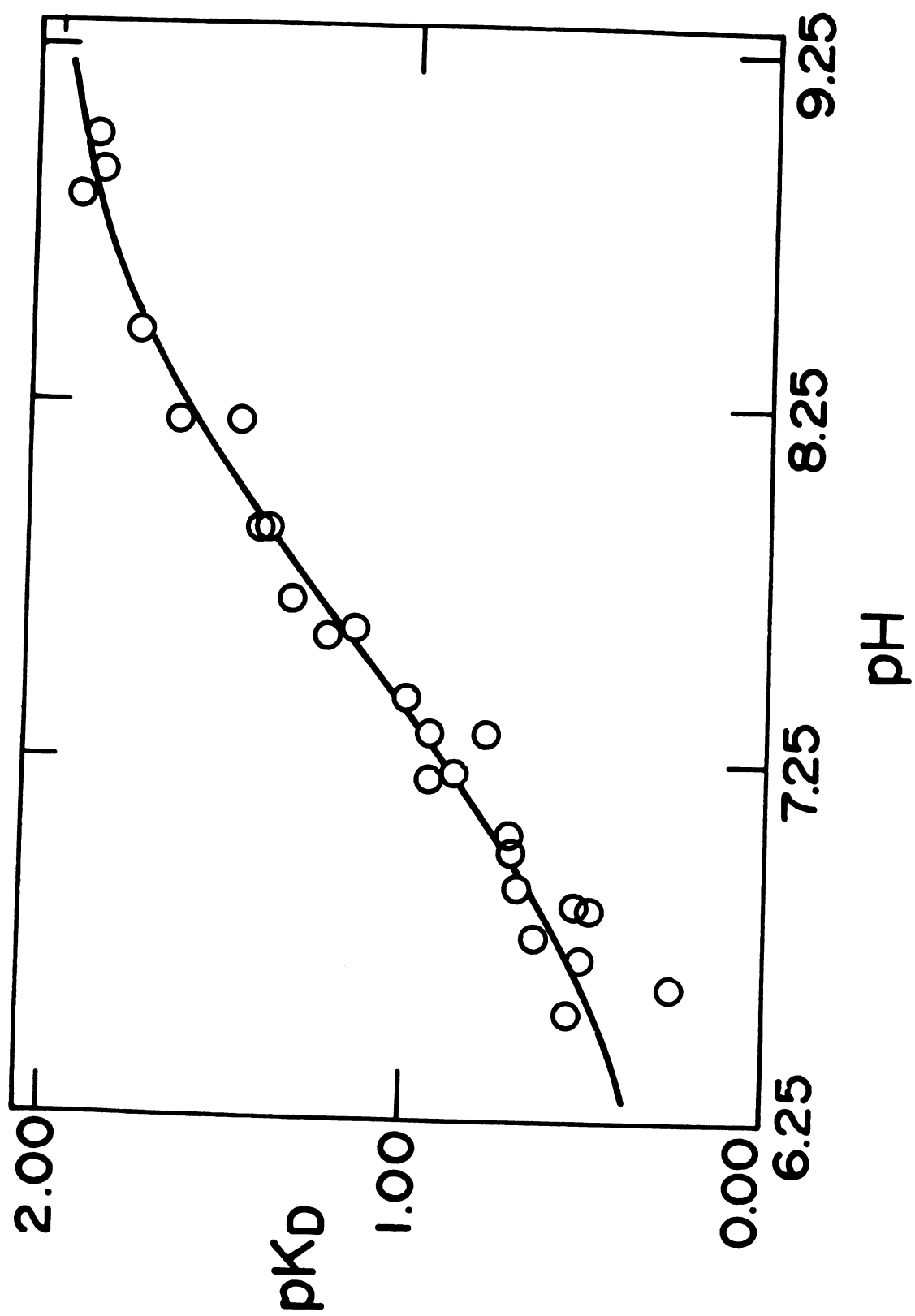


Figure 4

The apparent dissociation constant, K_D , at any pH is given by equation 2, taken from Cleland (14), where EH and E represent protonated and unprotonated enzyme, respectively.

$$K_D = \frac{K_i (1 + [H^+]/K_E)}{(1 + [H^+]/K_{EH})} \quad (2)$$

Analysis of the data in terms of this model using KINFIT (10) gave the following results: $pK_E = 8.47 \pm 0.10$, $K_i = 9.1 \pm 0.8$ mM. $pK_{EH} = 6.7$ and $K_j = 0.6$ M. K_{EH} and K_j are not well defined due to the experimental difficulty of saturating the enzyme with alanine at low pH values where the concentration of alanine would need to approach the value of 0.6 M to achieve half saturation of the enzyme. These results do imply, however, that under normal experimental conditions essentially no inhibitor binds to the EH form of the enzyme.

Kinetics of SOPC Degradation - Kinetic studies in the presence of 0.2 M KCl, 0.5 M KCl and 0.85 M LiCl reveal that V_{max} is constant with pH and that the K_m for SOPC varies with pH in a similar fashion under all three conditions. A plot of $\log (V/K)$ versus pH (Figure 5) reveals two downward inflection points. Since V/K is the apparent first order rate constant for the interaction of enzyme with substrate (15), these inflections imply that ionizations which occur on the free enzyme and/or free substrate affect binding. Data for the binding of alanine to tryptophanase as a function of pH showed that for all practical purposes only

Figure 5. Variation of the affinity of tryptophanase for SOPC and the maximal velocity (V) with pH. The kinetic parameters were determined as described in Materials and Methods in the presence of A) 0.2 M KCl; B) 0.5 M KCl; C) 0.85 M LiCl. The amount of purified tryptophanase used in each case was: A) 10 μ l of 1.3 mg ml⁻¹, B) 5 μ l of 1.0 mg ml⁻¹; C) 10 μ l of 8.8 mg ml⁻¹. The units of (V/K) are min⁻¹ and the units of V are μ mol min⁻¹ mg⁻¹. The lines were calculated with the parameters listed in Table II.

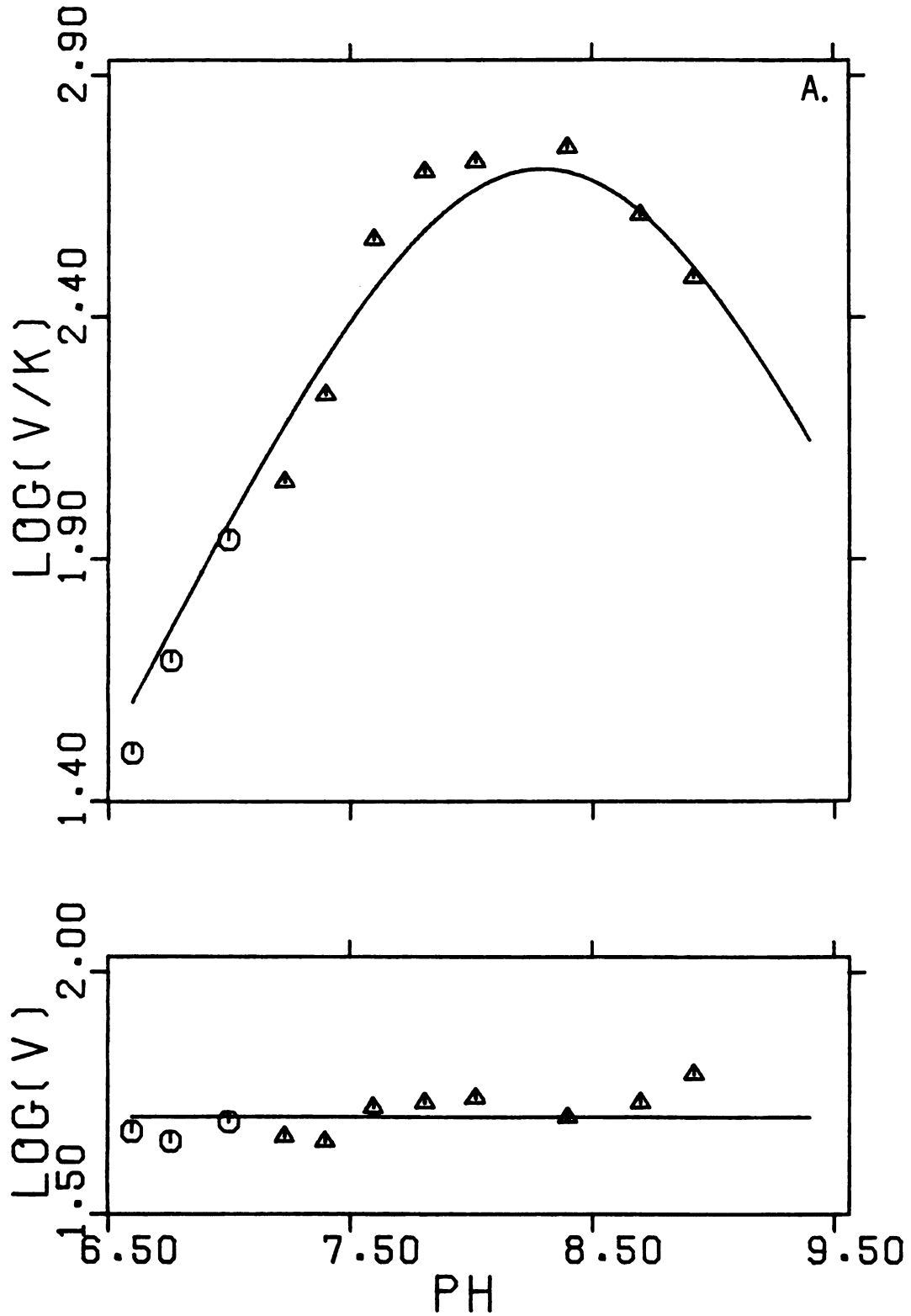


Figure 5A

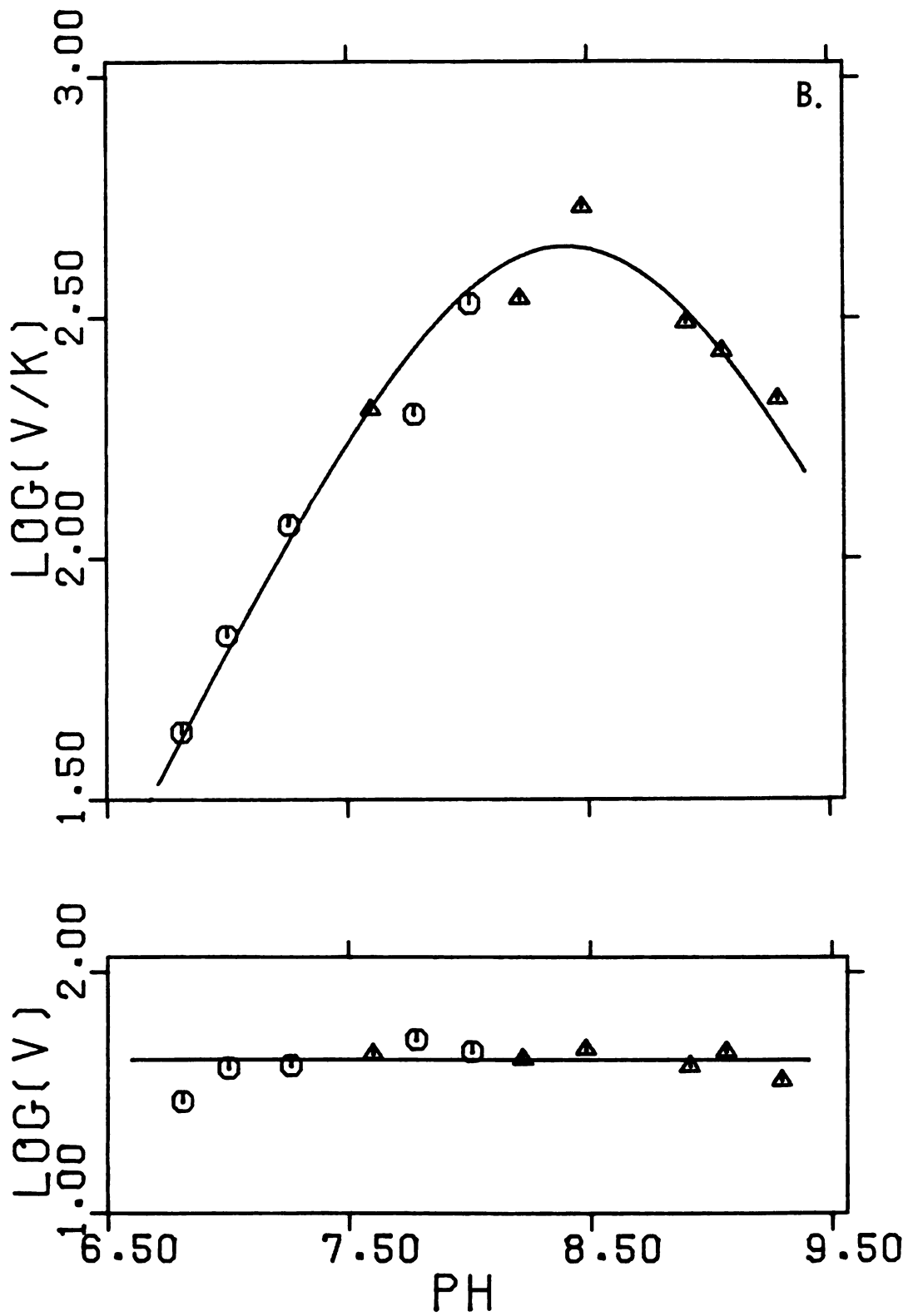


Figure 5B

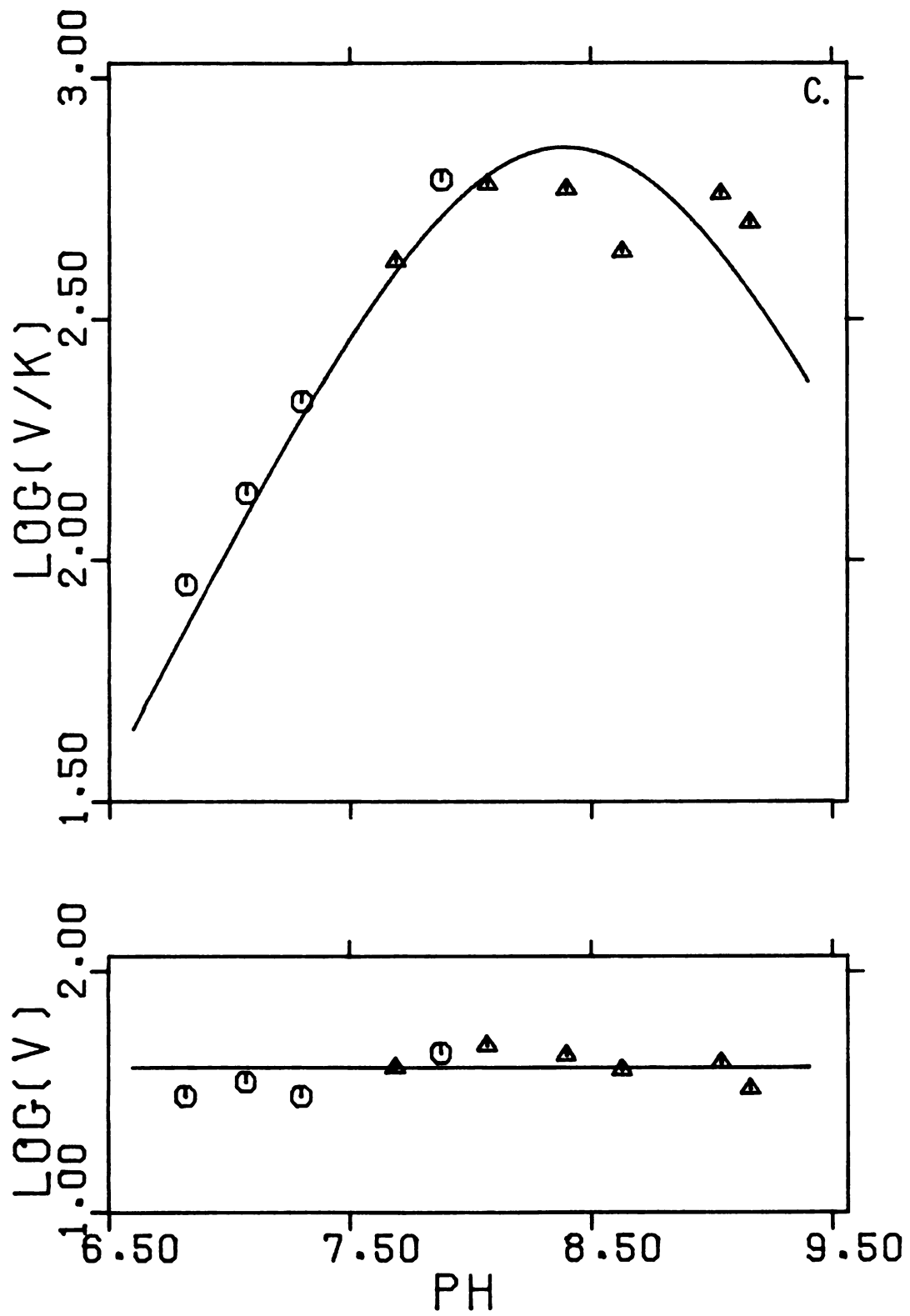
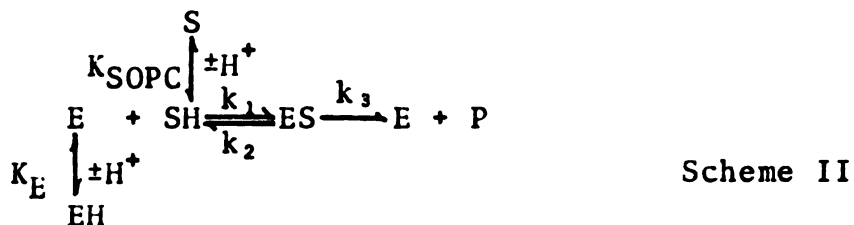


Figure 5C

the inhibitor in the zwitterionic form (pKa of α -amino group = 9.6) binds to unprotonated enzyme, E. Since the pKa of the α -amino group of SOPC was determined to be 8.44 ± 0.03 in 0.2 M KCl and 8.40 ± 0.04 in 0.5 M KCl at 30°C it was assumed that ionization of this group also dramatically lowered its affinity for the enzyme. If we assume that dipolar SOPC binds to unprotonated enzyme we arrive at the following mechanism:



where S and SH refer to unprotonated and protonated forms of SOPC, respectively. From steady-state considerations, assuming Michaelis-Menten behavior and that the protonation-deprotonation steps are in rapid equilibrium, one obtains the following:

$$v = \frac{V}{\left\{ \text{K}_m / [\text{SH}] (1 + [\text{H}^+] / \text{K}_E) \right\} + 1} \qquad (3)$$

where $\text{K}_m = (k_2 + k_3) / k_1$, and $\text{K}_E = (\text{E})(\text{H}) / (\text{EH})$.

After substituting an expression for [SH] in terms of S_o , total SOPC, we obtain

$$v = \frac{VS_o}{K_m (1 + [H^+]/K_E)(1 + K_{SOPC}/[H^+]) + S_o} \quad (4)$$

where K_{SOPC} is the dissociation constant for the α -amino group of SOPC. Since V is independent of pH, no Michaelis pH function (16) such as the ones appearing with K_m in equation 4 need be associated with this term.

All initial velocities obtained at various SOPC and hydrogen ion concentrations were then fitted by using equation 4 in program KINFIT To obtain pK_E , K_m and V_{max} in the presence of 0.2 M KCl, 0.5 M KCl and 0.85 M LiCl. The kinetic data with SOPC and the alanine titration data are summarized in Table II.

DISCUSSION

The results presented in this paper strongly support our previous conclusion that monovalent cations interact at or near the catalytic center of tryptophanase in such a way that they either participate directly in the reaction or are required for the critical alignment of one or more functional groups necessary for catalysis (5). The spectral titrations of tryptophanase as a function of pH demonstrate that the

Table II: Kinetic parameters for the degradation of SOPC and the formation of the quinonoid with L-alanine as a function of pH.

Substrate or Inhibitor	Monovalent Cation	pK _E	K _m (mM) ^a	V _{max} ^b	pK _{EH}	K _i (mM)	K _j (mM)
SOPC	0.2 M KCl	8.15 ± 0.10	0.034 ± 0.004	39 ± 1.5	--	--	--
SOPC	0.5 M KCl	8.43 ± 0.10	0.024 ± 0.002	43 ± 1.2	--	--	--
SOPC	0.85 LiCl	8.45 ± 0.15	0.016 ± 0.003	4 ± 0.2	--	--	--
Alanine	0.2 M KCl	8.47 ± 0.10	--	--	6.7	9.1 ± 0.8	600.

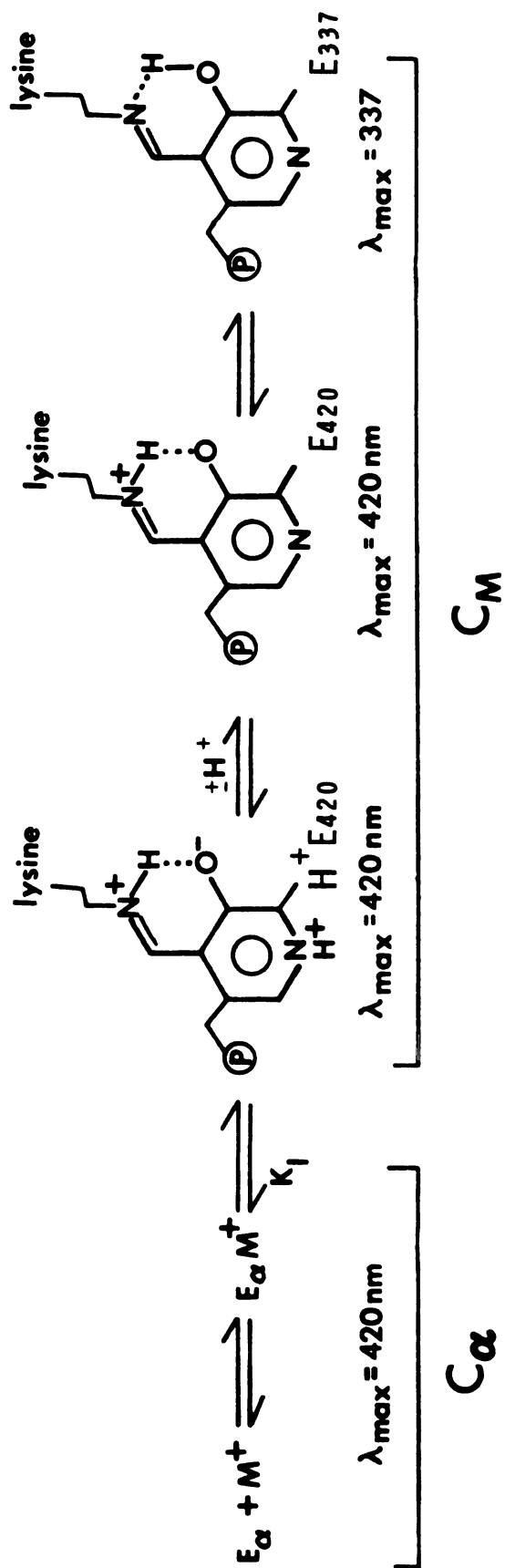
a. K_m for dipolar SOPC.

b. The units of V_{max} are μmol · min⁻¹ · mg⁻¹

cation has a dramatic effect on the equilibrium between the 337 nm and 420 nm forms of the enzyme. It is difficult to imagine that such large effects would be seen if the cation were bound at a site remote from the coenzyme.

These results are consistent with the scheme outlined by Davis and Metzler (1) in which deprotonation of the pyridinium nitrogen leads to a species absorbing at 337 nm. This mechanism is reproduced in Scheme III with the addition of a form corresponding to a conformer which exists in the absence of cations. That such a conformer exists is evident because in the absence of cations the enzyme is inactive and absorbs entirely at 420 nm. It is assumed that the coenzyme which gives rise to the inactive 420 nm absorption is similar in structure to H^+E_{420} or E_{420} , but is bound in such a manner as to preclude interaction with groups at the active site necessary for catalysis.

The different pK_a' values for the spectral interconversion and V_{max} values observed in the presence of the various cations are consistent with the assumption that the role of the cation is to affect the equilibrium between two conformers, C_a , a catalytically incompetent form that would exist in the absence of cations, and C_M , a conformer promoted to different extents by the various cations. By lowering the value of K_I (Scheme III), the cation could increase V_{max} and simultaneously decrease the apparent pK_a for conversion of



SCHEME III

420 nm absorption to an absorption with a maximum at 337 nm. Essentially identical values for the extinction coefficients of the various forms of the enzyme in the presence of NH_4^+ , K^+ and Rb^+ support this scheme. It should be pointed out that various conformations may exist under the general designations of C_α and C_M . In fact, this is almost surely the case for C_M which demonstrates at least two absorption maxima indicating different coenzyme environments. The fact that the absorbance at 337 nm does not go to zero at zero pH may be attributable to absorption contributed by the various 420 nm absorbers. According to Scheme III, absorption at 420 nm would not be expected to go to zero at high pH due to the pH-independent equilibrium between structures E_{420} and E_{337} .

We have also shown that although V_{max} is different in K^+ and Li^+ , it is independent of pH throughout the range investigated for both cations. This indicates that the cation does not act by altering the pK_a' of the α -hydrogen of the bound substrate molecule. If this were the case, one might expect to see an inflection point due to this ionization in the $\log V$ vs. pH plot for SOPC degradation in Li^+ . Of course, it is possible that this pK_a' is sensitive to the cation, but in all cases is below approximately 6.6.

The fact that the Li^+ enzyme shows activity even at low pH values despite its pK_a' value of approximately 9.75 also suggests that activity may be associated with a 420 nm form of the coenzyme rather than the 337 nm form as argued by Morino and Snell (4).

The affinity of enzyme for substrate as a function of pH is reflected in the $\log (V/K)$ plots for SOPC or in the case of the inhibitor, alanine, in the pK_D vs. pH plot. We have assumed for the analysis of the SOPC binding that it is the protonated form of the substrate that binds to an unprotonated enzyme. This is not evident from the SOPC data alone because the pK_a' for the α -amino group is similar to the pK_a' for the free enzyme. However, the pK_a for the L-alanine amino group is 9.6, and thus it is fully protonated throughout most of the pH range where binding studies were done. If we assume that alanine and SOPC are similar in this respect, then substrate must be protonated for binding to occur. The pK_a' obtained for free enzyme involved in binding obtained by equilibrium titration data with alanine and from kinetics data with SOPC (Table II) are not believed to be significantly different.

Therefore, the equilibrium binding data and kinetics data are consistent with a common model involving binding of protonated α -amino acids to an unprotonated enzyme. Binding of protonated alanine to unprotonated enzyme was some 65 times more effective ($K_j/K_i = 65.9$) than binding to protonated enzyme. Similar data could not be obtained with SOPC because inhibition was observed at elevated levels of SOPC (9). The value of $pK_{EH} = 6.7$ corresponds to the

value 6.65 given by Morino and Snell (4) for the loss of the alpha proton of L-alanine in the protein complex. Since attempts to fit the alanine binding data to the mechanism given by Morino and Snell (4) were not successful, we are not able to confirm this assignment.

Since pK_E is independent of the cation, the simplest explanation is that this group is on the protein itself and must be ionized for substrate to bind. However, the possibility remains that the process is more complex and involves more than one functional group.

REFERENCES

1. Davis, L., and Metzler, D. E. (1972) in The Enzymes (Boyer, P. D., ed.) Vol. 7, pp. 33-74.
2. Happold, F. C., and Struyvenberg, A. (1954) Biochem. J. 58, 379-382.
3. Newton, W. A., and Snell, E. E. (1964) Proc. Natl. Acad. Sci. U.S.A. 52, 382-389.
4. Morino, Y., and Snell, E. E. (1967) J. Biol. Chem. 242, 2800-2809.
5. Suelter, C. H., and Snell, E. E. (1977) J. Biol. Chem. 252, 1852-1857.
6. Watanabe, T., and Snell, E. E. (1972) Proc. Natl. Acad. Sci. U.S.A. 69, 1086-1090.
7. Suelter, C. H., Wang, J., and Snell, E. E. (1977) Anal. Biochem. 76, 221-232.
8. Högberg-Raibaud, A., Raibaud, O., and Goldberg, M. E. (1975) J. Biol. Chem. 250, 3352-3358.
9. Suelter, C. H., Wang, J., and Snell, E. E. (1976) FEBS Lett. 66, 230-232.
10. Dye, J. L., and Nicely, V. A. (1971) J. Chem. Ed. 48, 443-448.
11. Johnson, R. J., and Metzler, D. E. (1970) Methods Enzymol. 18A, 433-471.
12. June, D. S., Kennedy, B., Pierce, T. H., Elias, S. V., Halaka, F., Behbahani-Nejad, I., El-Bayoumi, A., Suelter, C. H., and Dye, J. L. (1979) J. Amer. Chem. Soc. 101, 2218-2219.
13. Schirch, L., and Diller, A. (1971) J. Biol. Chem. 246, 3961-3966.
14. Cleland, W. W. (1977) Adv. Enzymol. Relat. Areas Mol. Biol. 45, 273-387.
15. Cleland, W. W. (1970) in The Enzymes (Boyer, P. D. ed.) Vol. 2, pp. 1-65, Academic Press, New York.
16. Dixon, M., and Webb, E. C. (1964) Enzymes, 2nd edition, Academic Press, New York.

SECTION III

STUDIES ON THE KINETICS AND MECHANISM OF THE pH-DEPENDENT
INTERCONVERSION OF THE SPECTRAL FORMS OF TRYPTOPHANASE

Tryptophanase from *Escherichia coli* B/1t7-A is a pyridoxal-P dependent enzyme which catalyzes α,β -elimination reactions of amino acid substrates and requires monovalent cations for optimum activity (1). Above 280 nm the enzyme has absorption maxima at 337 nm and 420 nm whose relative amplitudes depend on both pH and monovalent cations (2). Equilibrium studies have shown that the apparent pKa (pKa') for the interconversion of these spectral forms varies with the nature and concentration of the monovalent cation and that this pKa' is related to the Vmax for the breakdown of the artificial substrate S-orthonitrophenyl-L-cysteine (3).

We reported previously (4) that the 420 nm and 337 nm forms of the enzyme interconvert in a complex fashion on the scanning stopped flow time scale following a rapid change in pH or monovalent cation. This observation provided us with a unique opportunity to study the spectral forms of tryptophanase in the absence of substrates or inhibitors.

The above-mentioned scanning stopped flow studies have been extended to include incremental pH jumps and drops over the range of enzyme stability. Major features of the data are interpreted in terms of a simple model including kinetic constants and postulated structures.

MATERIALS AND METHODS

Materials - KCl was Mallinckrodt, analytical reagent. 2(N-morpholino) ethane sulfonic acid (Mes), N-tris(hydroxymethyl) methyl-2-aminoethane sulfonic acid (Tes), N-2-hydroxyethylpiperazine propane sulfonic acid (Epps), N,N-bis (2-hydroxyethyl) glycine (Bicine), pyridoxal-5'-phosphate, and DL-dithiothreitol (DTT) were obtained from Sigma Chemical Co.

Tryptophanase - Tryptophanase was prepared according to the method of Suelter *et al.* (16). Stock apoenzyme was activated by incubation for 1 hr. at 37°C in 0.1 M potassium phosphate, pH 8.0, 1 mM EDTA, 7% $(\text{NH}_4)_2\text{SO}_4$, 0.2 mM pyridoxal-P and 20 mM DTT. The enzyme had a specific activity of 50 - 55 $\mu\text{mol min}^{-1}\text{mg}^{-1}$ when assayed at 30° C with 0.6 mM S-orthonitrophenyl-L-cysteine (SOPC) in 50 mM potassium phosphate, pH 8.0, and 50 mM KCl (3). Protein concentration was determined spectrophotometrically using $\epsilon_{278} = 0.795 \text{ ml mg}^{-1} \text{ cm}^{-1}$ (5).

Incremental pH jump experiments - Activated holotryptophanase ($\sim 20 \text{ mg ml}^{-1}$) was equilibrated with 1 mM Tes, pH 7.00, 0.2 M KCl, 15 μM pyridoxal-P, 1 mM EDTA and 0.2 mM DTT by dialysis at 4° C. Prior to use, the enzyme was diluted to a concentration of 2.9 mg ml^{-1} with the dialysis buffer. This solution was pushed against 50 mM Bicine, pH 7.00, 0.2 M KCl, 15 μM pyridoxal-P, 1 mM EDTA to give the final pH values of 7.69, 8.07, 8.56, 8.90 and 9.33.

Incremental pH drop experiments - Activated holotryptophanase ($\sim 20 \text{ mg ml}^{-1}$) was equilibrated with 1 mM Bicine, pH 8.70, 0.2 M KCl, 15 μM pyridoxal-P, 1 mM EDTA and 0.2 mM DTT by dialysis at 4° C. The enzyme was diluted to a concentration of 4.0 mg ml^{-1} prior to the experiment with the dialysis buffer. This solution was pushed against 50 mM Tes, pHi, 0.2 M KCl, 15 μM pyridoxal-P, 1 mM EDTA to give final pH values of 6.54, 7.03, 7.47, 7.77, 8.25 and 8.44.

Scanning Stopped Flow Kinetics - Stopped flow data were collected on a scanning instrument described elsewhere (6,7) at $24.0 \pm 0.1^\circ \text{ C}$. 150 spectra per second were collected over the wavelength range 280 nm - 550 nm for a period of 65 seconds in the pH jump experiments and 111 seconds in the pH drop experiments. A total of 50 and 56 spectra were stored in the pH jump and drop experiments, respectively, using an averaging scheme outlined previously (8). Control spectra were collected as described previously (4).

Data Analysis - Data were fitted to the appropriate mathematical function using the nonlinear curve-fitting program KINFIT (9). Errors listed are marginal standard deviations. All titration data were fitted to equation 1 previously given by Johnson and Metzler (10).

$$\Delta_{\text{obs}} = \frac{\Delta_{\text{A}}(10^{(\text{pH}-\text{pK})}) + \Delta_{\text{HA}}}{(1 + 10^{(\text{pH}-\text{pK})})} \quad (1)$$

where Δ_{obs} is equal to the observed change in absorbance at a given pH, Δ_{A} is the calculated absorbance change at infinite pH, Δ_{HA} is the calculated change in absorbance at zero pH and pK is the negative log of the dissociation constant for the monoprotic acid.

pH Measurements - pH values were determined with a Beckman Model 4500 digital pH meter at 24° C.

RESULTS

As pointed out earlier, Morino and Snell (2) originally showed that the 420 nm form of tryptophanase predominates at low pH values whereas at high pH values the 337 nm absorption predominates. The absorption spectra of tryptophanase at pH 7.00 and 8.70 obtained by scanning spectroscopy clearly confirm these results (Figure 1A). To investigate the time dependent interconversion of these spectral forms, the pH of an enzyme solution was increased (jumped) or decreased (dropped) in a scanning stopped flow spectrophotometer and the absorbance was scanned as a function of wavelength and time as outlined in Materials and Methods. Typical results of a pH drop experiment which are given in Figure 1B as a 3-dimensional difference absorbance-wavelength-time surface show the region of the spectrum where changes occur. These spectral changes were analyzed in terms of 3 distinct phases: 1) an abrupt phase, which is complete in less than

Figure 1: Absorbance spectrum of tryptophanase at low and high pH values and absorbance difference-wavelength-time surface observed in a pH drop experiment. A) Absorption spectrum of tryptophanase at pH 7.00 (O) and pH 8.70 (Δ); B) Absorbance difference-wavelength-time surface following a drop in pH from 8.70 to 6.54.

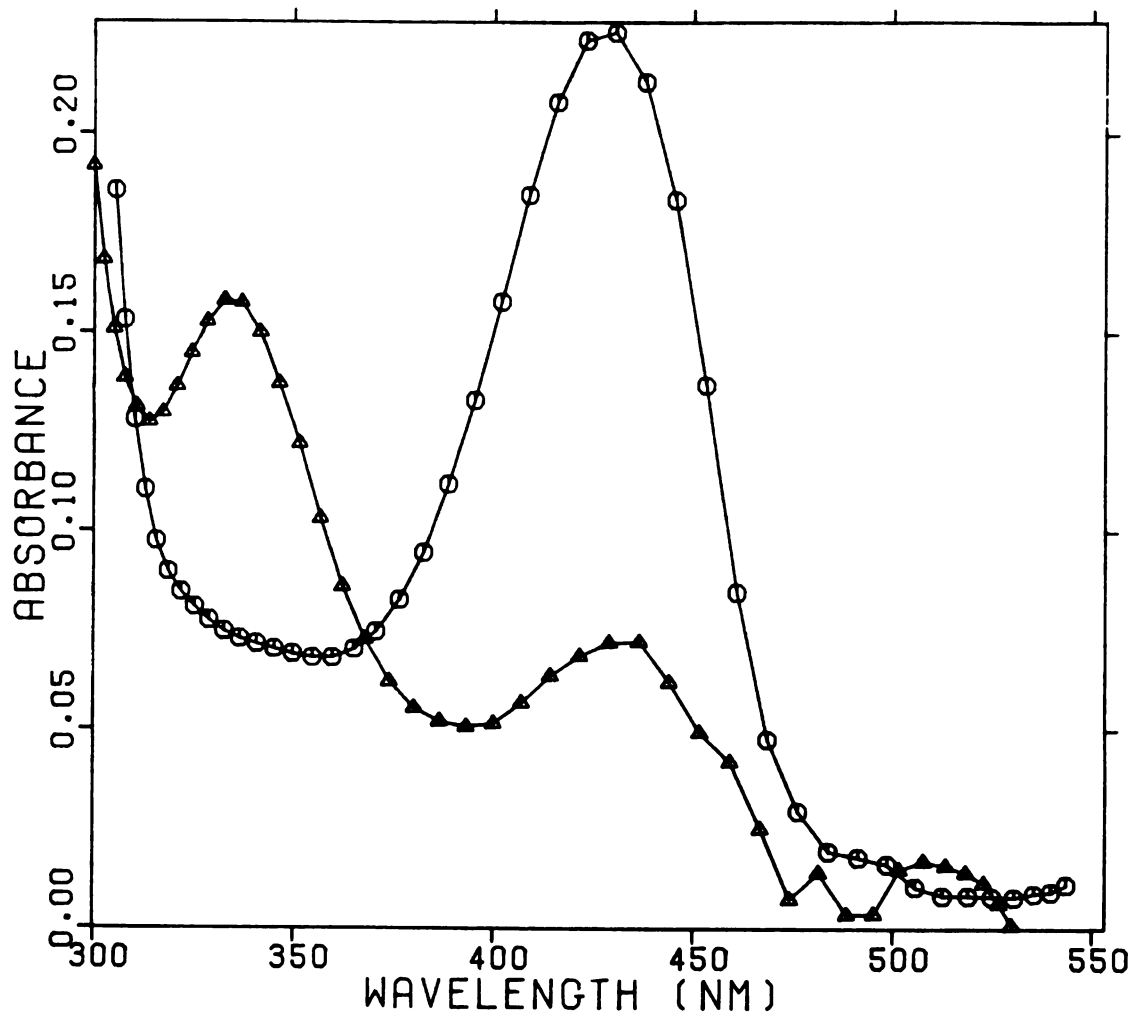


FIGURE 1A

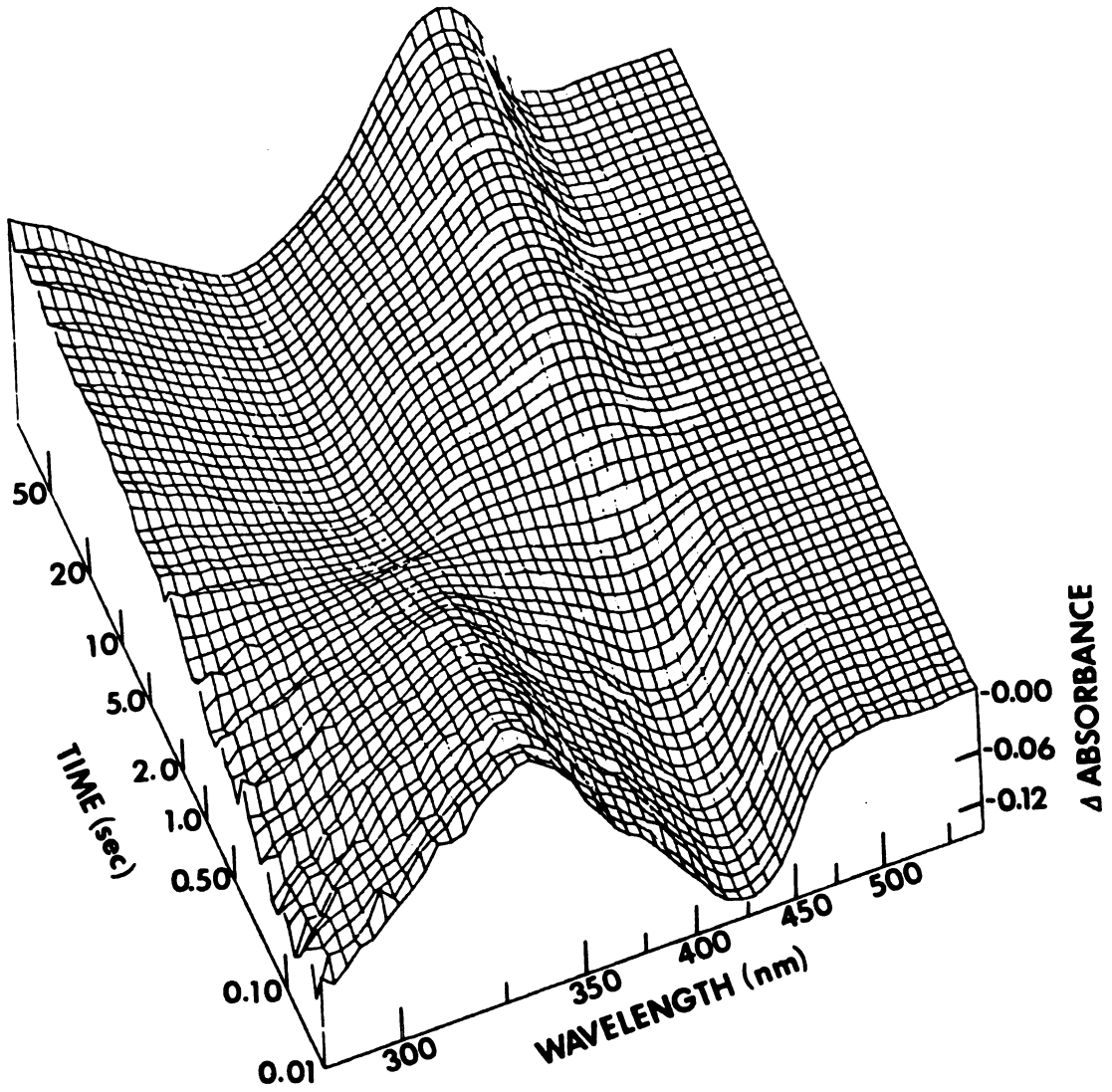


FIGURE 1B

5 msec, 2) a fast first order interconversion of 420 nm and 337 nm absorbance, and 3) a slow first order process involving growth at 355 nm coupled to two decays centered at 325 nm and 430 nm in the incremental pH jumps; and decay at 355 nm with concomitant growth at 430 nm and slight growth at 290 nm in the case of the incremental pH drop experiments. Each of these phases will be discussed separately.

Abrupt Spectral Changes - The First Phase - The difference spectra obtained by subtracting the enzyme spectrum at $t = 0$, prior to mixing, from the first spectrum after mixing (6 - 12 msec) are shown in Figure 2. These changes occurred during the 6.5 msec dead time (1.85 cm-path-length cell) and are referred to as the abrupt changes. A and B of Figure 2 show the difference spectra obtained in the incremental pH jump experiments. The overall features of the spectra include a peak at ~ 295 nm, a generalized increase in absorbance in the wavelength range ~ 330 nm - 420 nm, with possible peaks at ~ 340 nm and at ~ 395 nm, and a decrease in the range ~ 430 nm - 460 nm. C and D of Figure 2 are abrupt difference spectra obtained in the pH drop experiments. These spectra exhibit increases in absorbance centered at ~ 330 nm and ~ 420 nm and a decrease at ~ 295 nm.

The complexity of these difference spectra suggests that several processes, perhaps involving rapid subtle conformational changes and titration of various functional

Figure 2: Abrupt difference spectra obtained in the incremental pH jump and drop experiments. A) Incremental pH jumps from pH 7.00; pH 9.33 (O), pH 8.90 (Δ), pH 8.56 (+); B) Incremental pH jumps from pH 7.00; pH 8.07 (O), pH 7.69 (Δ); C) Incremental pH drops from pH 8.70; pH 6.54 (O), pH 7.03 (Δ), pH 7.47 (+); D) Incremental pH drops from pH 8.70; pH 7.77 (O), pH 8.25 (Δ), pH 8.44 (+).

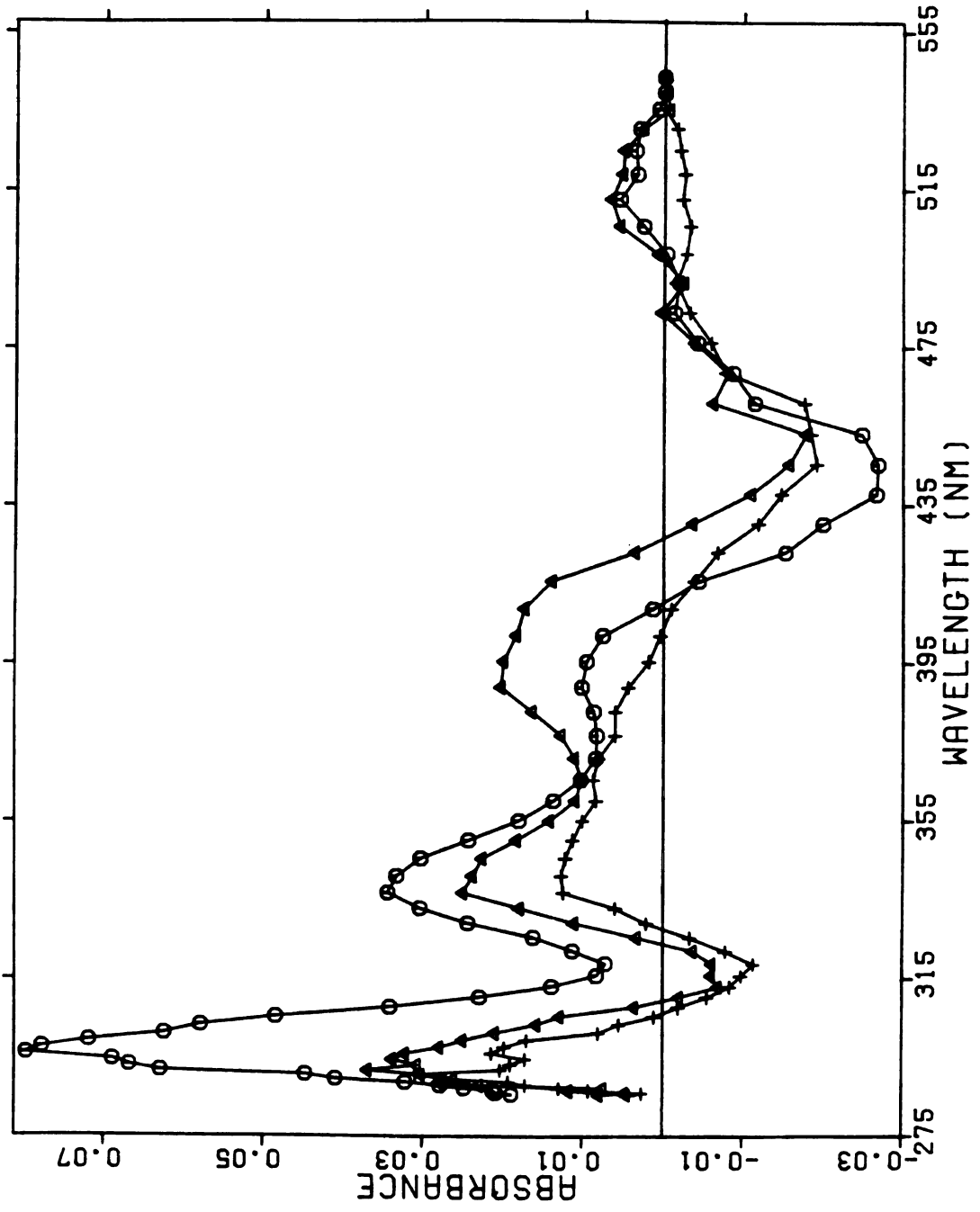


Figure 2A

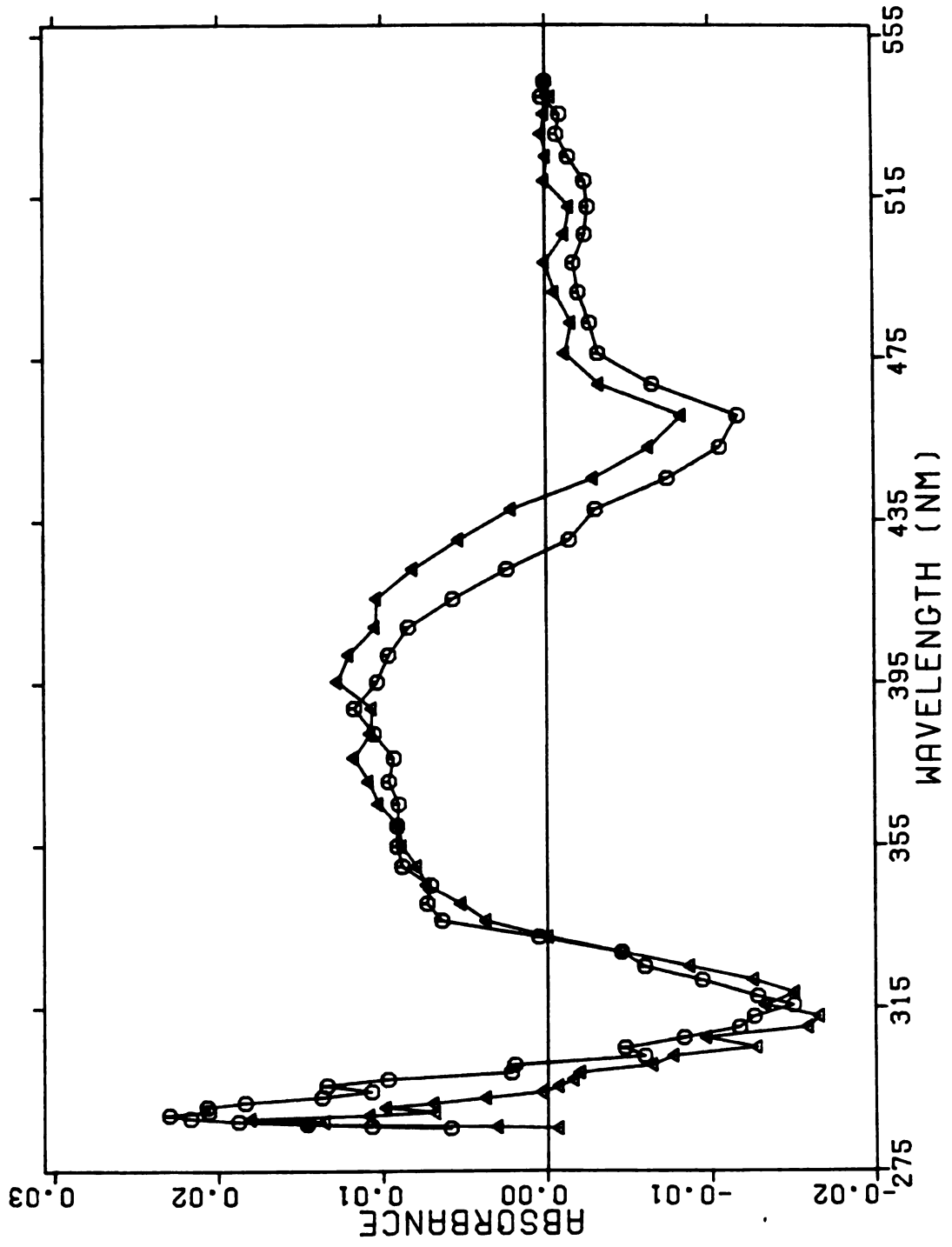


Figure 2B

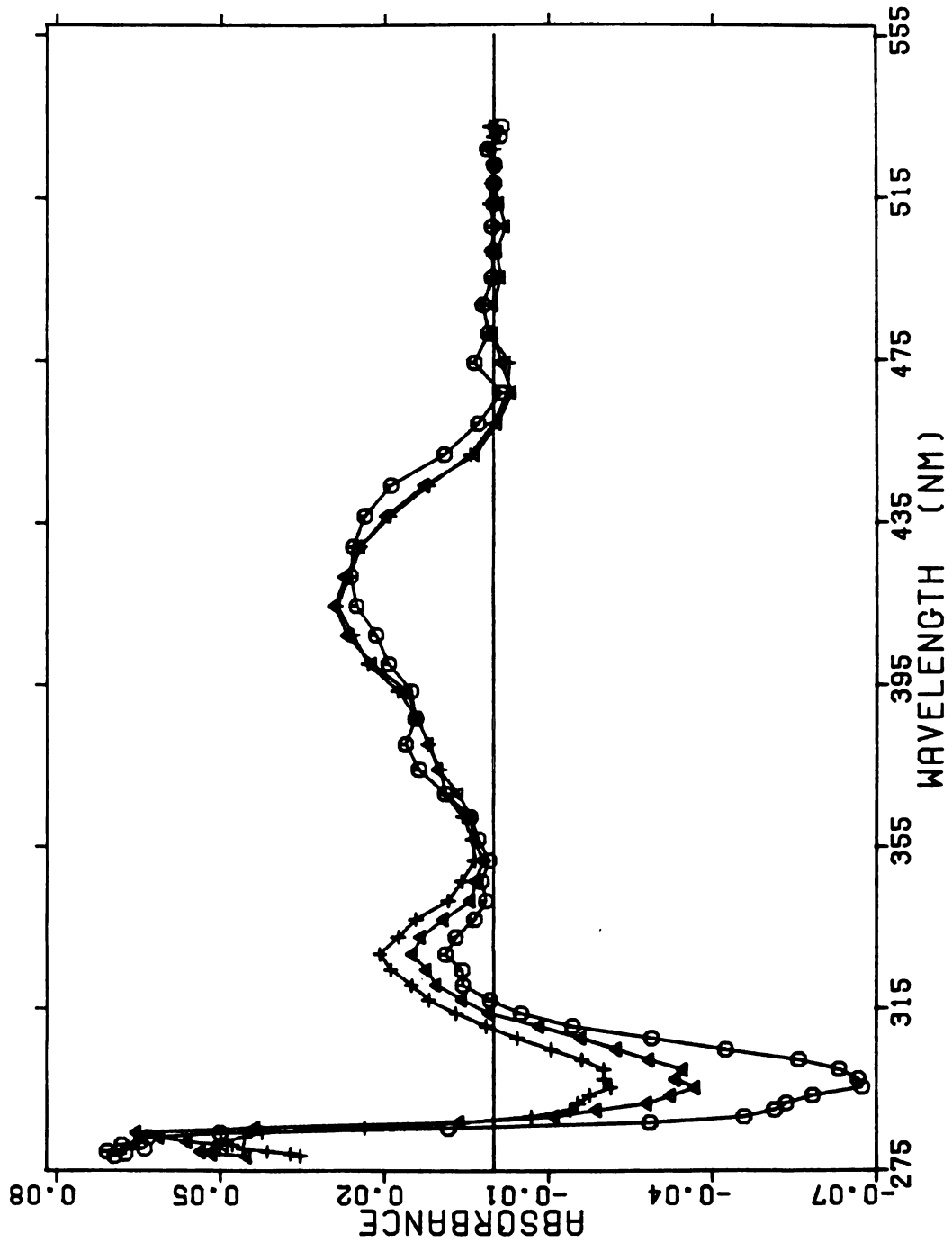


Figure 2C

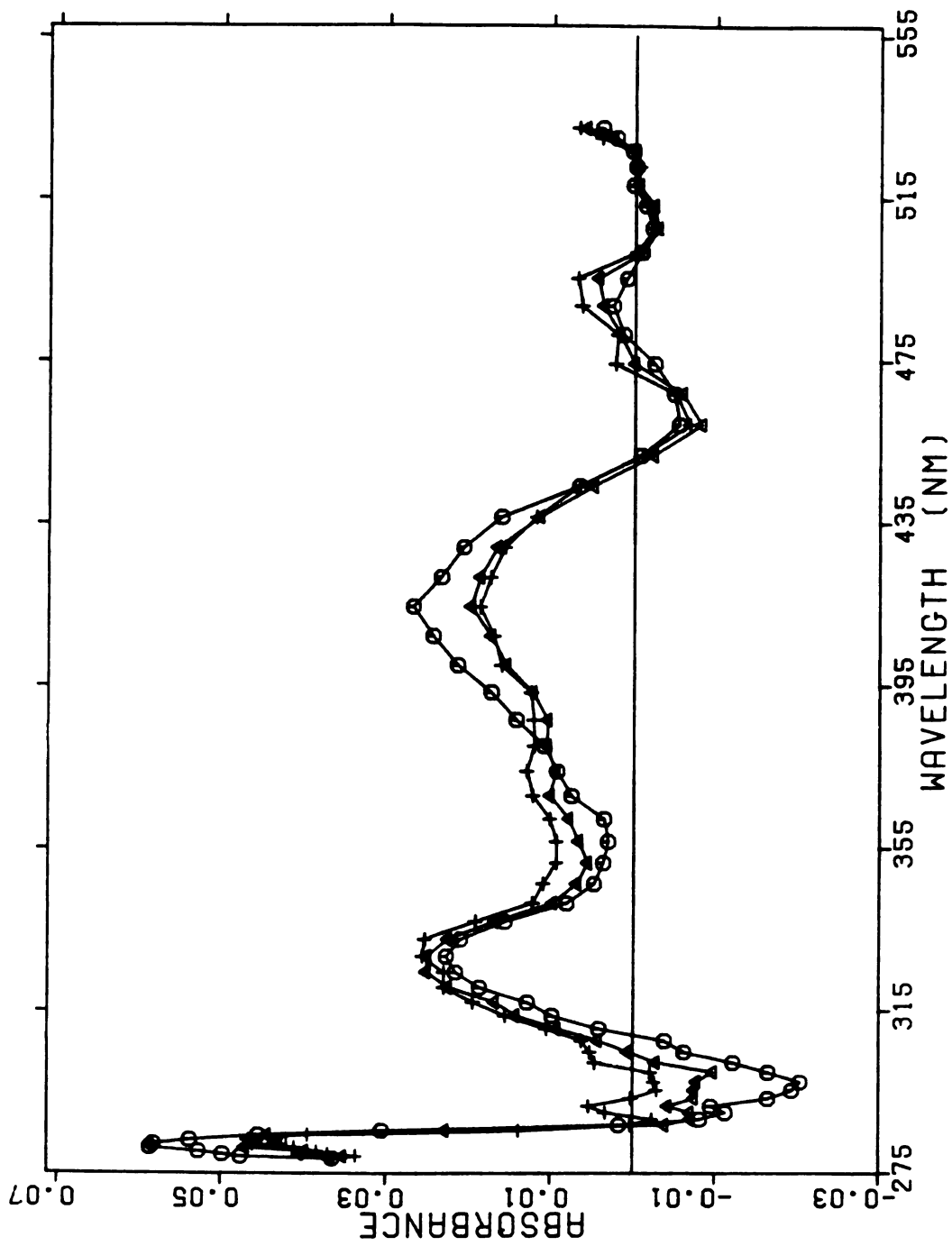


Figure 2D

groups, contribute to alterations in the original spectrum that give rise to the difference spectra. It is also likely that some wavelength instability in the scanning stopped flow instrument itself contributed to the nonuniformity of these difference spectra. Small wavelength shifts which occurred during the time between the collection of the various experimental spectra could cause wavelength shifts in these difference spectra.

Although the difference spectra for the pH jumps and drops are qualitatively different, the 295 nm peak which appears in the pH jump difference spectra (Figure 2A, B) occurs again, essentially as a mirror image, in the pH drop spectra (Figure 2C, D). To determine apparent pKa values for the process at 295 nm in the pH jump and drop experiments, the change in absorbance at 295 nm was examined as a function of pH in each case (Figures 3A and 3B).

The data are not sufficient to clearly define pKa' values in either case. Nevertheless, some qualitative features can be discerned. It is clear, for example, that the pKa' at 295 nm in the pH jumps is above 9.0. To illustrate this the theoretical line was drawn with a pKa' value of 9.6 ± 1.2 , obtained by fitting the data to equation 1 with KINFIT (9). The data for the pH drop experiments, which extend the lower range of pH investigated to 6.54,

Figure 3. The change in absorbance at 295 nm as a function of pH for the abrupt spectral changes observed in the incremental pH jump and drop experiments. A) Incremental pH jumps. The line was calculated using equation 1 with a pK value of 9.63. B) Incremental pH drops. The line was calculated with pK values of 6.3 and 9.4.

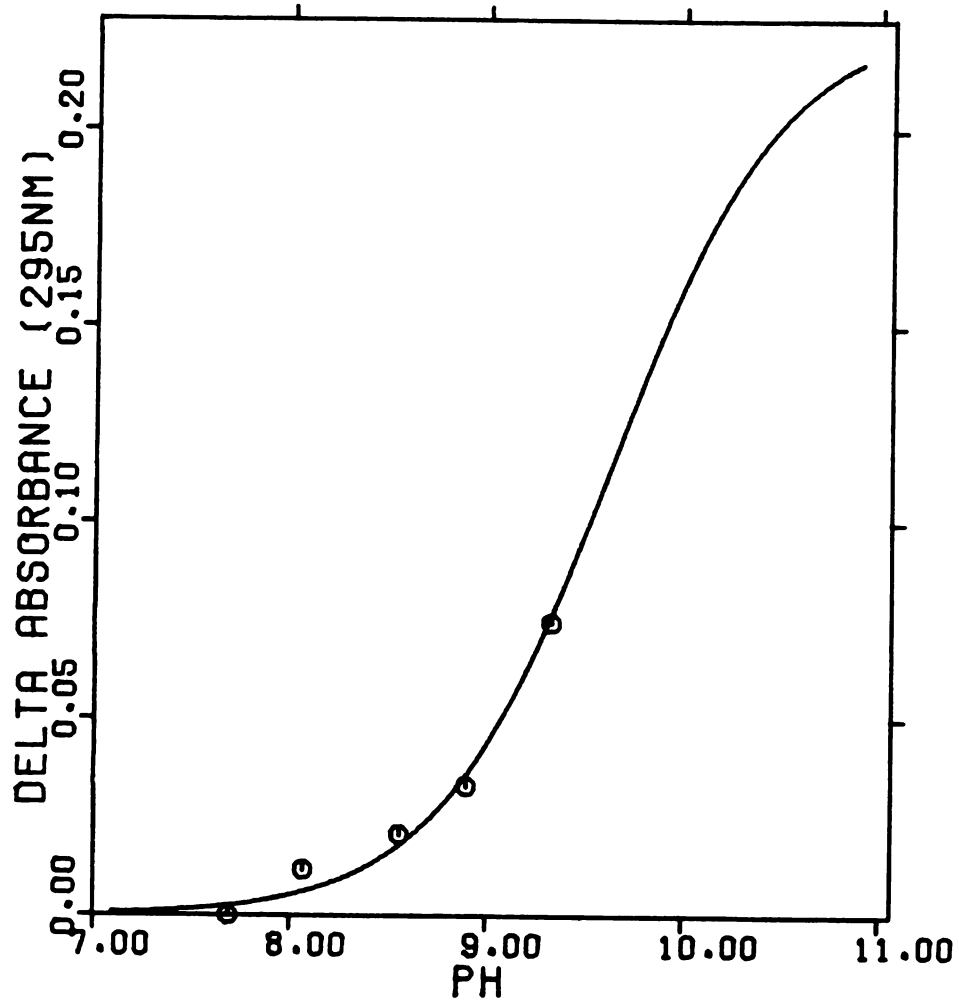


FIGURE 3A

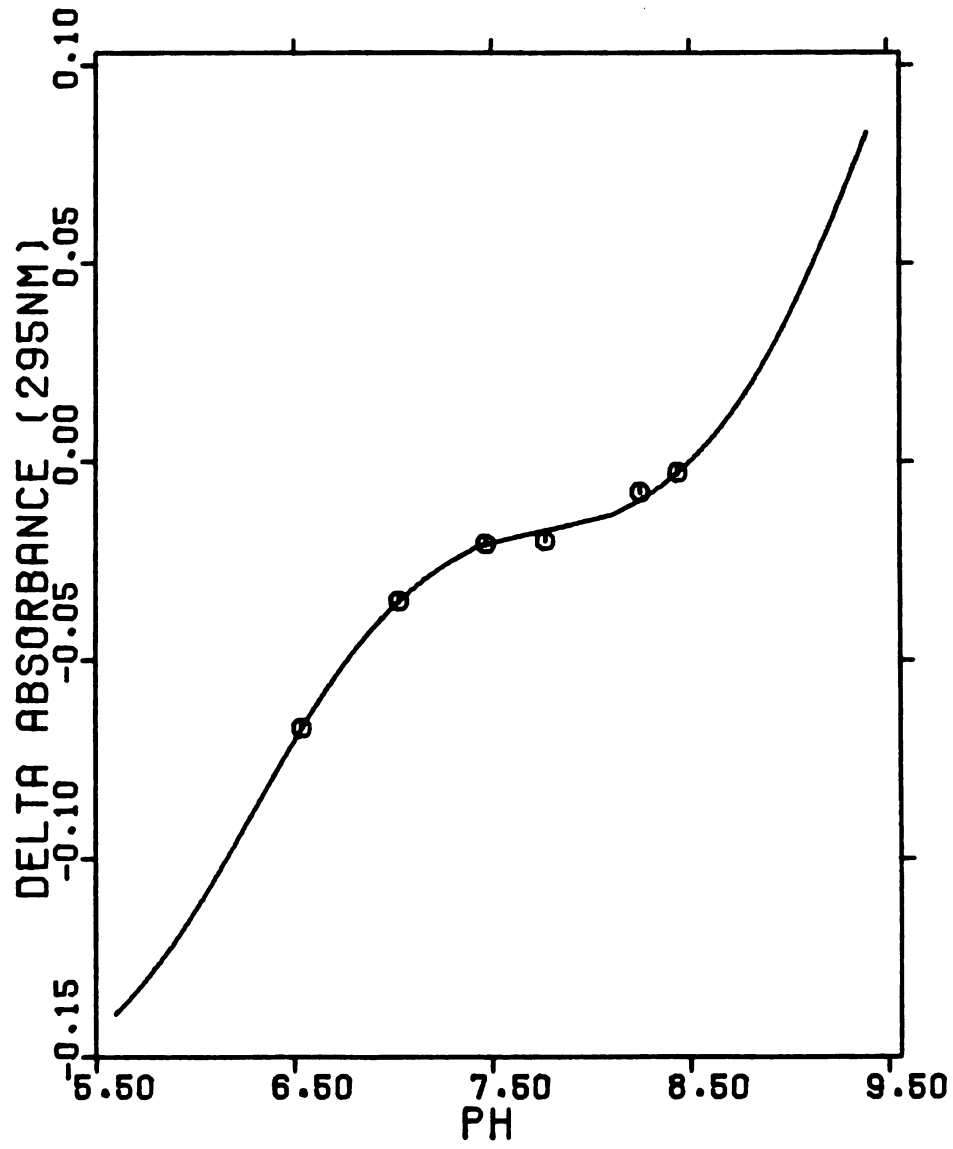


FIGURE 3B

indicate that two groups may be involved when the pH is dropped incrementally from a starting pH of 8.70. The theoretical line was drawn with $pK_{a_1}' = 6.3$ and $pK_{a_2}' = 9.4 \pm 4.7$.

Fast First Order Interconversion of 420 nm and 337 nm Forms of Tryptophanase - The Second Phase - The second phase, which occurs after a change in pH, is a fast first order interconversion of 420 nm and 337 nm absorption. A and B of Figure 4 show the spectral changes observed as a function of time following an increase in pH from 7.00 to 9.33 and a decrease in pH from 8.70 to 6.54, respectively. After such a pH jump, there is a growth centered at ~337 nm coupled to decays at ~420 nm and ~290 nm. The changes observed after a decrease in pH mirror those seen after a pH increase. Isosbestic points occur at ~300 nm and ~360 nm in both cases.

The first order rate constants for the changes at 420 nm and 337 nm were obtained by fitting the absorbance vs. time data at each wavelength to equation 2 with KINFIT (9). The adjustable parameters were A^∞ , the absorbance at infinite time, ΔA , the

$$A_{\text{obs}} = A^\infty \pm \Delta A e^{-k_1' t} \quad (2)$$

change in absorbance [i.e., $(A^\infty - A_0)$, where A_0 is the absorbance at $t = 0$], and k_1' , the apparent first order rate constant.

Figure 4. Spectral changes occurring during the fast first order interconversion of 420 nm and 337 nm absorptions. These difference spectra were obtained by subtracting the spectrum collected before any changes occurred from the spectrum collected after the fast first order changes were complete. A) A pH jump from pH 7.00 to 9.33; B) A pH drop from pH 8.70 to 6.54.

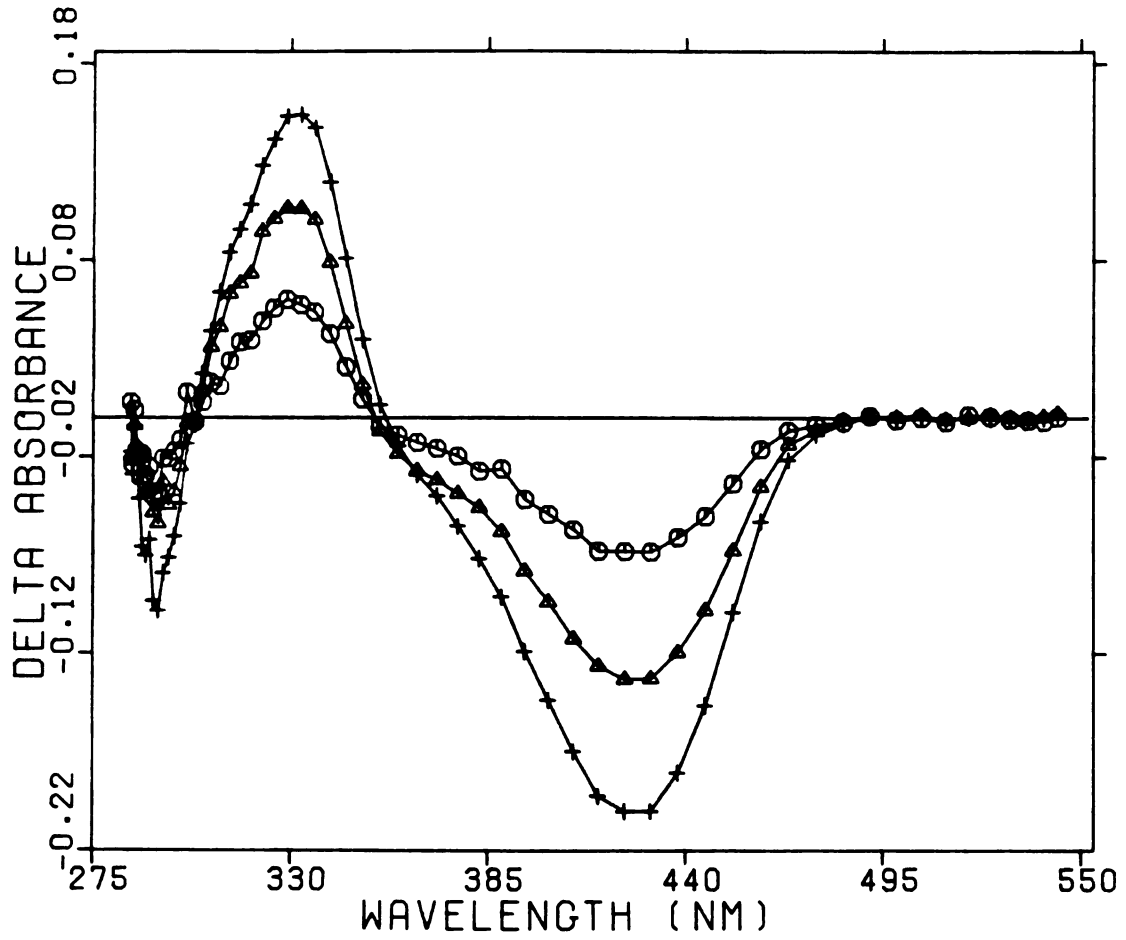


FIGURE 4A

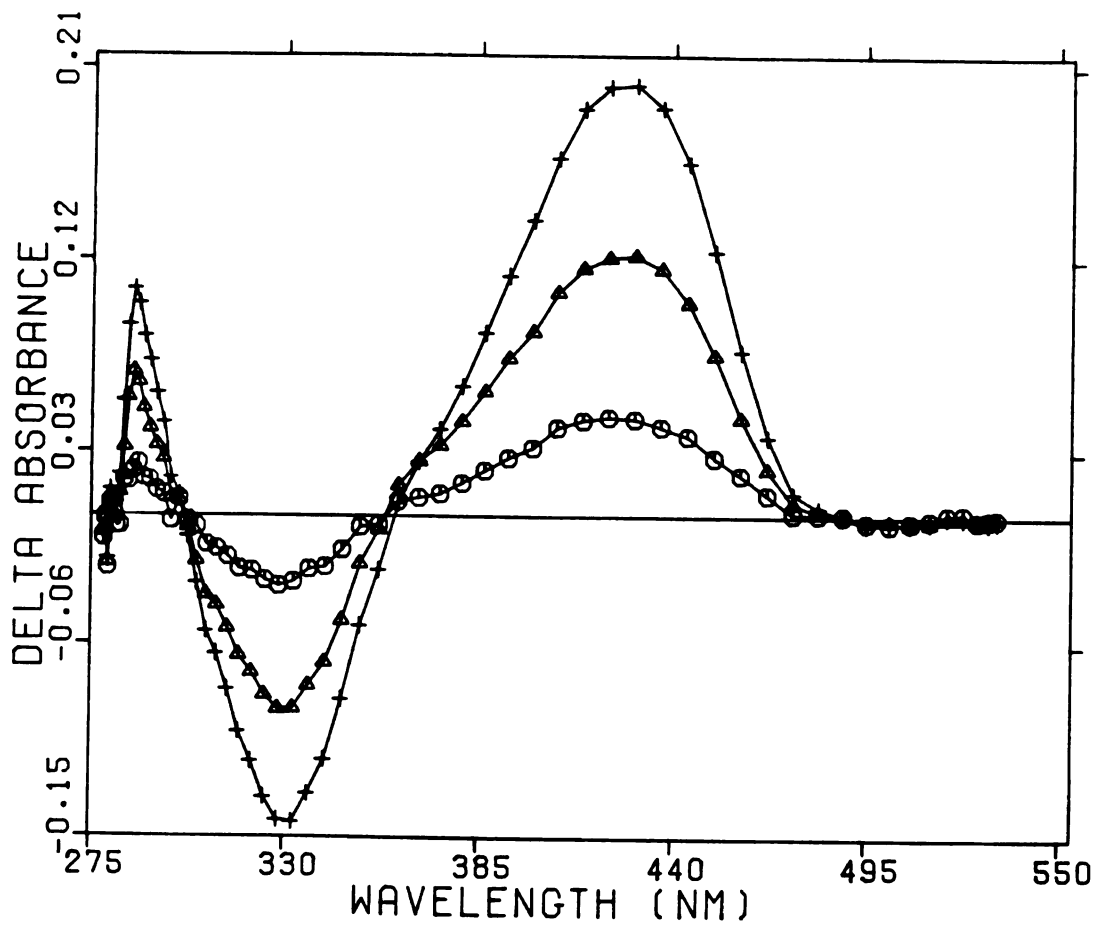


FIGURE 4B

Apparent pKa values for this interconversion process were obtained by fitting the absolute values of ΔA , obtained as described above, at 337 nm and 420 nm as a function of the final pH to equation 1 as a multiple data set (Figures 5A and 5B). This gave pKa' values, respectively, of 8.30 ± 0.02 and 8.08 ± 0.04 for the pH jump and drop experiments.

The first order rate constants for the changes in absorbance at 337 nm and 420 nm obtained in each pH jump or drop experiment were essentially identical. However, they varied with pH in a systematic manner as indicated in Table I and Figure 9. The data for the change centered at 290 nm appeared to show the same kinetic behavior as the 420 nm and 337 nm data. However, the noise encountered at this low wavelength coupled with small absorbance changes, especially in the smaller increments of pH change, made analysis difficult. Values are reported in Table I for those instances where the analysis was successful.

Representative plots showing the changes occurring at 295 nm, 337 nm and 420 nm as a function of time for a pH jump from 7.00 to 9.33 are shown in Figures 6A, B and C. The theoretical lines were calculated with equation 2 using the parameters listed in Table I.

Figure 5. The changes in absorbance at 337 nm and 420 nm observed in the incremental pH jump and drop experiments as a function of pH. A) Incremental pH jumps; 337 nm (O), 420 nm (Δ). The lines were calculated using equation 1 with a pK value of 8.30; B) Incremental pH drops; 337 nm (O), 420 nm (Δ). The lines were calculated using equation 1 with a pK value of 8.08.

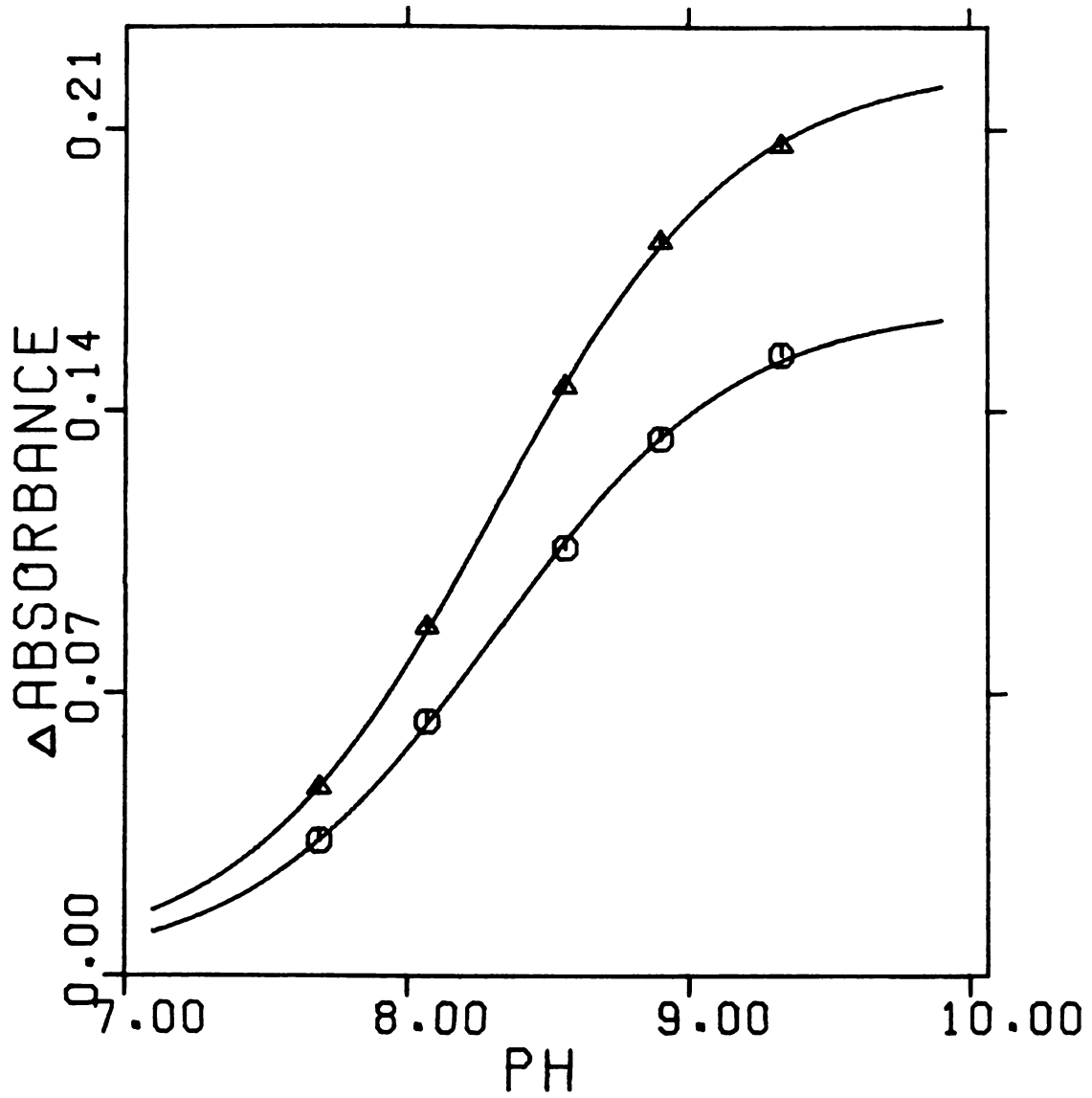


FIGURE 5A

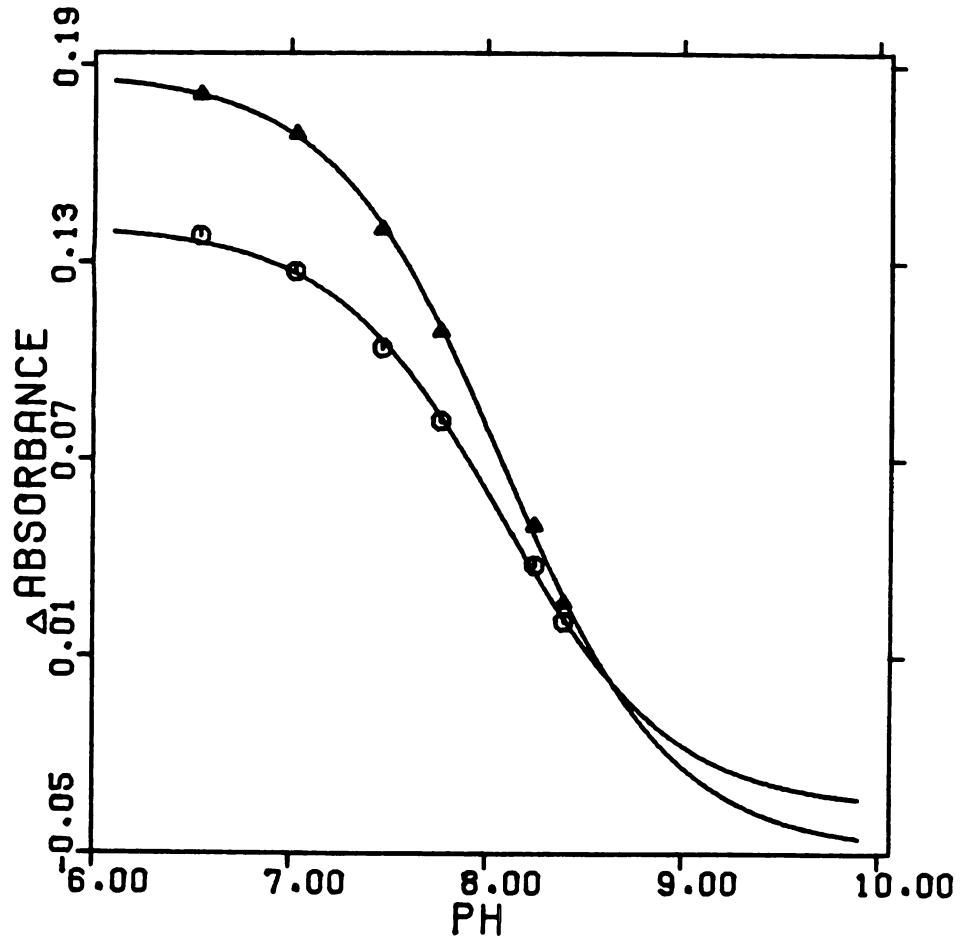


FIGURE 5B

Table I: Kinetic parameters for the fast first order interconversion of 420 nm and 337 nm absorbance in the pH jump and drop experiments. These parameters were obtained by fitting the changes in absorbance at each wavelength to equation 2.

INCREMENTAL pH JUMP EXPERIMENTS:

Final pH	Wave-length (nm)	A_{∞}	ΔA	k_1' (sec ⁻¹)
9.33	295	0.711 ± 0.007	0.0674 ± 0.0020	1.79 ± 0.38
	337	0.325 ± 0.003	0.154 ± 0.003	2.78 ± 0.08
	420	0.169 ± 0.003	0.206 ± 0.003	2.63 ± 0.01
8.90	295	0.687 ± 0.008	0.0553 ± 0.0260	1.06 ± 0.35
	337	0.229 ± 0.003	0.133 ± 0.002	1.44 ± 0.01
	420	0.207 ± 0.002	0.182 ± 0.003	1.38 ± 0.04
8.56	295	0.687 ± 0.005	0.0362 ± 0.0035	0.620 ± 0.156
	337	0.273 ± 0.002	0.106 ± 0.002	0.882 ± 0.004
	420	0.248 ± 0.002	0.146 ± 0.001	0.838 ± 0.004
8.07	337	0.236 ± 0.002	0.0630 ± 0.0005	0.464 ± 0.015
	420	0.310 ± 0.004	0.0863 ± 0.0013	0.423 ± 0.007
7.69	337	0.213 ± 0.001	0.0334 ± 0.0004	0.359 ± 0.006
	420	0.353 ± 0.004	0.0466 ± 0.0007	0.338 ± 0.004

INCREMENTAL pH DROP EXPERIMENTS:

6.54	295	0.879 ± 0.019	0.070 ± 0.012	0.483 ± 0.016
	337	0.186 ± 0.002	0.138 ± 0.001	0.541 ± 0.010
	420	0.329 ± 0.003	0.181 ± 0.003	0.519 ± 0.004
7.03	295	0.889 ± 0.005	0.048 ± 0.001	0.487 ± 0.123
	337	0.207 ± 0.003	0.127 ± 0.001	0.414 ± 0.002
	420	0.319 ± 0.003	0.169 ± 0.001	0.409 ± 0.003
7.47	337	0.236 ± 0.001	0.104 ± 0.001	0.366 ± 0.005
	420	0.296 ± 0.001	0.140 ± 0.001	0.362 ± 0.004
7.77	337	0.258 ± 0.001	0.0818 ± 0.0010	0.384 ± 0.003
	420	0.264 ± 0.001	0.109 ± 0.001	0.377 ± 0.007
8.25	337	0.304 ± 0.001	0.0377 ± 0.0011	0.534 ± 0.032
	420	0.209 ± 0.001	0.0498 ± 0.0005	0.507 ± 0.009
8.40	337	0.323 ± 0.002	0.0205 ± 0.0006	0.665 ± 0.118
	420	0.186 ± 0.002	0.0262 ± 0.0005	0.620 ± 0.053

Figure 6. Changes in absorbance at 295 nm, 337 nm and 420 nm as a function of time during the fast first order conversion of 420 nm to 337 nm absorbance following a jump in pH from 7.00 to 9.33. A) first order decay of 295 nm, B) first order growth at 337 nm, C) first order decay at 420 nm. The lines through the data were calculated from equation 2 and the parameters listed in Table I.

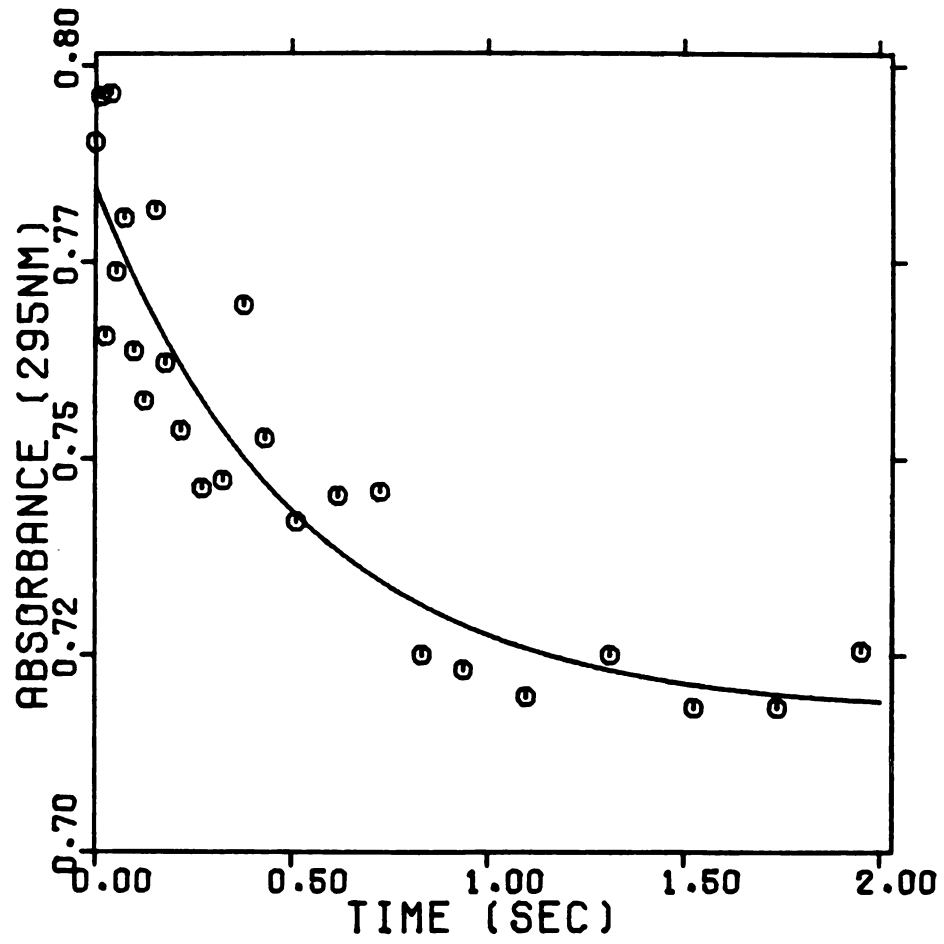


FIGURE 6A

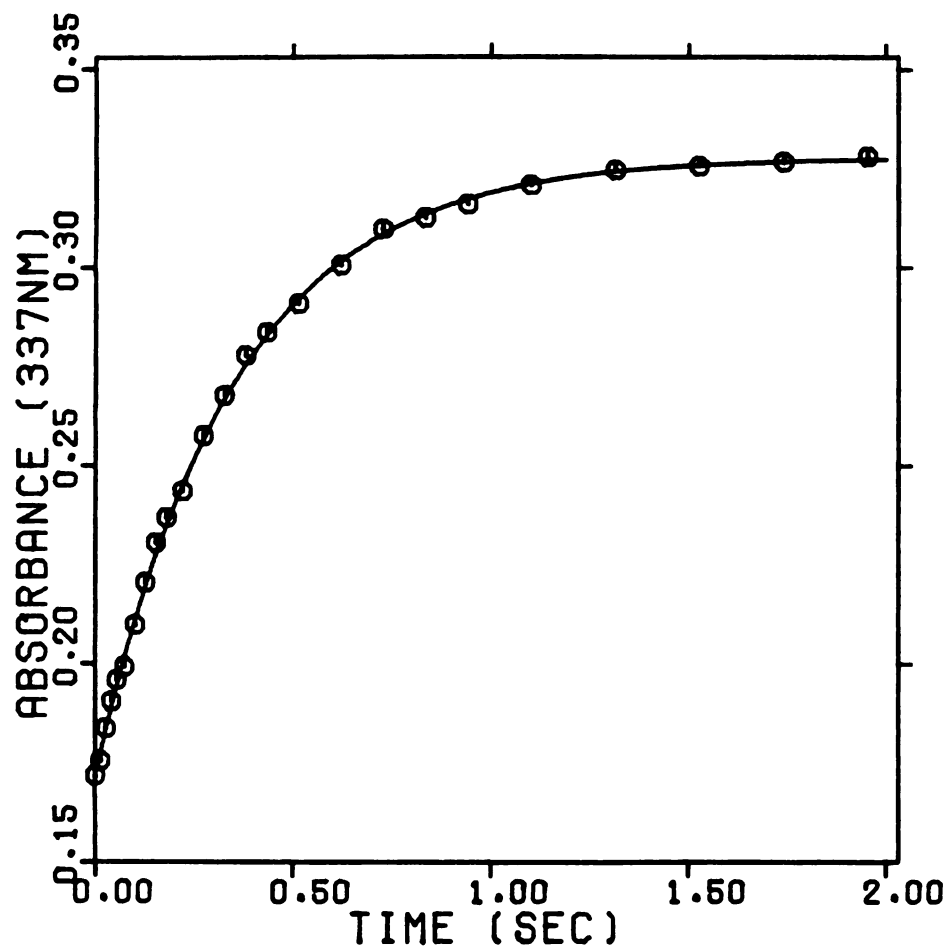


FIGURE 6B

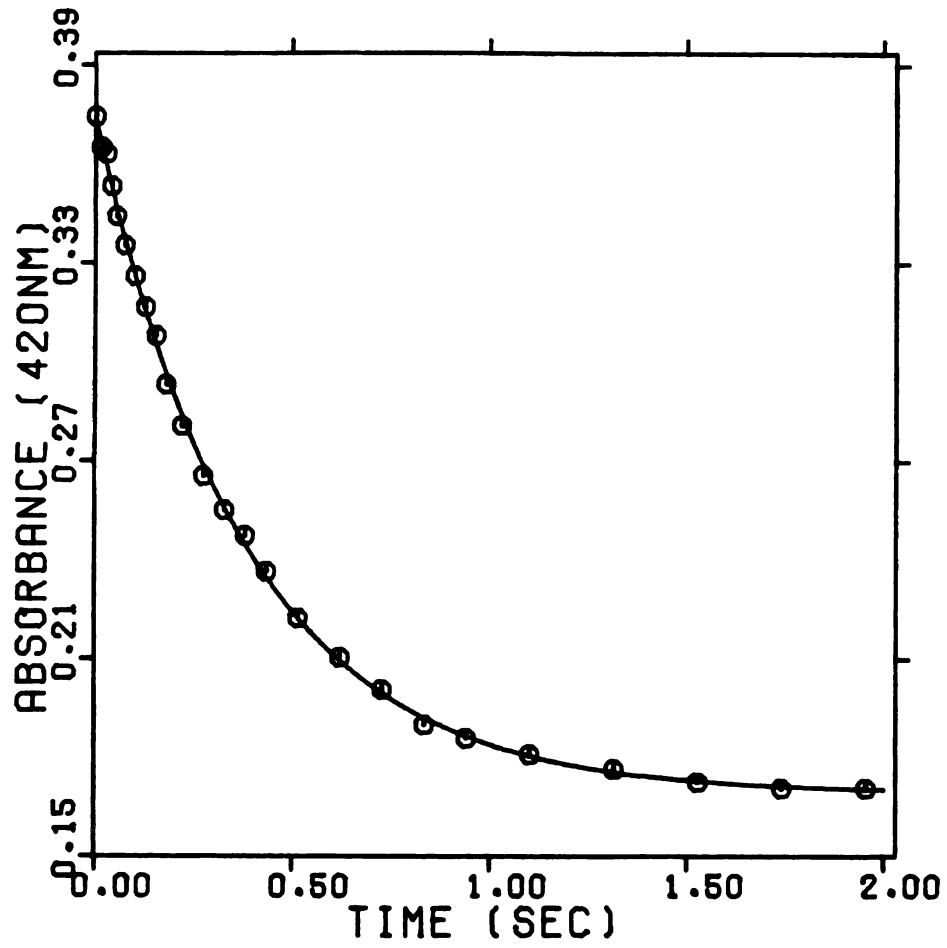


FIGURE 6C

Slow First Order Processes - The Third Phase - Incremental pH Jump Experiments - Figure 7A shows the time dependence of the changes in spectra which occur in the so-called slow first order process following a sudden increase in pH from 7.00 to 9.33. These changes involve growth at ~355 nm with concomitant decays centered at ~325 nm and ~430 nm. Similar changes were observed at the four other final pH values. The absorbance vs. time data at the above three wavelengths were fitted to equation 2 to obtain values for A^∞ , ΔA and k_2' , the apparent first order rate constant for the slow phase.

The rate of the slow third phase, k_2' , was independent of wavelength and pH and gave an average value of $0.064 \pm 0.005 \text{ sec}^{-1}$ for five determinations at 355 nm and 420 nm. The data at ~325 nm were somewhat noisier than data collected at higher wavelengths and consequently the analysis was less successful at this wavelength. Table II lists the values for A^∞ , ΔA and k_2' for the incremental pH jumps. Analysis of the change in absorbance at 355 nm as a function of pH using equation 1 in KINFIT yielded a pK_a' value of 8.10 ± 0.06 (Figure 8). Thus, this slow process exhibits essentially the same pH dependence as the fast interconversion of the 420 nm and 337 nm forms of the enzyme in the pH jump and drop experiments.

Figure 7. Spectral changes occurring during the slow first order process following a rapid change in pH. These difference spectra were obtained by subtracting the spectrum collected after the fast first order changes were essentially complete, but before the slow first order process had begun, from the last spectrum collected. A) A pH jump from 7.00 to 9.33; B) A pH drop from 8.70 to 6.54.

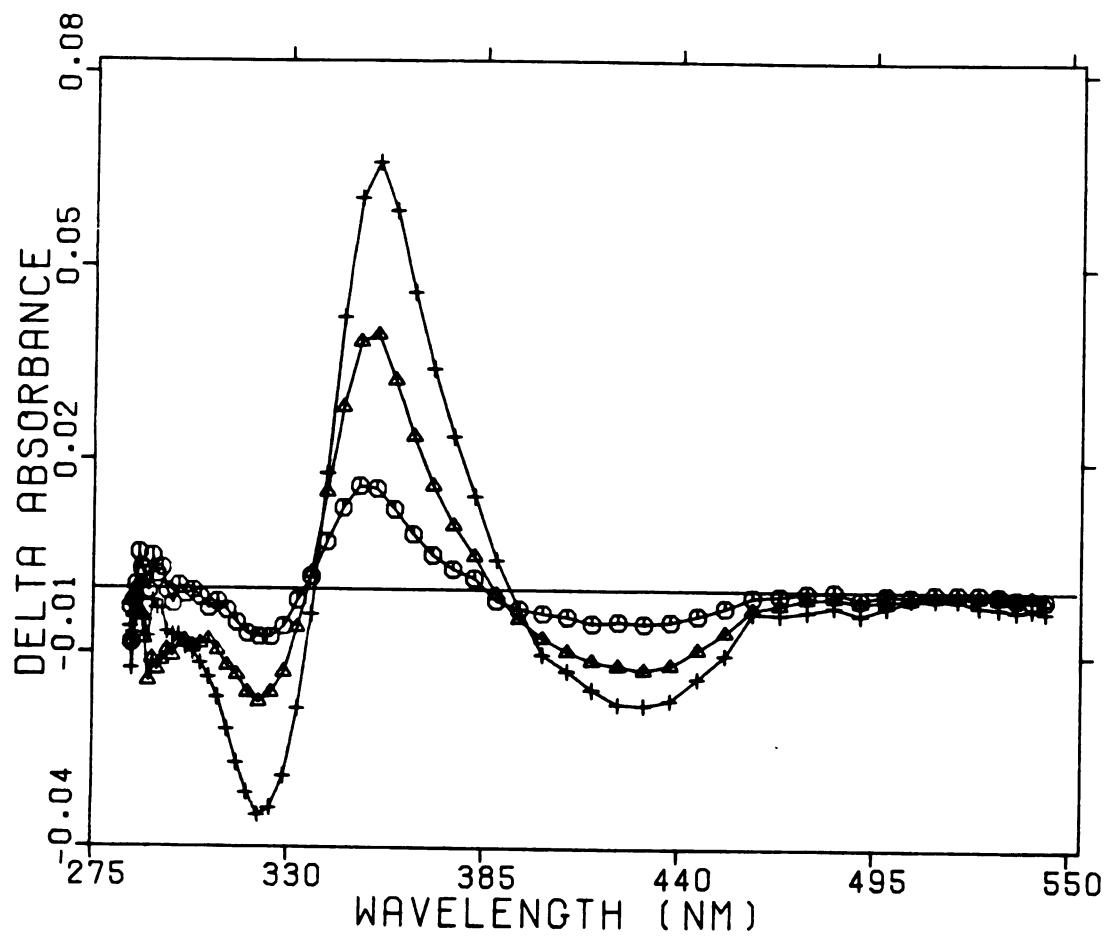


FIGURE 7A

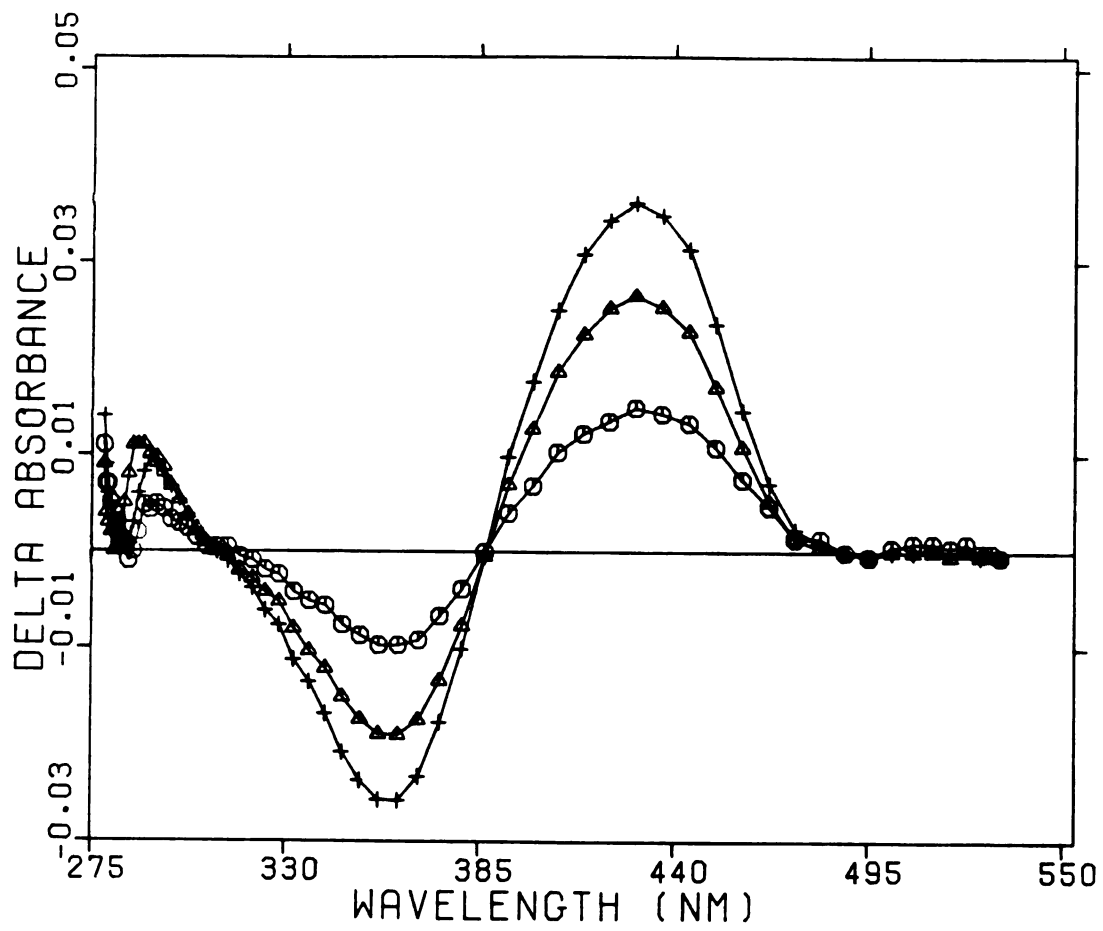


FIGURE 7B

Table II: Kinetic parameters for the slow first order process in the incremental pH jump experiments. These parameters were obtained by fitting the changes in absorbance at each wavelength to equation 2.

Final pH	Wave-length (nm)	A_{∞}	ΔA	k_2' (sec ⁻¹)
9.33	325	0.279 ± 0.002	0.040 ± 0.003	0.042 ± 0.005
	355	0.270 ± 0.003	0.082 ± 0.001	0.058 ± 0.002
	430	0.146 ± 0.003	0.024 ± 0.001	0.068 ± 0.013
8.90	325	0.268 ± 0.003	0.025 ± 0.004	0.043 ± 0.008
	355	0.265 ± 0.004	0.076 ± 0.001	0.062 ± 0.003
	430	0.174 ± 0.002	0.039 ± 0.002	0.068 ± 0.006
8.56	325	0.254 ± 0.003	0.013 ± 0.003	0.029 ± 0.015
	355	0.252 ± 0.002	0.065 ± 0.001	0.065 ± 0.002
	430	0.213 ± 0.002	0.048 ± 0.001	0.066 ± 0.001
8.07	355	0.225 ± 0.003	0.037 ± 0.001	0.062 ± 0.002
	430	0.287 ± 0.005	0.040 ± 0.005	0.062 ± 0.009
7.69	355	0.207 ± 0.001	0.018 ± 0.001	0.073 ± 0.006
	430	0.340 ± 0.003	0.023 ± 0.001	0.060 ± 0.009

Figure 8. The change in absorbance at 355 nm as a function of pH observed in the slow first order process in the incremental pH jump experiments. The line was calculated using equation 1 with a pK value of 8.10.

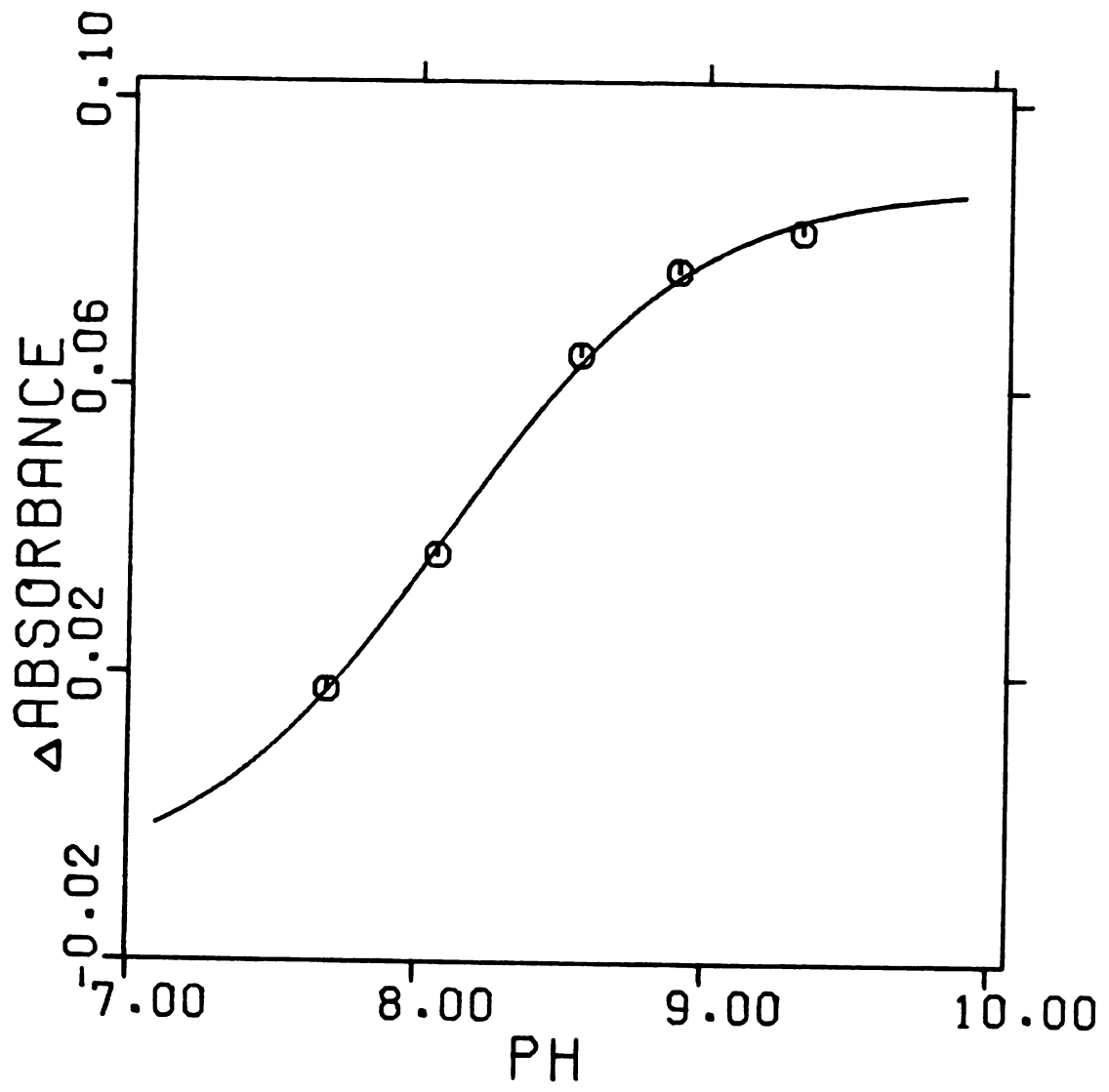


FIGURE 8

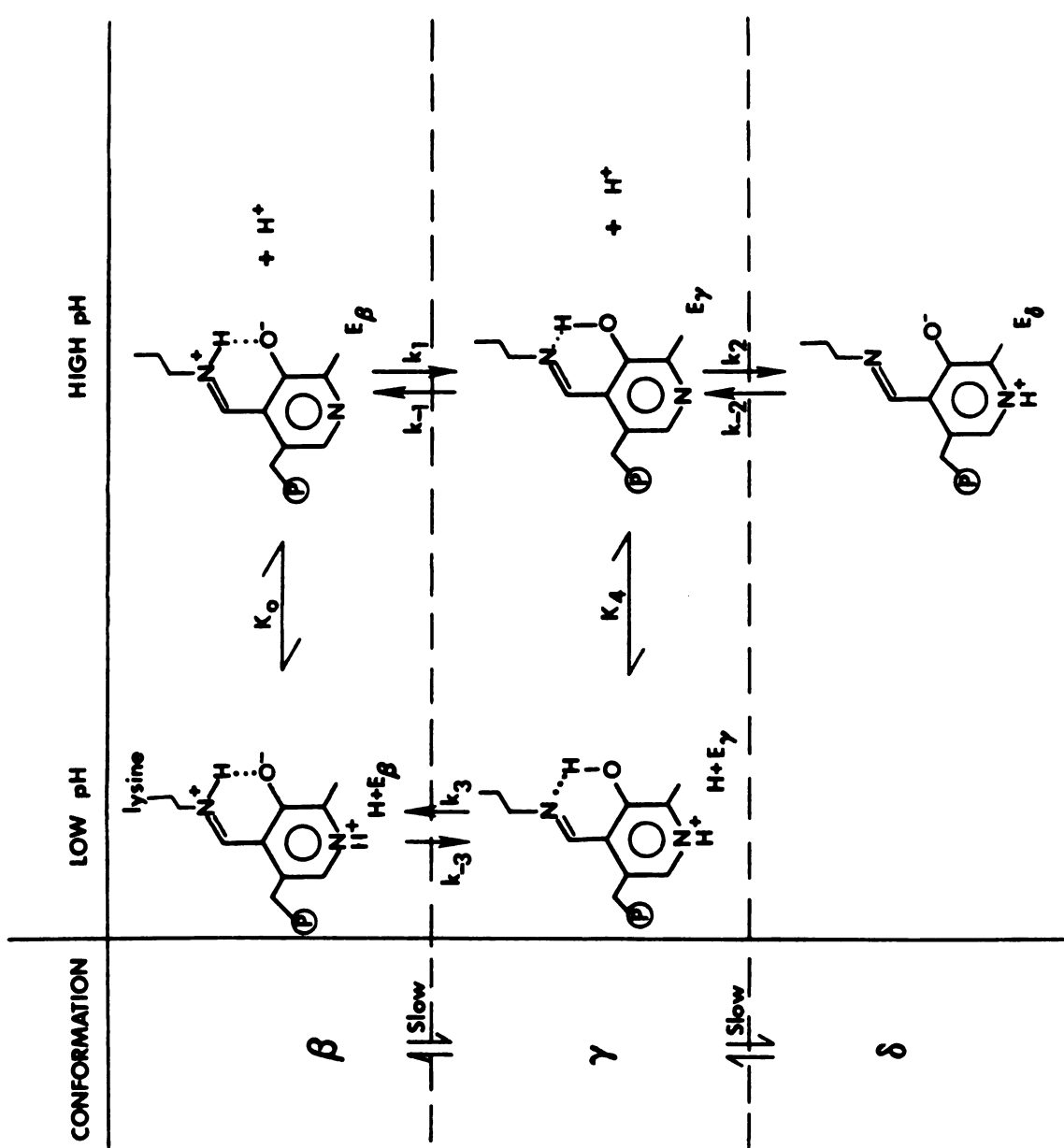
Incremental pH Drop Experiments - Changes in Spectra

which occur during the slow first order process following a drop in pH from 8.70 to 6.54 (Figure 7B) involve a decay at ~355 nm and growths at ~430 nm and ~290 nm. These changes are essentially the same as those observed at the other five final pH values. The growth at 290 nm, however, becomes negligible as the extent of the pH drop becomes smaller.

The values of k_2' , for the pH drop from 8.70 to 6.54 were $0.009 \pm 0.004 \text{ sec}^{-1}$ and $0.008 \pm 0.001 \text{ sec}^{-1}$ at 355 nm and 430 nm respectively. The rate constants are just estimates since the data were collected for less than two half times. This made it impossible to obtain a reliable value of A_∞ so that the apparent pKa for the conversion of the 355 nm absorbance to that at 430 nm could not be obtained.

Interpretation of Experimental Results and Discussion -

The experimental data presented above were analyzed in terms of the kinetic model outlined in Scheme I. This scheme assumes that the enzyme can exist in at least three conformations and that interconversion between these forms is a relatively slow process on the stopped flow time scale. In addition, each of these enzyme conformations has associated with it forms of pyridoxal-P which exhibit different absorption maxima. For example, conformation β contains forms of



SCHEME I

the coenzyme which absorb at ~420 nm while conformations γ and δ have forms that absorb at ~337 nm and ~360 nm, respectively. The structures giving rise to these various absorptions are known from both model studies and studies on other pyridoxal-P dependent enzymes (10).

In two of the three conformations, namely β and γ , the forms of the coenzyme within each conformational manifold appear to differ only by their state of protonation at the pyridinium nitrogen. Protonation at this site does not greatly alter the location of the absorption maxima of pyridoxal-P Schiff's bases although the extinction coefficient may vary somewhat (10). Thus both H^+E_β and E_β would be expected to show an absorption maximum at ~420 nm, while the H^+E_γ and E_γ absorption would be centered at ~337 nm. E_δ , which absorbs at ~355 nm, appears to be essentially the form of the coenzyme which is associated with activity in aspartate aminotransferase (11). This is also approximately the wavelength associated with the maximal rate of photoinactivation of tryptophanase, (12) and thus E_δ may play a role in this process.

The abrupt changes presumably reflect protonations or deprotonations occurring within conformation manifolds. According to Scheme I these abrupt changes would involve protonation or deprotonation at the pyridinium nitrogen. The fast and slow first order processes would then reflect

conversions between conformations. The fast process involves the 420 nm and 337 nm absorption bands and reflects conversions between conformations β and γ . The slow process which shows absorption changes at ~ 325 nm, ~ 355 nm and ~ 430 nm in the pH jumps and at ~ 355 nm and ~ 430 nm in the pH drops involves all three conformations.

If we assume that the fast first order process involves conformations β and γ as well as the four structures of pyridoxal-P therein, we can obtain an expression for the apparent first order rate of appearance or disappearance of the 420 nm or 337 nm absorbance (see Appendix A, part A, for derivation):

$$k_1' = \frac{(k_{-1}K_4/[H^+] + k_3)}{(1 + K_4/[H^+])} + \frac{(K_0/K_4)(k_1/k_{-1})k_3 + (k_1K_0/[H^+])}{(1 + K_0/[H^+])} \quad (3)$$

The rate and equilibrium constants are defined in Scheme I. The parameters obtained from a fit to equation 3 of the apparent first order rate constants at 337 nm and 420 nm as a function of pH for both the pH jump and drop experiments are $pK_0 = 9.5 \pm 0.1$, $pK_4 = 6.2 \pm 0.3$, $k_1 = 6.3 \pm 0.9 \text{ sec}^{-1}$, $k_{-1} = 0.23 \pm 0.02 \text{ sec}^{-1}$, $k_3 = 1.1 \pm 0.3 \text{ sec}^{-1}$, $k_{-3} = 0.015 \pm 0.004 \text{ sec}^{-1}$. The theoretical curve through the experimental values for k_1' in Figure 9 was drawn using these parameters. If we ignore conformation δ , which is always formed to a small extent even at high pH values, the percentage of

Figure 9. Variation of the apparent first order rate constant for the fast first order interconversion of 420 nm and 337 nm absorptions in the incremental pH jump and drop experiments. The apparent first order rate constant was determined at 337 nm and 420 nm for each individual push. Each symbol on the graph represents the average of three pushes. Incremental pH jump experiments; k_1' from 337 nm data (O), k_1' from 420 nm data (Δ). Incremental pH drop experiments; k_1' from 337 nm data (+), k_1' from 420 nm data (\diamond). The line was calculated using equation 4 with the parameters listed in the text.

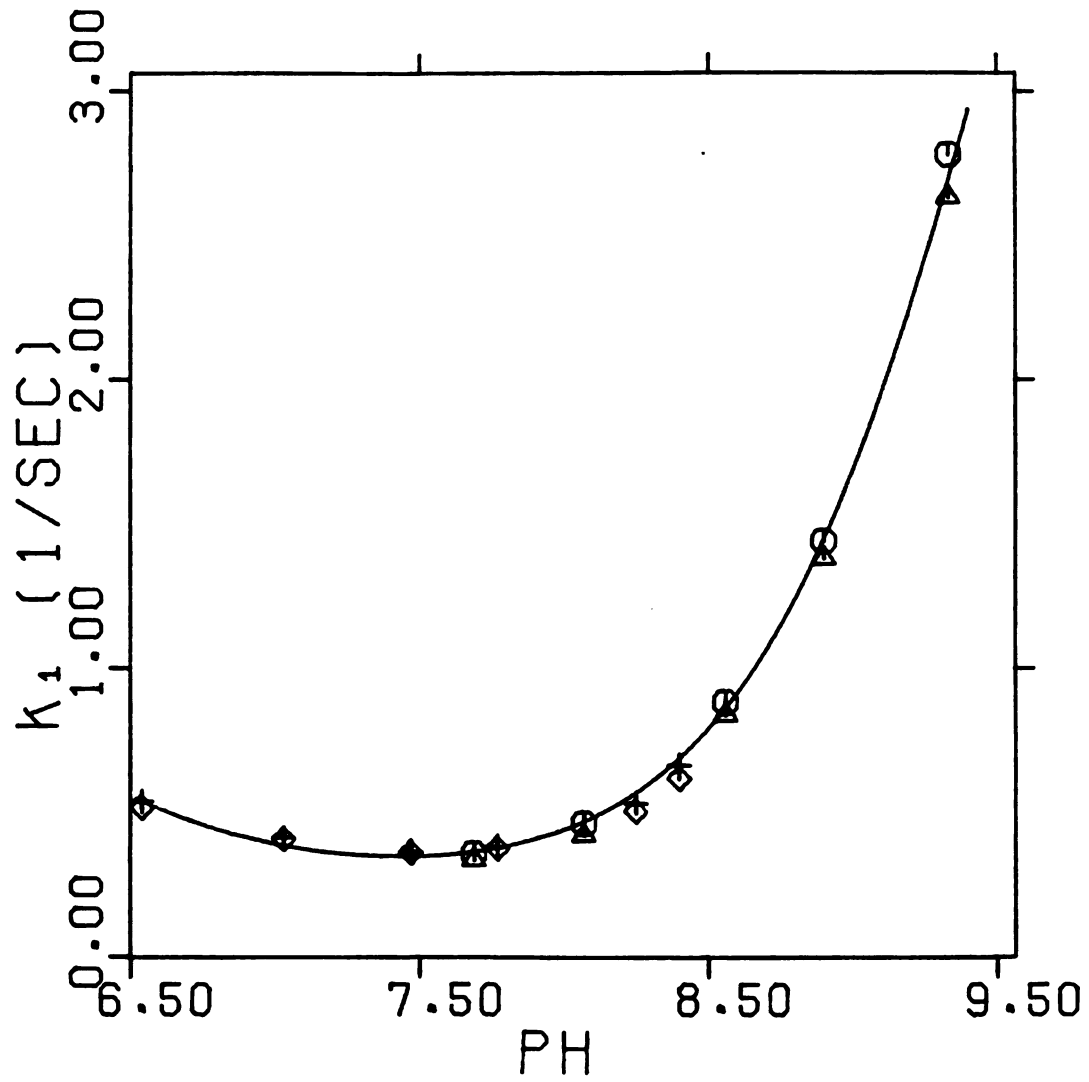


Figure 9

enzyme in each of the forms H^+E_β , E_β , H^+E_γ and E_γ can be calculated with the parameters obtained with equation 3. Table III which lists the percentages of these four species at three pH values reveals that E_β and H^+E_γ are always relatively minor components. H^+E_β and E_γ make the largest contribution to the absorbance at 420 nm and 337 nm, respectively. The distribution between these two absorption bands at a given pH value depends on the effective pKa, $p[K_0(k_1/k_{-1})] = 8.1$. This effective pKa is in close agreement with the value of 8.3 obtained by equilibrium titrations for the pH dependent interconversion of the 420 nm to 337 nm absorption in 0.2 M KCl. This close agreement between equilibrium and kinetic results supports our contention that at any given pH most of the enzyme is in the forms H^+E_β and E_γ . Thus, changes in these forms dominate the equilibrium spectrum.

Table III: The percentages of total enzyme that exists in each of the four forms H^+E_β , E_β , H^+E_γ and E_γ at three pH values.

pH	% H^+E_β	% E_β	% H^+E_γ	% E_γ
7.00	91.	.27	1.2	7.3
8.00	54.	1.6	.72	44.
9.00	11.	3.2	.14	86.

As mentioned previously, the abrupt spectral changes observed in the pH jump and drop experiments (Figure 2) are complex and cannot be interpreted in terms of one or two ionizing groups. However, it is interesting to note that the titration curves obtained by plotting the change in absorbance at 295 nm vs. pH for the pH jumps (Figure 3A) and the pH drops (Figure 3B) reveal pKa' values of approximately 9.6 and 6.3, respectively. There is also an indication of a higher pKa of uncertain value in the pH drop experiments (Figure 3B). Although these pKa' values are not well determined, the values of 9.6 and 6.3 are consistent with the values obtained by analysis of the more reliable kinetic data to give 9.5 and 6.2 for pK_0 and pK_4 , respectively. Thus, the change in absorption at 295 nm, as well as other features in the abrupt difference spectra may arise as a result of protonation of E_γ in the case of a pH drop or deprotonation of H^+E_β in the case of a pH jump, at the pyridinium nitrogen.

Figure 10 shows the absorption spectra of the pyridoxal-P valine Schiff's base forms H_2PL , HPL, and PL which correspond to H^+E_β , E_γ and E_δ respectively. H_2PL and HPL have similar spectra with peaks at ~413 nm and ~280 nm.

Figure 11 is the difference spectrum that results when the H_2PL spectrum is subtracted from the HPL spectrum. This corresponds to the difference spectrum obtained during the

Figure 10. Absorption spectra of various ionic forms of pyridoxal-P. H₂PL (O), HPL (Δ), PL (+). Spectra were kindly supplied by Prof. D. E. Metzler, Iowa State University.

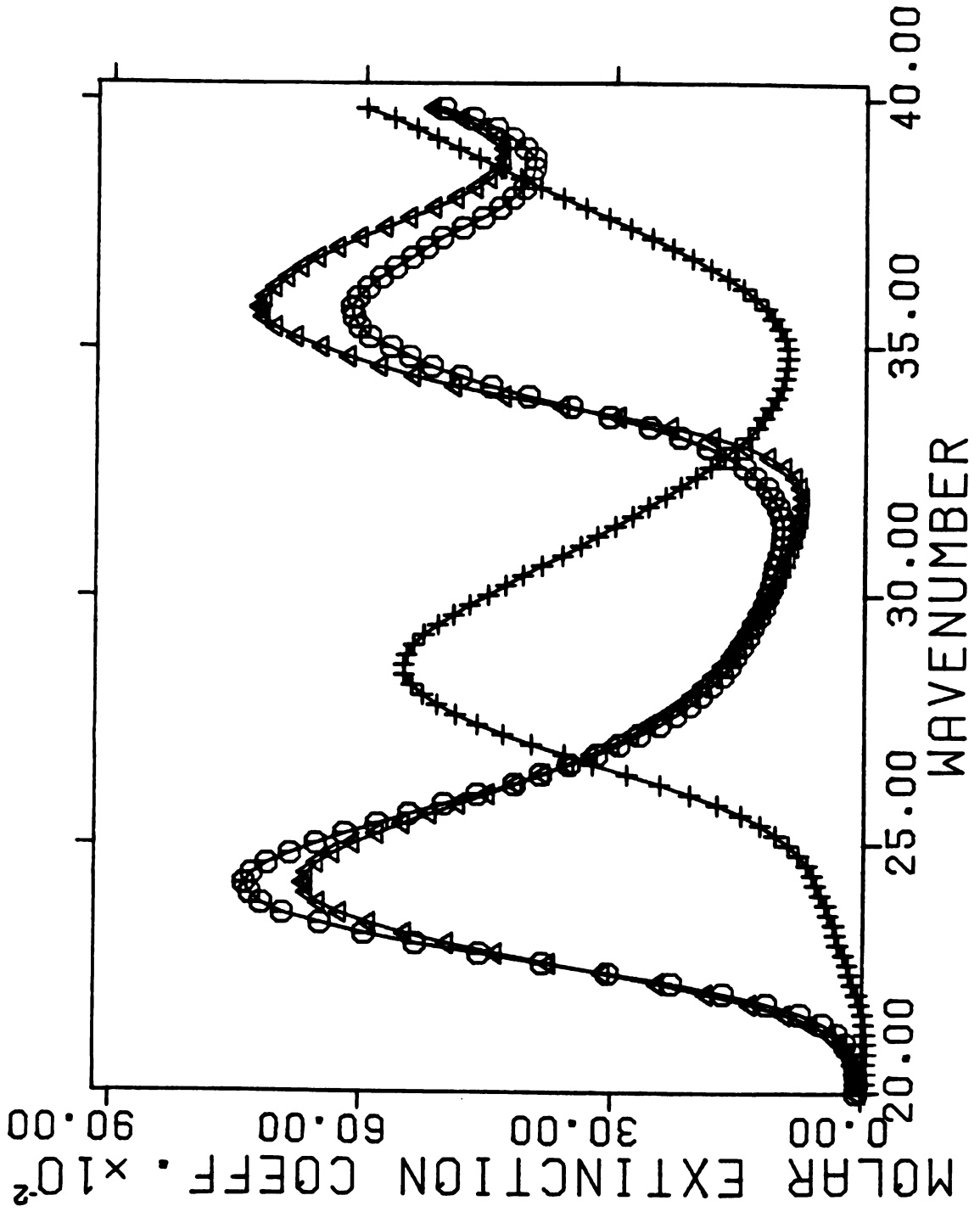


FIGURE 10

Figure 11. Difference spectrum obtained by subtracting the H₂PL spectrum from the HPL spectrum, both given in Figure 10.

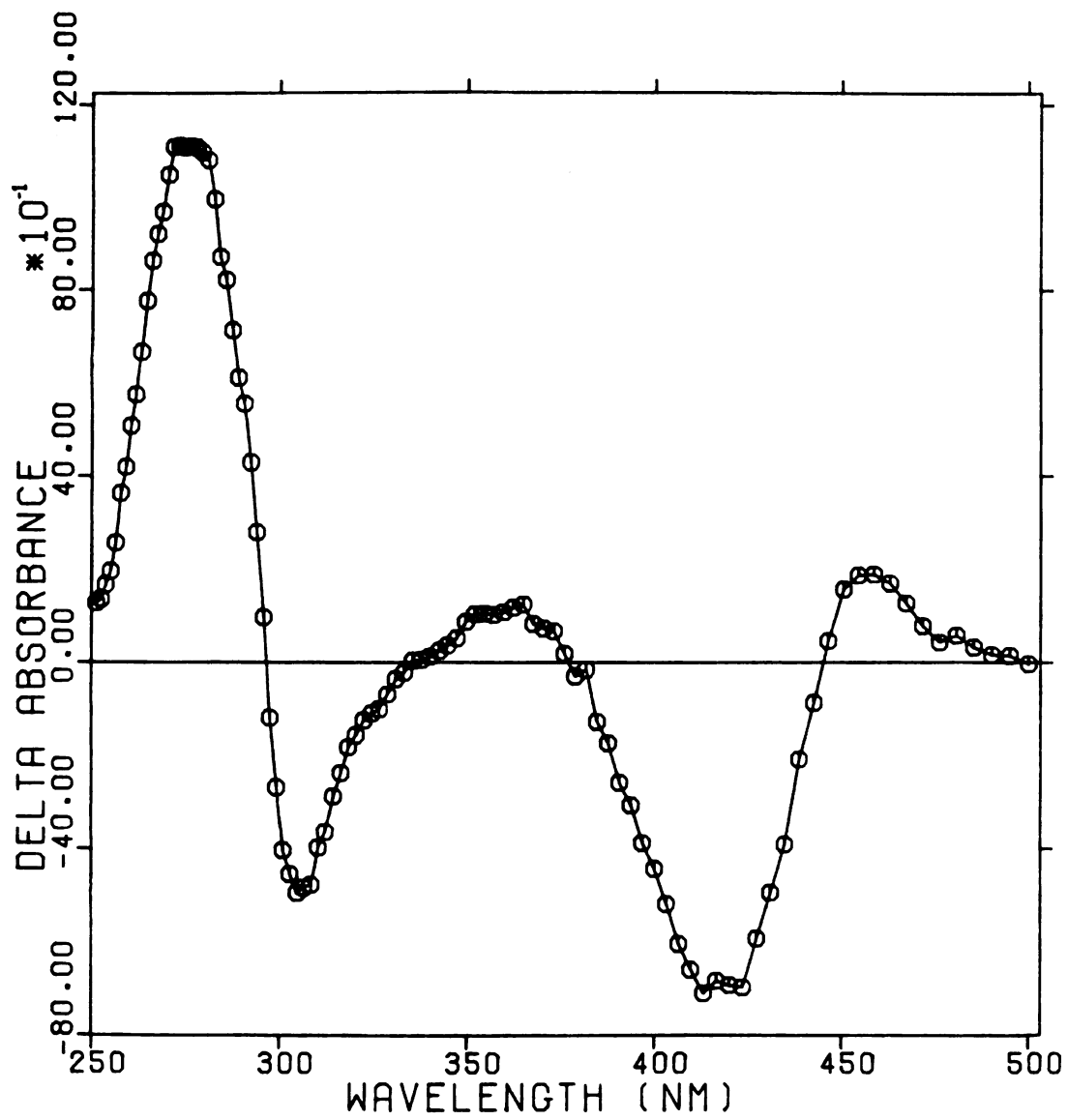


FIGURE 11

during the abrupt changes of a pH jump with tryptophanase. A comparison of Figure 11 with Figures 2A and B reveals definite similarities in spectral shapes in support of our argument that deprotonation at the ring nitrogen contributes to these difference spectra. Figures 2C and D are essentially the reverse of Figure 11 in the sense that these would represent a protonation at the pyridinium nitrogen. The discrepancies between wavelength maxima for difference peaks and valleys between Figures 2 and 11 may arise as a result of the differing environments of the pyridoxal-P imine in tryptophanase and the model compound. The changes at 295 nm, on the other hand, could reflect a rapid change in the environment of one or more enzyme tryptophan residues since this is the wavelength of maximum difference for tryptophan perturbations (13). This interpretation would be consistent with the results of Tokushige *et al.* (14) who suggest that there is a tryptophyl residue at the active site of tryptophanase in close proximity to the coenzyme moiety, which is necessary for catalytic activity and pyridoxal-P binding. This tryptophyl residue may be very sensitive to slight perturbations caused by changes in the conformation or the change distribution of the bound coenzyme. Regardless of which mechanism pertains, the change centered at 295 nm is the most constant feature in the abrupt difference spectra for the pH jumps and drops

and appears to reflect the pKa values obtained in the kinetic analysis. Spectral changes at 295 nm may be the most sensitive probe for the state of protonation at the pyridinium nitrogen of the bound pyridoxal-P of tryptophanase.

The addition of the conformation manifold δ , containing the species E_δ serves to rationalize the changes seen in the incremental pH jump and drop experiments during the slow first order process. For example, in the pH jump experiments there is an increase in absorbance at approximately 355 nm corresponding to the formation of E_δ . The decreases in absorbance at ~430 nm and ~325 nm which occur at the same rate as the appearance of 355 nm absorbance correspond to the conversion of H^+E_β and E_γ , respectively, into E_δ . The rate constants obtained for the interconversion of the β and γ manifolds show that these steps are fast enough to remain at equilibrium during the formation of the δ conformation. This is the explanation of why the first order rates are the same at these three wavelengths.

In the case of the pH drop experiments there was a decrease in absorbance at ~355 nm with a concomitant increase at ~430 nm. These changes would correspond to the disappearance of E_δ and the appearance of H^+E_β , respectively. Absorbance at ~325 nm would not be expected

to build up according to the proposed mechanism because as soon as E_γ is formed from E_δ it rapidly forms H^+E_β at a rate which is much faster than the rate of conversion of E_δ to E_γ .

A derivation (see Appendix A, part B) of the rate of change of E_δ as a function of time for the above mechanism gives the following equation for the apparent first order rate constant for the appearance or disappearance of E_δ at any final pH:

$$k_2' = \frac{k_2}{(1 + K_1 + [H^+]/K_0K_1 + [H^+]/K_0K_1K_3)} + k_{-2}$$

Although the value of K_2 , the equilibrium constant for the formation of E_δ from E_γ , is not known, it must be less than one because E_δ is not formed to any great extent even at pH 9.33 where most of the enzyme is in the form of E_γ . Since $K_2 = k_2/k_{-2}$, this implies that k_2 is then less than k_{-2} . Substituting the known values of K_0 , K_1 and K_3 of $2.95E-10M$, 27.2 and 73.3 respectively, into equation 4 reveals that the contribution of the terms $(H^+)/K_0K_1$ and $(H^+)/K_0K_1K_3$ in the denominator, through which any pH dependence is expressed, is small at all pH values studied in the pH jump experiments compared to 28.2, the sum of $1 + K_1$. This, coupled to the fact that k_2 is small in comparison to k_{-2} gives rise to the observed pH independence of k_2' as a function of pH in the incremental pH jump experiments.

It should be pointed out that this derivation does not explain the 7.5-fold difference between k_2' observed in the pH jump and drop experiments. In a somewhat related study on the pyridoxal-P dependent enzyme glutamate decarboxylase (15) O'Leary and Brummund observed that the rate of conversion of a species absorbing at 420 nm following a rapid decrease in pH was affected by the nature and concentration of the buffer used. It is conceivable that the rate of interconversion of the γ and δ conformation manifolds is also sensitive to buffer effects. Additional experimentation under various buffer conditions will be required to resolve this discrepancy.

The increase in absorbance at ~295 nm during the slow phase at the lowest pH values may be indicative of yet another group on the enzyme with a very low pK_a' or further perturbation of tryptophan residues. Essentially no information is available about this process, however, due to enzyme instability at low pH values.

REFERENCES

1. Snell, E. E., (1975) Adv. Enzymol. Relat. Areas Mol. Biol. 42, 287-333.
2. Morino, Y., and Snell, E. E. (1967) J. Biol. Chem. 242, 5591-5601.
3. Suelter, C. H., Wang, J., and Snell, E. E. (1976) FEBS Lett. 66, 230-232.
4. June, D. S., Kennedy, B., Pierce, T. H., Elias, S. V., Halaka, F., Behbahani, Nejad, I., El-Bayoumi, A., Suelter, C. H., and Dye, J. L., (1979) J. Amer. Chem. Soc. 101, 2218-2219.
5. Högberg-Raibaud, A., Raibaud, O., and Goldberg, M. E. (1975) J. Biol. Chem. 250, 3352-3358.
6. Coolen, R. B., Papadakis, N., Avery, J., Enke, C. G., and Dye, J. L. (1975) Anal. Chem. 47, 1649-1655.
7. Papadakis, N., Coolen, R. B., and Dye, J. L. (1975) Anal. Chem. 47, 1644-1649.
8. Suelter, C. H., Coolen, R. B. and Dye, J. L. (1975) Anal. Biochem. 69, 155-163.
9. Dye, J. L., and Nicely, V. A. (1971) J. Chem. Ed. 48, 443-448.
10. Johnson, R. J., and Metzler, D. E. (1970) Methods Enzymol. 18A, 433-471.
11. Ivanov, V. I., and Karpeisky, M. Ya. (1969) Adv. Enzymol. Relat. Areas Mol. Biol. 32, 21-53.
12. Coetzee, W. F., and Pollard, E. C. (1975) Photochem. and Photobiol. 22, 29-32.
13. Kayne, F. J., and Suelter, C. H. (1965) J. Amer. Chem. Soc. 87, 987-900.
14. Tokushige, M., Fukada, Y., and Watanabe, Y. (1979) Biochem. Biophys. Res. Comm. 86, 976-981.

References - continued

15. O'Leary, M. H., and Brummund, W. (1974) J. Biol. Chem. 249, 3737-3745.
16. Suelter, C. H., Wang, J., and Snell, E. E. (1977) Anal. Biochem. 76, 221-232.

SECTION IV
SCANNING STOPPED FLOW STUDIES ON THE MECHANISM OF QUINONOID
FORMATION WITH TRYPTOPHANASE USING
COMPETITIVE INHIBITORS

An absorption band centered around 500 nm appears following addition of certain amino acid inhibitors to several pyridoxal-P dependent enzymes (1 - 6). This band has been attributed to a quinonoid complex at the enzyme active site formed by the loss of a leaving group from the α -carbon of the amino acid-pyridoxal-P Schiff's base (7). Morino and Snell (3) demonstrated that a stable, dead-end quinoid complex, characterized by an intense absorption band centered at 502 nm was produced when the competitive inhibitor, L-alanine, interacted with tryptophanase and that the α -proton of alanine was labilized in the process. Watanabe and Snell (8) later identified a number of inhibitors that formed quinonoid derivatives with tryptophanase.

The formation of the tryptophanase-quinonoid complex with ethionine has an absolute requirement for monovalent cations (9). Suelter and Snell showed that in the absence of cations, ethionine interacted with the enzyme, presumably forming a Schiff's base with coenzyme, but was unable to proceed to quinonoid until KCl was added.

The purpose of this study was to examine the transient kinetics of quinonoid production with inhibitors in an attempt to gain insight into the mechanism of tryptophanase catalysis up to and including α -proton abstraction. Specifically, this paper describes the results of stopped flow

studies of the kinetics of formation of the quinonoid derivative with L-ethionine and L-alanine. The effects of pH, concentration of inhibitor, differing monovalent cations, and the substitution of deuterium at the α -position of alanine on this reaction are reported. These observations are integrated with previous results into a simple mechanism of tryptophanase catalysis.

MATERIALS AND METHODS

Materials - KCl and NH_4Cl were Mallinckrodt, analytical reagents. CsCl and RbCl were obtained from Ventron, Danvers, Mass. as ultrapure products. Pyridoxal-5'-phosphate, L-alanine, DL-dithiothreitol (DTT), and N-2-hydroxyethyl-piperazine propane sulfonic acid (Epps) were obtained from Sigma Chemical Co. L-ethionine was from Vega Biochemicals and L- $[\alpha\text{-}^2\text{H}]$ alanine was purchased from Merck and Co., Inc., Rahway, N.J. $(\text{CH}_3)_4\text{NCl}$ from Aldrich Chemical Co. was recrystallized from isopropyl alcohol before use. $(\text{CH}_3)_4\text{NOH}$ was prepared fresh before use by passage of recrystallized $(\text{CH}_3)_4\text{NCl}$ over Dowex-1-OH.

Tryptophanase - Tryptophanase was prepared according to the method of Suelter *et al.* (10). Stock apoenzyme was activated by incubation for one hour at 37°C in 0.1 M potassium phosphate, pH 8.0, 1 mM EDTA, 7% $(\text{NH}_4)_2\text{SO}_4$,

0.2 mM pyridoxal-P and 20 mM DTT. Unless otherwise indicated, the enzyme had a specific activity of 50 - 55 $\mu\text{mol min}^{-1} \text{mg}^{-1}$ when assayed at 30° C with 0.6 mM S-orthonitrophenyl-L-cysteine (SOPC) in 50 mM potassium phosphate, pH 8.0, and 50 mM KCl (11). Protein concentration was determined spectrophotometrically using $\epsilon = 0.795 \text{ ml mg}^{-1} \text{cm}^{-1}$ (12).

Scanning Stopped Flow Experiments - These experiments were completed with a computerized double beam rapid scanning stopped flow instrument described elsewhere (13, 14) at $24.0 \pm 0.1^\circ \text{C}$ using a 1.85 cm path length. Scanning data were collected using an averaging scheme previously described (15) at a rate of 150 spectra per second over the wavelength range 280 nm - 600 nm. Control spectra were collected as outlined previously (16). Experimental conditions for individual experiments are described below.

Tryptophanase vs. L-ethionine and L-alanine - Activated holotryptophanase ($\sim 20 \text{ mg ml}^{-1}$) was equilibrated by dialysis at 4° C with 25 mM K-Epps, pH 8.0, 0.1 M KCl, 1 mM EDTA, 0.1 mM pyridoxal-P, 0.2 mM DTT and diluted to a concentration of 1.4 mg ml^{-1} with the same buffer. This enzyme solution was pushed against various concentrations of L-ethionine and L-alanine in 25 mM K-Epps, pH 8.0, 0.1 M KCl.

For the data presented in Figures 1, 3 and 5 holotryptophanase was equilibrated with 25 mM K-Epps, pH 8.0, 0.2 M KCl, 1 mM EDTA, 10 μ M pyridoxal-P, 0.2 mM DTT and then diluted to a concentration of 2.0 mg ml⁻¹ before being pushed against 20 mM L-ethionine in the same buffer.

Tryptophanase vs. L-[α -¹H]alanine and L-[α -²H]alanine - Activated holotryptophanase (~20 mg ml⁻¹) was equilibrated by dialysis at 4° C with 25 mM K-Epps, pH 8.0, 0.1 M KCl, 1 mM EDTA, 0.1 mM pyridoxal-P and 0.2 mM DTT and diluted to a concentration of 1.8 mg ml⁻¹. This enzyme solution was pushed against 25 mM K-Epps, pH 8.0, 0.1 M KCl, 1 mM EDTA, 0.1 mM pyridoxal-P containing 0.45 M L-[α -¹H]alanine or L-[α -²H]alanine.

Tryptophanase vs. L-ethionine at three pH values - Activated holotryptophanase (~20 mg ml⁻¹) was equilibrated by dialysis at 4° C with 25 mM K-Epps, pH 8.0, 0.1 M KCl, 1 mM EDTA, 0.1 mM pyridoxal-P and 0.2 mM DTT. The enzyme was divided into three equal volumes at a concentration of 1.6 mg ml⁻¹. These three solutions were adjusted to pH values of 7.2, 8.0 and 8.7, with 0.1 M HCl or 0.1 M KOH at 24° C and pushed against 25 mM K-Epps, 0.1 M KCl and 10 mM L-ethionine at a pH of 7.2, 8.0 or 8.7.

Tryptophanase-ethionine complex (minus cations) vs. NH₄Cl, KCl, RbCl and CsCl - Activated holotryptophanase (~25 mg ml⁻¹) was dialyzed at 4° C against 25 mM (CH₃)₄N-Epps, pH 8.0, 0.2 mM pyridoxal-P, 0.2 mM DTT and 1 mM

$[(\text{CH}_3)_4\text{N}]_2\text{-EDTA}$ to remove activating cations. After this treatment the enzyme had a specific activity of $30 \mu\text{mol min}^{-1} \text{mg}^{-1}$ when assayed as described above with SOPC at 30°C .

The enzyme was diluted with the above buffer containing 10 mM L-ethionine to a concentration of 1.9 mg ml^{-1} . This solution was pushed against 25 mM $(\text{CH}_3)_4\text{N-Epps}$, pH 8.0, containing 0.05 M NH_4Cl , 0.2 M KCl , 0.5 M RbCl or 1.0 M CsCl . No attempt was made to control ionic strength due to the lack of a suitable non-activating salt [$(\text{CH}_3)_4\text{NCl}$ is known to inhibit tryptophanase at concentrations greater than 50 mM (9)].

Data Analysis - Data were fitted to the appropriate mathematical function using the nonlinear curve fitting program KINFIT (17). Errors listed are marginal standard deviations.

All single exponential data were fitted to equation 1

$$A_t = A_\infty \pm \Delta A e^{-k_1' t} \quad (1)$$

where A_∞ , the absorbance at infinite time, ΔA , the total change in absorbance [i.e. $(A_\infty - A_0)$ where A_0 equals the absorbance at $t = 0$] and k_1' , the apparent first order rate constant, were the three adjustable parameters.

Biphasic data were analyzed as the sum of two exponential growths according to equation 2

$$A_t = A_\infty - \Delta A_1(e^{-k_1't}) - \Delta A_2(e^{-k_2't}) \quad (2)$$

where A_∞ is the absorbance at infinite time, ΔA_1 and ΔA_2 are the total changes in absorbance due to the fast and slow phases, respectively, and k_1' and k_2' are the apparent first order rate constants for the fast and slow phases.

pH Measurements - pH values were determined with a Beckman Model 4500 digital pH meter at 24° C.

RESULTS

The first studies to be described were designed to investigate the interaction of the dead-end inhibitors, alanine and ethionine, with tryptophanase on the stopped flow time scale. Digitized data, which were collected with the rapid scanning stopped flow device (13, 14, 15) and stored on floppy disk, were displayed on a cathode ray tube for visual inspection. Figure 1 is a photograph of this display showing a composite of 55 spectra collected over a 65 second time period during the reaction between tryptophanase and ethionine. Spectra displayed in this fashion (absorbance vs. wavelength) point out the existence of channels which are themselves composed of absorbance vs. time data at a particular wavelength.

Figure 1. Tryptophanase spectra collected as a function of time after mixing with ethionine at 24° C in 25 mM K-Epps, pH 8.0, 0.2 M KCl, 1 mM EDTA, 10 µM pyridoxal-P, 0.2 mM DTT. After mixing: 10 mM ethionine and 1.0 mg ml⁻¹tryptophanase.

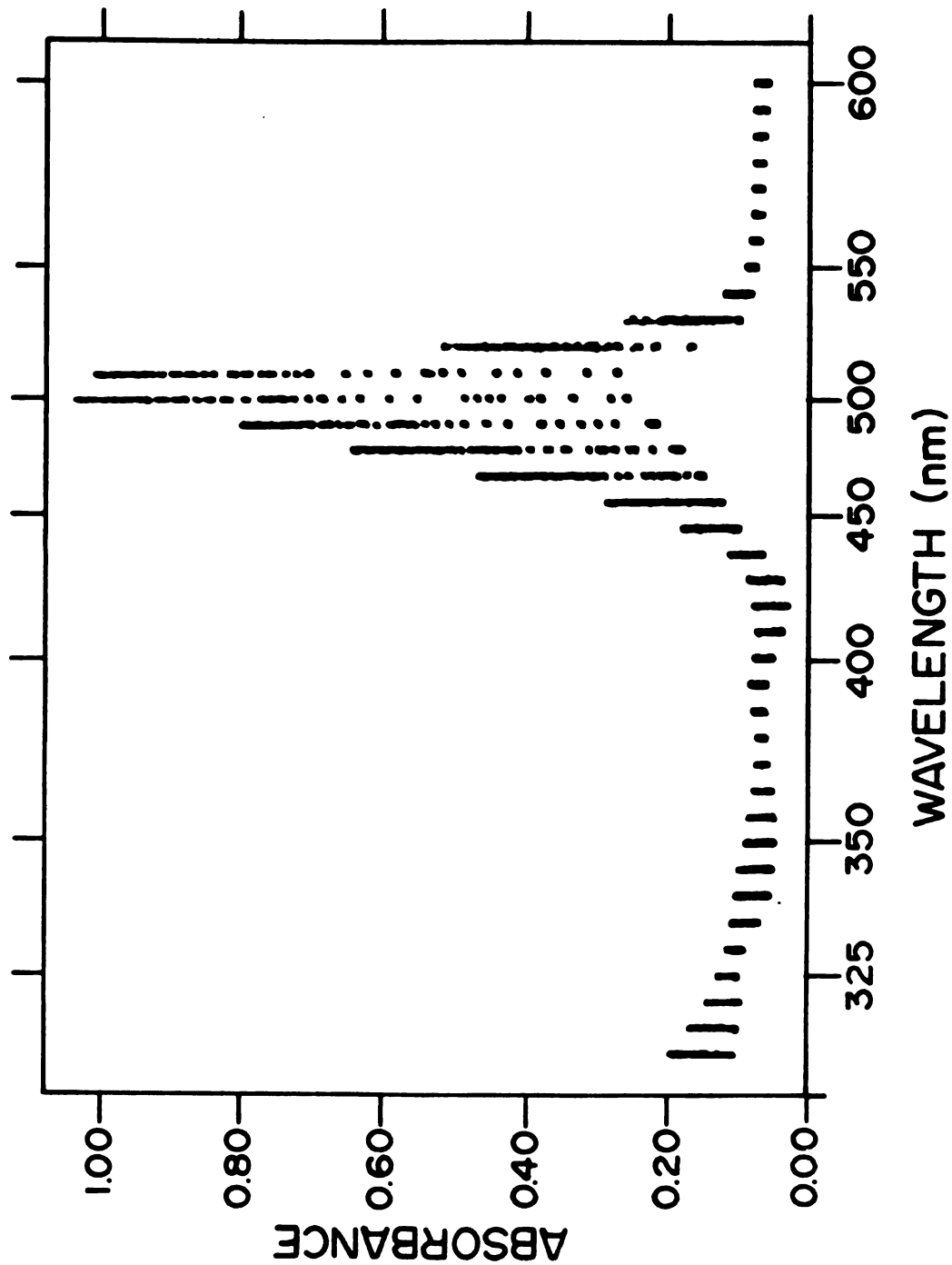


FIGURE 1

Examination of these spectra reveals small changes in absorbance in the wavelength region 300 nm - 450 nm and a large growth, centered at 508 nm, corresponding to the growth of the quinonoid complex. Although it is not readily apparent from Figure 1, there is a shoulder at approximately 480 nm associated with this long wavelength band (3). A similar growth of quinonoid, but centered at 502 nm was observed when alanine was mixed with tryptophanase (Figure 2). However, the growth at 502 nm was accompanied by a slower growth centered at ~430 nm with concomitant decay over the range 300 nm - 390 nm. A clean isosbestic point occurred at ~390 nm as shown by the difference spectra in Figure 2. The absorption due to quinonoid appeared to be unaffected by this slower process. The explanation for this phenomenon is unknown and awaits further experimentation.

Analysis of the biphasic growth at 508 nm observed with ethionine using equation 2 in KINFIT (17) demonstrated that the first six to eight seconds of the growth could be adequately described as the sum of two first order processes, k_1' and k_2' (Figure 3). The rate constants k_1' and k_2' were the same at 470 nm, 480 nm, 485 nm, 490 nm, 500 nm and 510 nm, i.e. at several selected wavelengths through the 500 nm absorption manifold. Data taken at longer times revealed yet a third slower first order

Figure 2. Tryptophanase spectra collected as a function of time after mixing with alanine at 24° C in 25 mM K-Epps, pH 8.0, 0.1 M KCl, 1 mM EDTA, 0.1 mM pyridoxal-P and 0.2 mM DTT. After mixing: 0.225 M alanine and 0.88 mg ml⁻¹ tryptophanase. The first spectrum has been subtracted from all of the other spectra to give rise to this set of difference spectra.

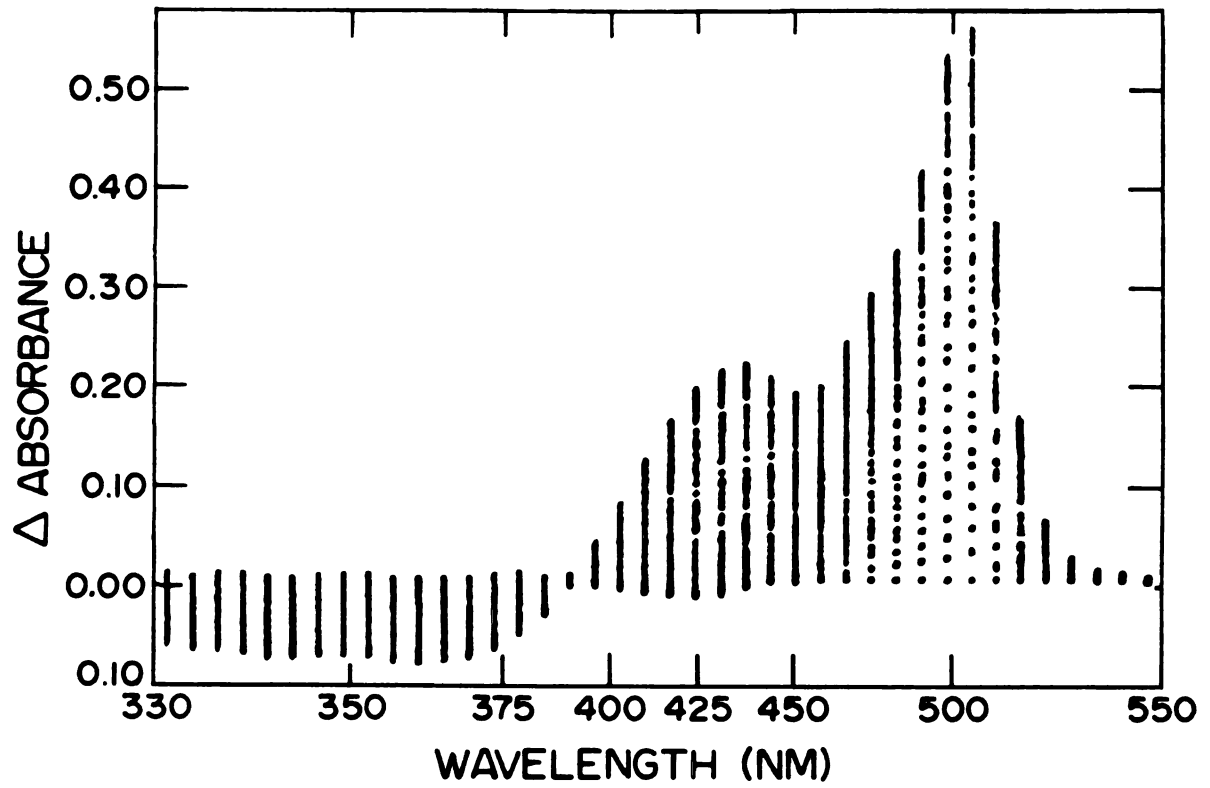


FIGURE 2

Figure 3. The biphasic growth in absorbance at 508 nm after mixing tryptophanase with ethionine at 24° C in 25 mM K-Epps, pH 8.0, 0.2 M KCl, 1 mM EDTA, 10 μM pyridoxal-P and 0.2 mM DTT. After mixing: 10 mM ethionine and 1.0 mg ml⁻¹ tryptophanase. The solid line was calculated with equation 2 using the parameters listed in Table III.

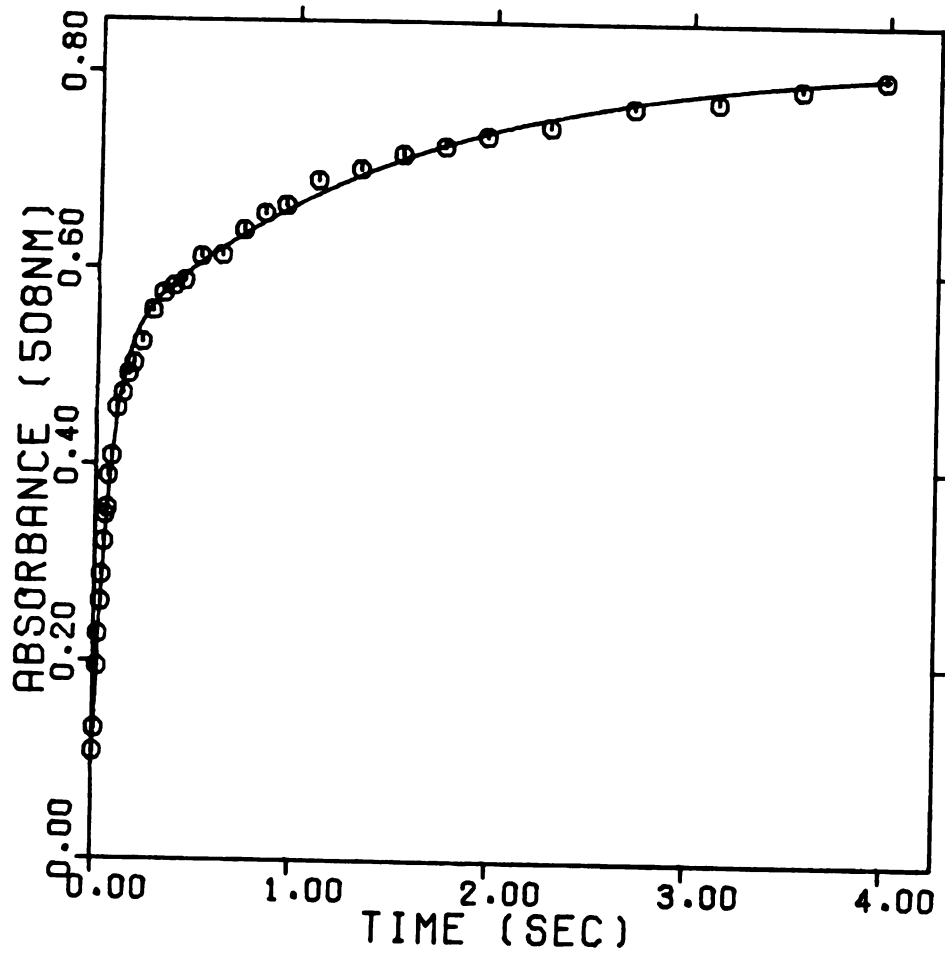


FIGURE 3

growth. The majority of the results presented in this paper deal only with the first two phases. The relatively long times required to collect data during the third phase made it technically difficult to define the fast phase in those cases where the fixed wavelength mode was used.

Additional information available from the analysis was the total absorbance change (here represented as the sum of ΔA_1 and ΔA_2) and the fraction of the absorbance change attributable to each phase. Since data for this experiment were collected for only 6 seconds the contribution of the slow third phase is not included. Assuming that the percent of the contribution of the third phase is independent of the concentration of ethionine, a $K_D = 0.67 \pm 0.04$ mM for the interaction of ethionine was determined by a weighted least squares analysis as suggested by Wilkinson (18), of the reciprocal of the total ΔA at 508 nm given in Table 1 as a function of the reciprocal ethionine concentration. This is in close agreement with the value of 0.52 mM given by Watanabe and Snell (8). Similar treatments of ΔA_1 and ΔA_2 gave values for $K_D = 0.50 \pm 0.004$ mM and 0.90 ± 0.14 mM, respectively. Of particular interest, however, was the observation that under these conditions (pH, etc.) ΔA_1 and ΔA_2 were roughly of equal amplitude.

Table I. Kinetic parameters for the biphasic growth of quinonoid as a function of ethionine concentration. Values were obtained by fitting the data for the change in absorbance at 508 nm as a function of time to equation 2. Total ΔA is defined as the sum of the absorbance changes in the fast and slow phases. Percent ΔA_1 and ΔA_2 are the percent of the total absorbance change attributable to each phase.

[L-ethionine] (mM)	k_1' (sec ⁻¹)	k_2' (sec ⁻¹)	Total ΔA	% ΔA_1	% ΔA_2
.30	2.3 \pm 0.023	0.38 \pm 0.004	0.172	70	30
.40	3.1 \pm 0.014	0.41 \pm 0.012	0.247	64	36
.75	4.4 \pm 0.017	0.42 \pm 0.008	0.340	59	41
1.0	5.2 \pm 0.081	0.42 \pm 0.001	0.381	56	44
1.5	7.2 \pm 0.064	0.44 \pm 0.004	0.452	54	46
5.0	14. \pm 0.11	0.61 \pm 0.005	0.562	52	48
10.	17. \pm 0.29	0.71 \pm 0.003	0.591	55	45
20.	18. \pm 0.55	0.72 \pm 0.017	0.442*	57	43

* These data were collected at a slightly lower wavelength and therefore the absorbance change was smaller.

In order to determine if k_1' and k_2' , the apparent first order rate constants for the fast and slow phases, respectively, showed any dependence on inhibitor concentration, the biphasic rate of quinonoid formation at 508 nm was examined over a range of ethionine concentrations from 0.3 mM to 20 mM. The results of these studies are presented in Figure 4 and Table I. It can be seen from Figure 4 that k_1' exhibits a hyperbolic dependence on concentration while k_2' is essentially independent of ethionine concentration. The fact that k_2' , that is the slow phase, is essentially unchanged over this wide range of inhibitor concentrations suggests that k_2' reflects an enzyme conformational change. When the data for k_1' from Figure 4 were plotted in reciprocal form, a value of $20.6 \pm 0.6 \text{ sec}^{-1}$ was obtained for k_1' at infinite ethionine concentration.

Table II contains kinetic parameters for quinonoid growth obtained with 50 mM, 100 mM and 200 mM alanine. Although the dissociation constant for the interaction of alanine with tryptophanase (8) is not known precisely, it appears that the three concentrations of alanine used were saturating, or that k_1' is insensitive to the concentration of alanine, as no variation in k_1' was observed. It is interesting to note that although under saturating conditions k_1' for alanine is significantly slower than k_1'

Figure 4. The variation of the apparent first order rate constants, k_1' (O) and k_2' (Δ), for the fast and slow phases, respectively, of the biphasic growth of quinonoid with ethionine concentration. The conditions under which these experiments were carried out are described in Materials and Methods.

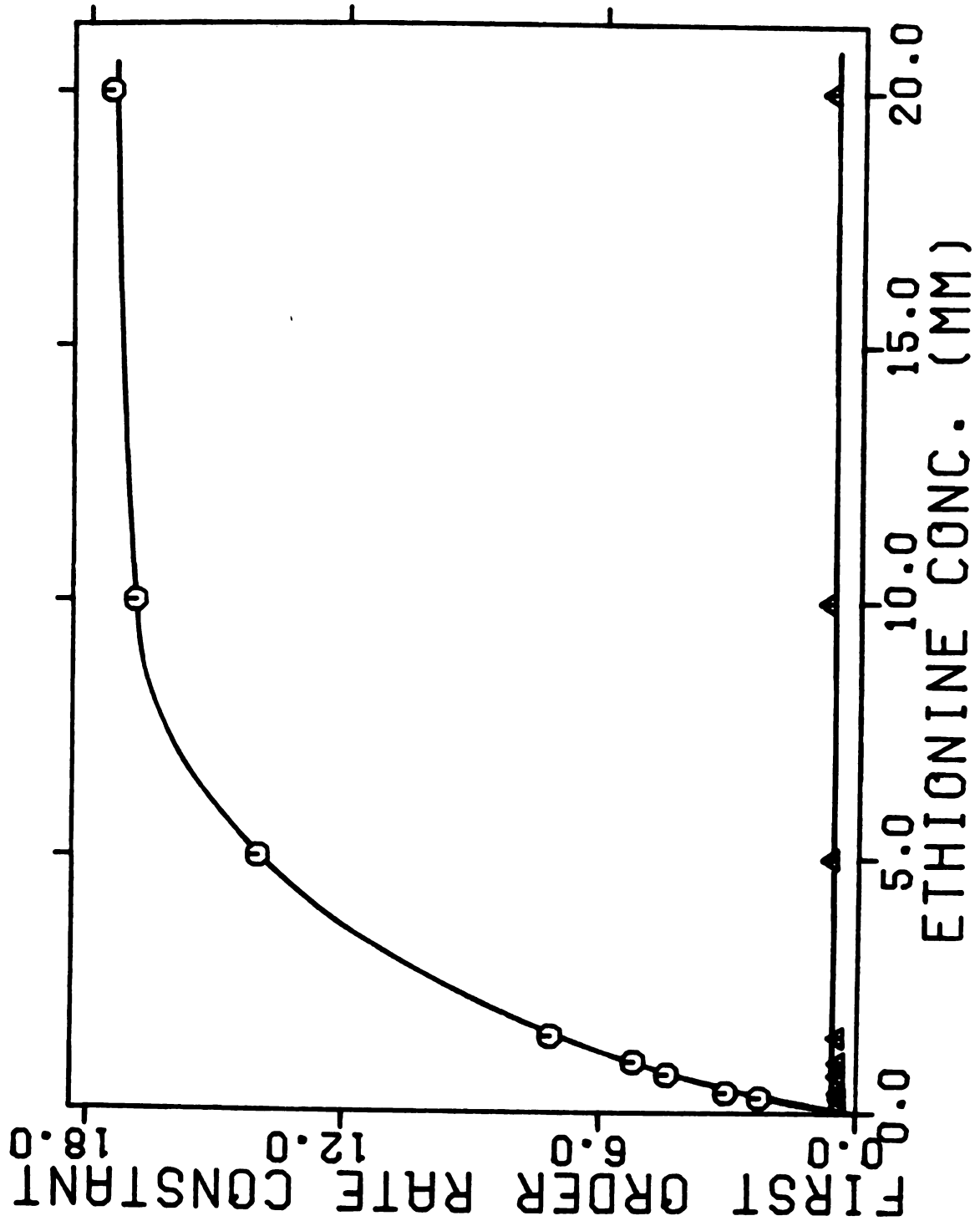


FIGURE 4

Table II. Kinetic parameters for biphasic quinonoid growth at three concentrations of alanine. Values were obtained by fitting the data for the change in absorbance as a function of time to equation 2. Total ΔA and percent ΔA_1 and ΔA_2 are defined in Table I.

[L-alanine] (mM)	k_1' (sec ⁻¹)	k_2' (sec ⁻¹)	Total ΔA^*	% ΔA_1	% ΔA_2
50	2.2 ± 0.064	0.39 ± 0.011	0.457	50	50
100	2.2 ± 0.12	0.44 ± 0.028	0.317	50	50
200	2.7 ± 0.12	0.59 ± 0.044	0.351	49	51

* Differences in total absorbance change reflect the fact that these data for the different alanine concentrations were collected at slightly different wavelengths.

for ethionine, k_2' is comparable for both inhibitors. This is consistent with our previous suggestion that k_2' reflects an enzyme conformational change. Again with alanine the fast and slow phases each account for roughly fifty percent of the total absorbance change in the two phases.

Changes at 337 nm and 420 nm - Holotryptophanase exhibits absorption bands due to bound coenzyme centered at 337 nm and 420 nm whose relative amplitudes vary with pH (3). Morino and Snell (3) associated the 337 nm form of tryptophanase with active enzyme on the basis that at pH values above 8.0, where tryptophanase appeared to exhibit its greatest activity, the 337 nm form predominated. In addition, the more effective monovalent cation activators appeared to stabilize the 337 nm form. The pH dependent

interconversion of the 420 nm and 337 nm forms had a pKa of 8.14 ± 0.06 in our hands which was at variance with the value of 7.2 reported by Morino and Snell (3). Thus, significant amounts of 420 nm absorbance exist at the apparent pH optimum of 8.3 for tryptophanase. Also, the fact that we observed activity in the presence of LiCl, which is essentially always in the 420 nm form prompted us to investigate these enzyme forms in a more quantitative manner in an attempt to determine the roles played by the 337 nm and 420 nm forms in catalysis. We reasoned that by following the changes in absorbance at 337 nm, 420 nm and 508 nm after mixing tryptophanase with ethionine in the scanning stopped flow spectrophotometer, we might be able to correlate the rates of change at 337 nm or 420 nm with the 508 nm absorbance and thus assess the importance of each form in the activity of the enzyme.

Figures 5A, B show the changes which occur in the tryptophanase spectrum at 420 nm upon addition of ethionine. Recall that all wavelengths in the range 280 nm - 600 nm are monitored in the same experiment. The change in absorbance at 420 nm is composed of a fast first order decay with an apparent first order rate constant of $18 \pm 2.2 \text{ sec}^{-1}$ (see Figure 5B) followed by a slow first order growth with an apparent first order rate constant of $0.38 \pm 0.05 \text{ sec}^{-1}$. Following the fast first order depletion

Figure 5. The changes in the tryptophanase absorption spectrum at 337 nm and 420 nm as a function of time after mixing with ethionine in 25 mM K-Epps, pH 8.0, 0.2 M KCl, 1 mM EDTA, 10 μ M pyridoxal-P, 0.2 mM DTT. After mixing: 10 mM ethionine and 1.0 mg ml⁻¹ tryptophanase. A) The overall absorbance changes at 420 nm; B) The rapid decrease in absorbance at 420 nm; C) The overall absorbance changes at 337 nm. The solid lines were calculated with equation 1 using the parameters listed in Table III.

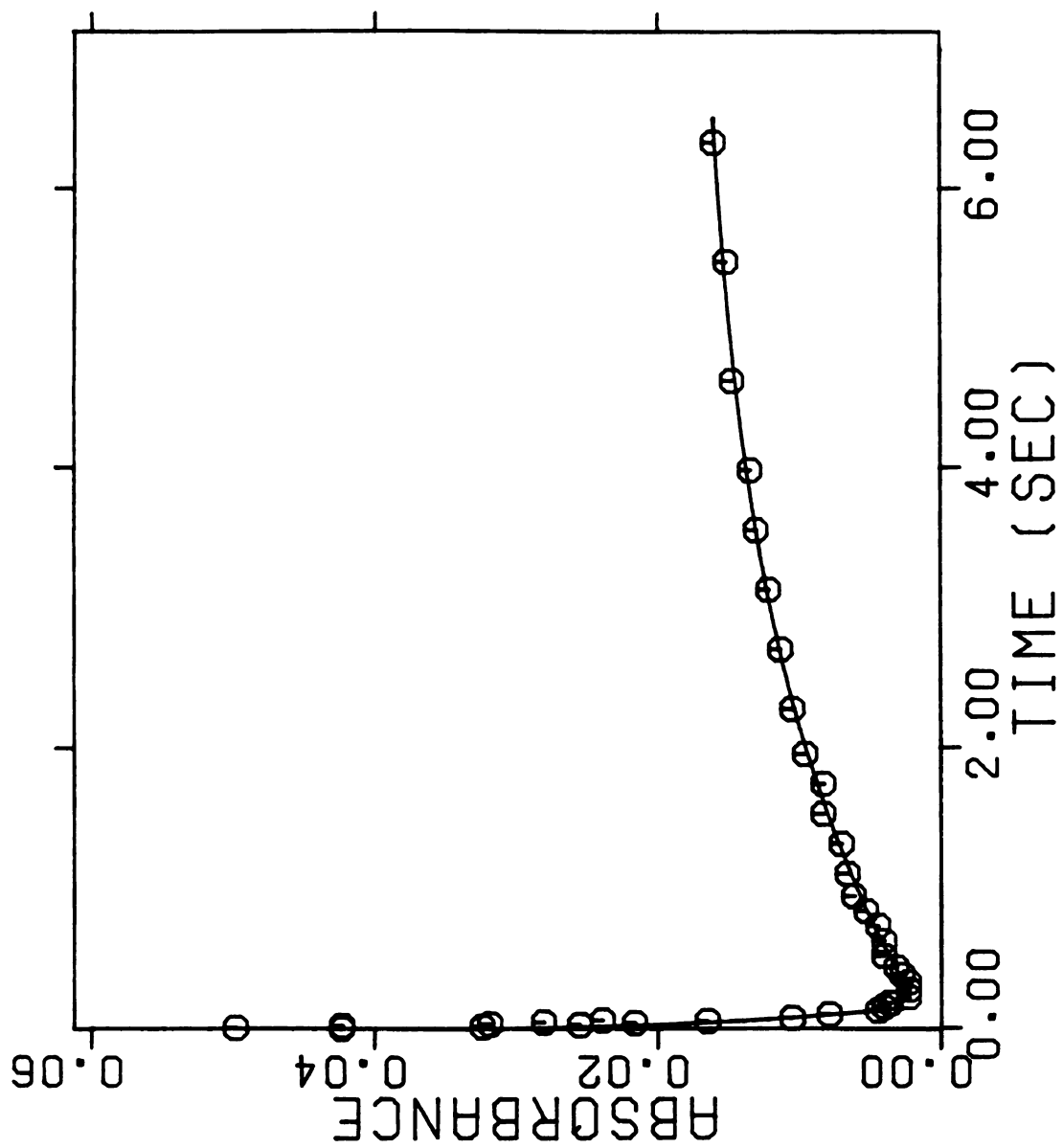


FIGURE 5A

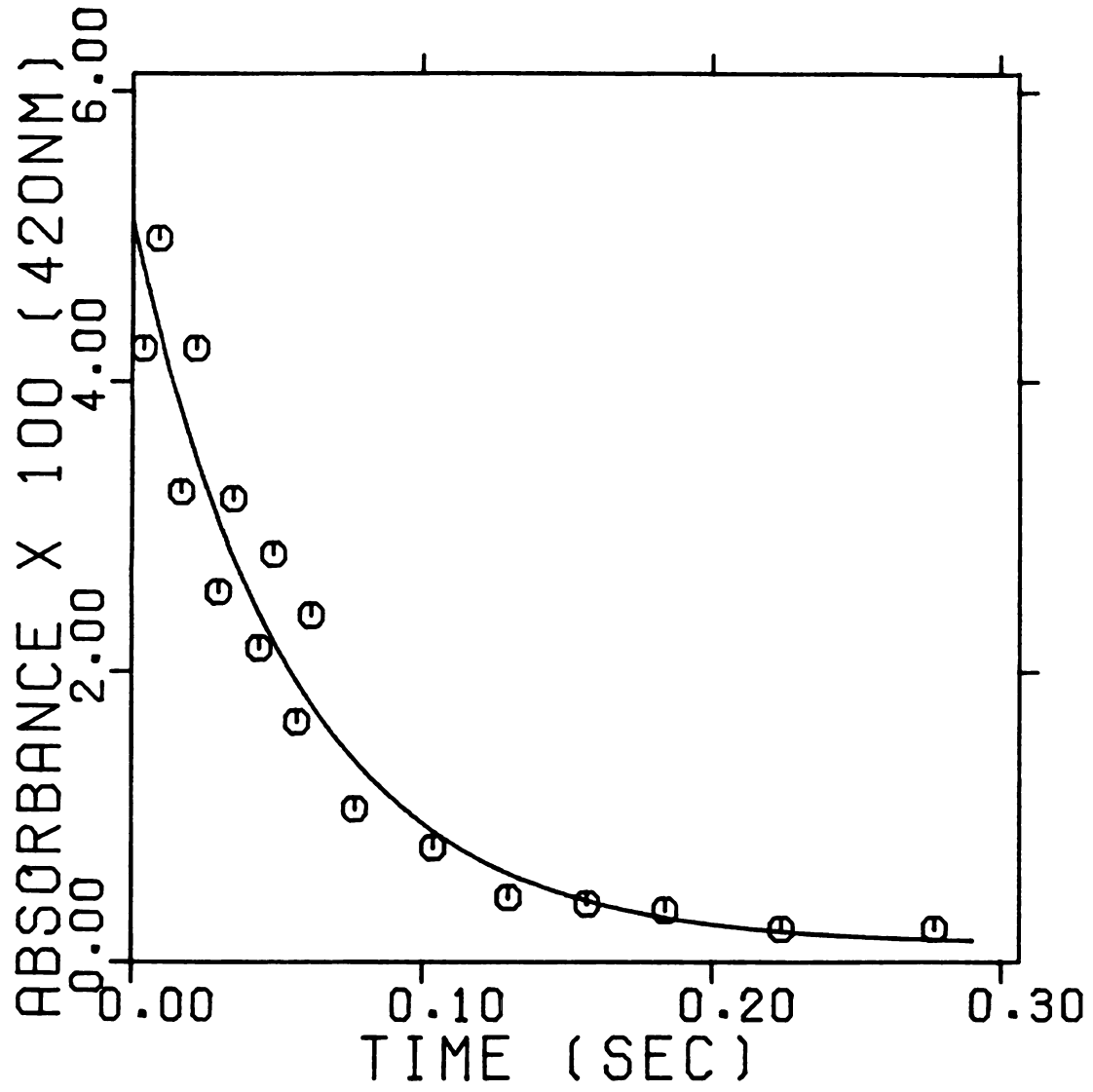


FIGURE 5B

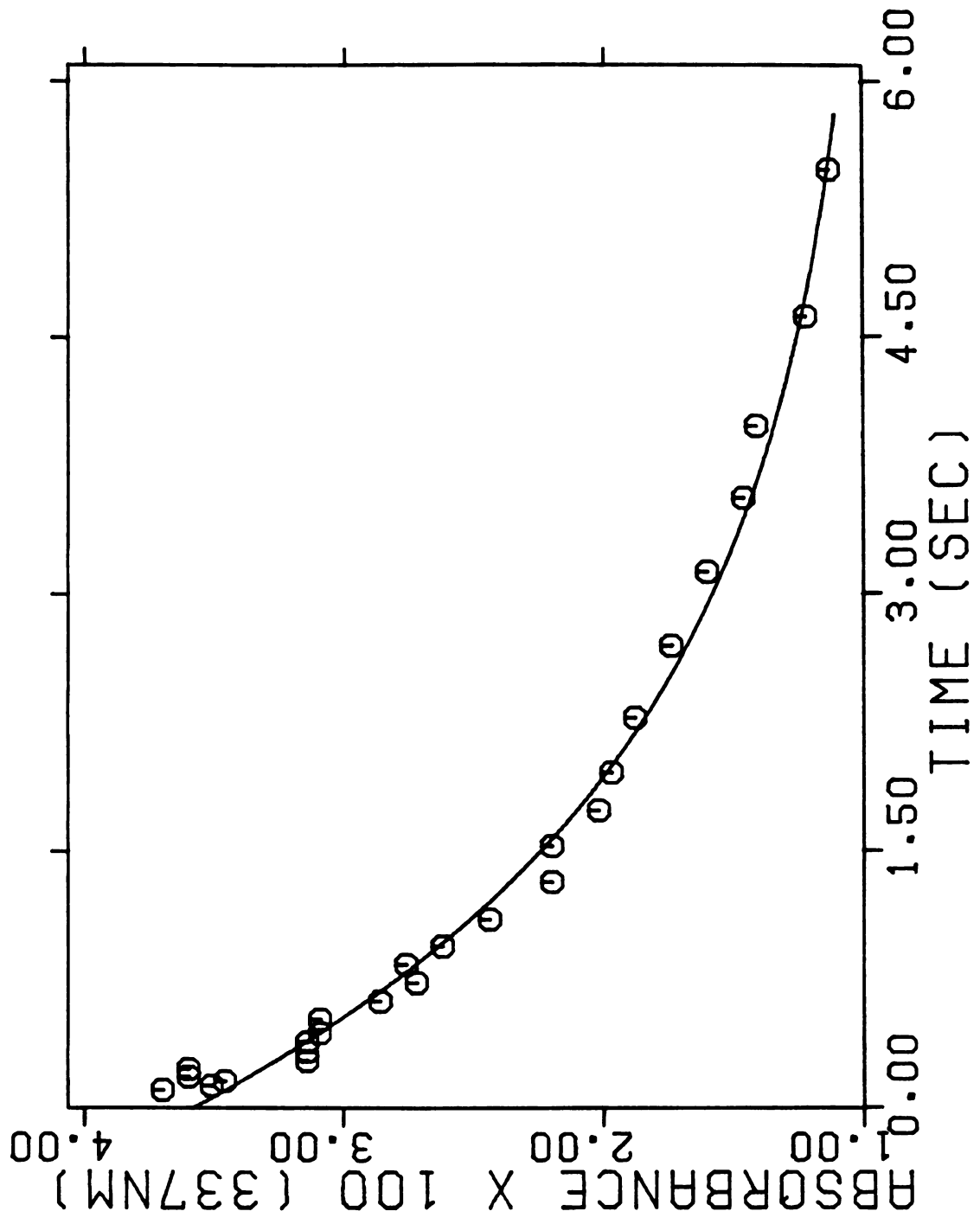


FIGURE 5C

of 420 nm absorbance, the 337 nm form of the coenzyme disappeared slowly with an apparent first order rate constant of $0.56 \pm 0.08 \text{ sec}^{-1}$ (Figure 5C). In these experiments values of k_1' and k_2' for the fast and slow phases of quinonoid formation at 508 nm were $15. \pm 1.2 \text{ sec}^{-1}$ and $0.62 \pm 0.06 \text{ sec}^{-1}$, respectively. Therefore, the rapid phase of quinonoid growth ($k_1' = 15. \pm 1.2 \text{ sec}^{-1}$) occurs simultaneously with a rapid loss of a 420 nm absorbing coenzyme species ($k_1' = 18. \pm 2.2 \text{ sec}^{-1}$). This suggests that the 420 nm form is the form poised for activity. The observed slow increase at 420 nm following the fast phase ($k' = 0.38 \pm 0.05 \text{ sec}^{-1}$) presumably arises from what was originally coenzyme in the 337 nm form being redistributed among 337 nm, 420 nm and 508 nm absorptions according to the new equilibrium which exists in the presence of ethionine. Alternatively, this could be due to a build-up of a 420 nm absorber of unknown identity as was observed with alanine. These data are summarized in Table III.

Effect of pH on Quinonoid Formation - Morino and Snell

(3) demonstrated that more quinonoid is formed with alanine as the pH is increased. A similar relationship was observed with serine transhydroxymethylase (2) for the quinonoid formed with D-alanine, and for tryptophanase with ethionine (Figure 6). Because the amount of the 337 nm form and the

Table III. Kinetic parameters for the absorbance changes at 337 nm, 420 nm and 508 nm which occur when tryptophanase is mixed with ethionine. The data at 508 nm were fitted to equation 2. The data at 337 nm were fitted to equation 1. The data at 420 nm is composed of two parts as described in the text. Each part was fitted separately to equation 1. Total ΔA and percent ΔA_1 and ΔA_2 are defined in Table I.

Absorbance changes at 508 nm:

k_1' (sec ⁻¹)	k_2' (sec ⁻¹)	Total ΔA	% ΔA_1	% ΔA_2
15. \pm 1.2	0.63 \pm 0.058	0.747	58	42

Absorbance changes at 337 nm and 420 nm:

wavelength (nm)	k' (sec ⁻¹)	ΔA
337 nm	0.56 \pm 0.080	0.026 \pm 0.0012
420 nm (decay)	18. \pm 2.2	0.049 \pm 0.0010
420 nm (growth)	0.38 \pm 0.050	0.017 \pm 0.0004

Figure 6. The rate and extent of quinonoid formation as a function of pH. Tryptophanase was pushed against ethionine at three pH values as described in Materials and Methods and quinonoid growth was monitored at 508 nm. pH 7.2, (O); pH 8.0, (Δ); pH 8.7 (+). The solid lines were calculated using the parameters listed in Table IV.

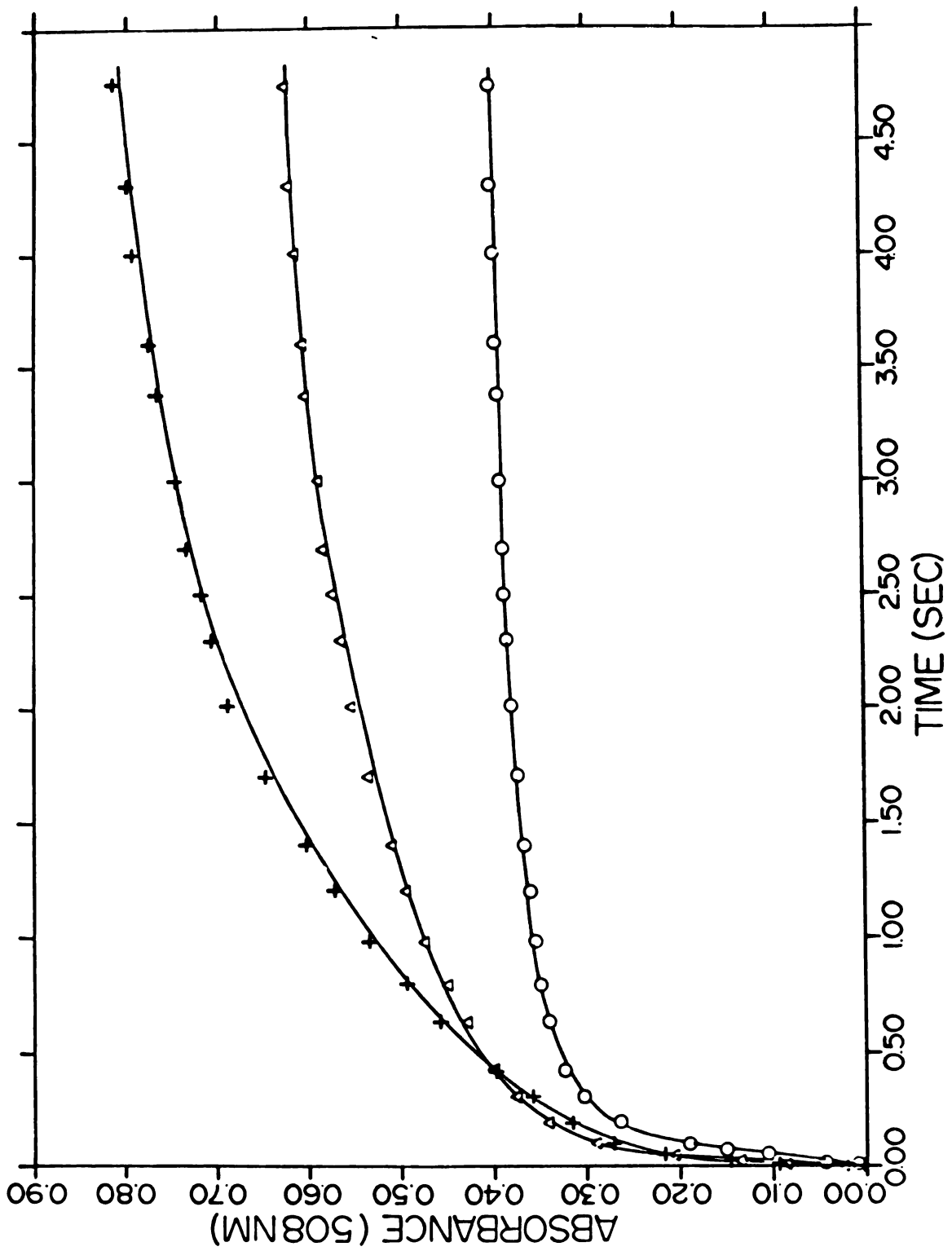


FIGURE 6

420 nm form depended on pH and since the 420 nm form appeared to be poised for activity, we examined the rate of quinonoid formation and the amount of quinonoid formed at equilibrium when tryptophanase was mixed with 5 mM ethionine at pH 7.2, 8.0 and 8.7 as described in Materials and Methods. The data at each pH which were collected for a period of 16.5 seconds, were analyzed as the sum of three exponentials, the first two phases of which are presented in Figure 6. The kinetic constants and amplitudes for all three phases are summarized in Table IV.

Examination of Table IV reveals that as the pH is increased, k_1' also increases, from $8.7 \pm 0.28 \text{ sec}^{-1}$ at pH 7.2 to $13. \pm 0.89 \text{ sec}^{-1}$ at pH 8.0 and $19. \pm 2.3 \text{ sec}^{-1}$ at pH 8.7. In contrast, k_2' and k_3' appear to be relatively insensitive to pH. This is consistent with the notion that k_2' and k_3' reflect enzyme conformational changes.

The relative amplitudes attributable to each phase given in Table IV are also of interest. As the pH is increased the contribution of the fast phase to the total absorbance change diminishes, while the second and third phases contribute more.

Tryptophanase-ethionine (minus cations) vs NH_4Cl , KCl , RbCl and CsCl - Suelter and Snell (9) have shown that ethionine interacts with tryptophanase in the absence of cations, presumably forming a Schiff's base with enzyme

Table IV: Kinetic parameters for the triphasic growth of quinonoid at pH values 7.2, 8.0 and 8.7. Values were obtained by fitting the data for the change in absorbance at 508 nm as a function of time to an equation similar to 2 involving the sum of three exponentials. Total ΔA is defined as the sum of the absorbance changes in the three phases. Percent ΔA_1 , ΔA_2 and ΔA_3 are the percent of the total absorbance change attributable to each phase.

pH	k_1' (sec ⁻¹)	k_2' (sec ⁻¹)	k_3' (sec ⁻¹)	Total ΔA	% ΔA_1	% ΔA_2	% ΔA_3
7.2	8.7 ± 0.28	0.74 ± 0.080	0.14 ± 0.024	0.401	68	22	10
8.0	13. ± 0.80	0.72 ± 0.040	0.098 ± 0.010	0.603	42	40	18
8.7	19. ± 2.3	1.1 ± 0.56	0.30 ± 0.30	0.866	24	56	20

in the α -conformation. However, no quinonoid is formed until activating cations are added. In an attempt to gain more information on the role of cations in this process, tryptophanase was prepared as described in Materials and Methods in the presence of 10 mM ethionine and $(\text{CH}_3)_4\text{N-Epps}$ in the absence of activating cations.

Figure 7 shows the results obtained when this enzyme solution was pushed against saturating concentrations of NH_4^+ , K^+ , Rb^+ and Cs^+ . Quinonoid growth at 508 nm was again biphasic. The kinetic parameters obtained for each cation are given in Table V along with the percentages of the total absorbance change attributable to the fast and slow phases.

The amount of quinonoid formed at equilibrium was approximately the same in NH_4^+ , K^+ and Rb^+ , but considerably less in Cs^+ which is consistent with what was previously shown (9). However, the percentage of the total absorbance change occurring in the fast phase is larger in the case of the more effective monovalent cation activators. Values of k_1' and k_2' , the apparent first order rate constants for the fast and slow phases, respectively, appear to increase as the effectiveness of the activator decreases.

Figure 7. The rate and extent of quinonoid formation in the presence of various monovalent cations. A tryptophanase solution containing ethionine was prepared in the absence of activating cations as described in Materials and Methods. This enzyme solution was pushed against saturating concentrations of four monovalent cations and quinonoid growth was monitored at 508 nm. 0.025 M NH_4Cl , (O); 0.1 M KCl , (Δ); 0.25 M RbCl , (+); 0.5 M CsCl (\diamond). The solid lines were calculated with equation 2 using the parameters listed in Table V.

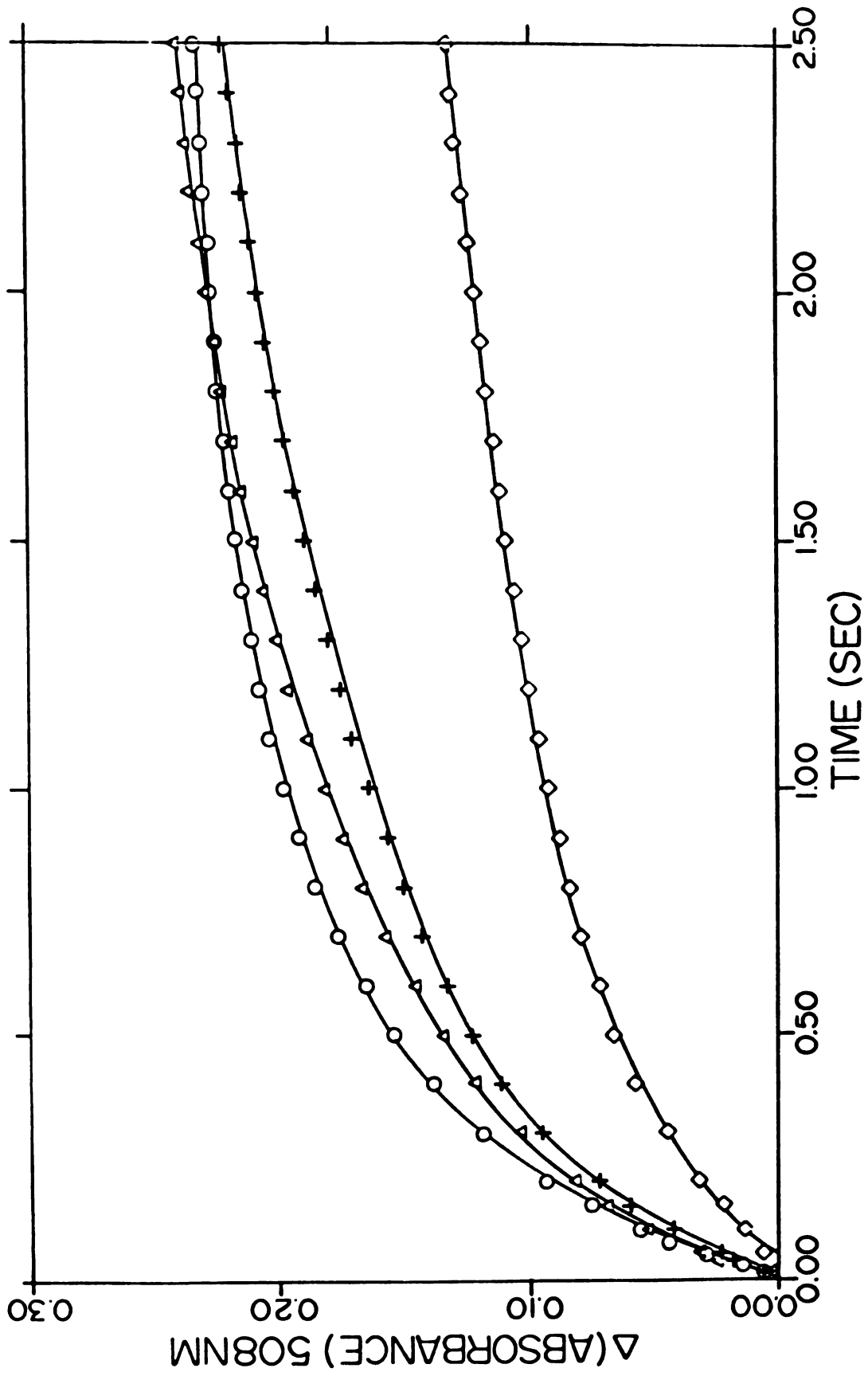


FIGURE 7

Table V. Kinetic parameters for the biphasic growth of quinonoid observed when a tryptophanase-ethionine complex is mixed with monovalent cations. Values were obtained by fitting the data for the change in absorbance at 508 nm as a function of time to equation 2. Total ΔA and percent ΔA_1 and ΔA_2 are defined in Table I.

Cation	Concentration (M)	k_1' (sec ⁻¹)	k_2' (sec ⁻¹)	Total ΔA	% ΔA_1	% ΔA_2
NH ₄ ⁺	0.025	2.8 ± 0.050	0.31 ± 0.019	0.263	70	30
K ⁺	0.10	2.4 ± 0.091	0.44 ± 0.012	0.277	49	51
Rb ⁺	0.25	3.9 ± 0.37	0.48 ± 0.027	0.266	36	64
Cs ⁺	0.50	5.5 ± 0.29	0.58 ± 0.029	0.188	27	73

Deuterium Isotope Effect on Quinonoid Formation -

Figure 8 shows the results obtained when tryptophanase was mixed with L-[α - ^1H]alanine and L-[α - ^2H]alanine. Substitution of deuterium at the α position of the inhibitor effects both the extent and rate of quinonoid formation. At equilibrium, approximately 4.5 times more quinonoid is formed from L-[α - ^1H]alanine than from L-[α - ^2H]alanine. The progress curve for quinonoid formation from L-[α - ^1H]alanine was biphasic giving a value for k_1' of $2.2 \pm 0.02 \text{ sec}^{-1}$ and $0.38 \pm 0.003 \text{ sec}^{-1}$ for k_2' . On the other hand, with deuterium at the α position, the two apparent first order rate constants, k_1' and k_2' , were too close in value to be separated by our curve fitting procedures. Therefore, these data were fitted to a single exponential giving a value for k' or $0.49 \pm 0.005 \text{ sec}^{-1}$. It thus appears that the effect of deuterium substitution is to slow down the fast phase of quinonoid growth while leaving the slow phase virtually unchanged. This is interpreted as additional evidence that k_2' reflects an enzyme conformational change. The deuterium kinetic isotope effect of approximately four-fold also shows that loss of the α -proton is the rate-limiting step when quinonoid is formed from the competitive inhibitor of tryptophanase, L-alanine.

Figure 8. The effect of deuterium substitution at the α -position of alanine on the rate and extent of quinonoid formation with tryptophanase. Tryptophanase was pushed against 0.45 M L- $[\alpha\text{-}^1\text{H}]$ -alanine (O) and L- $[\alpha\text{-}^2\text{H}]$ -alanine (Δ) as described in Materials and Methods. The top line was calculated with equation 2 using the values: $A_\infty = 0.70$, $\Delta A_1 = 0.43$, $\Delta A_2 = 0.22$, $k_1' = 2.4 \text{ sec}^{-1}$, and $k_2' = 0.38 \text{ sec}^{-1}$. The bottom line was calculated with equation 1 using the values $A_\infty = 0.17$, $\Delta A = 0.14$, and $k_1' = 0.49 \text{ sec}^{-1}$.

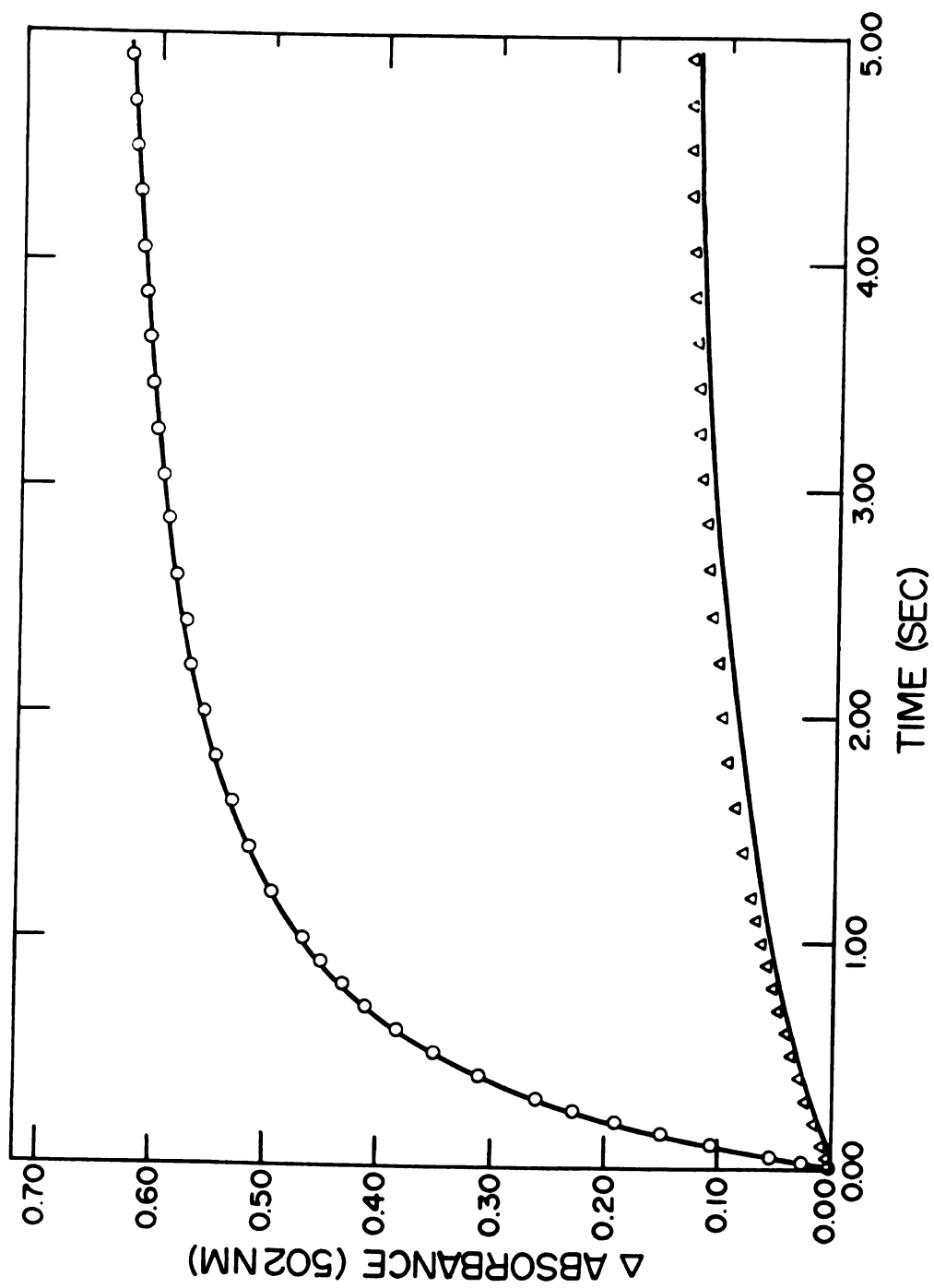
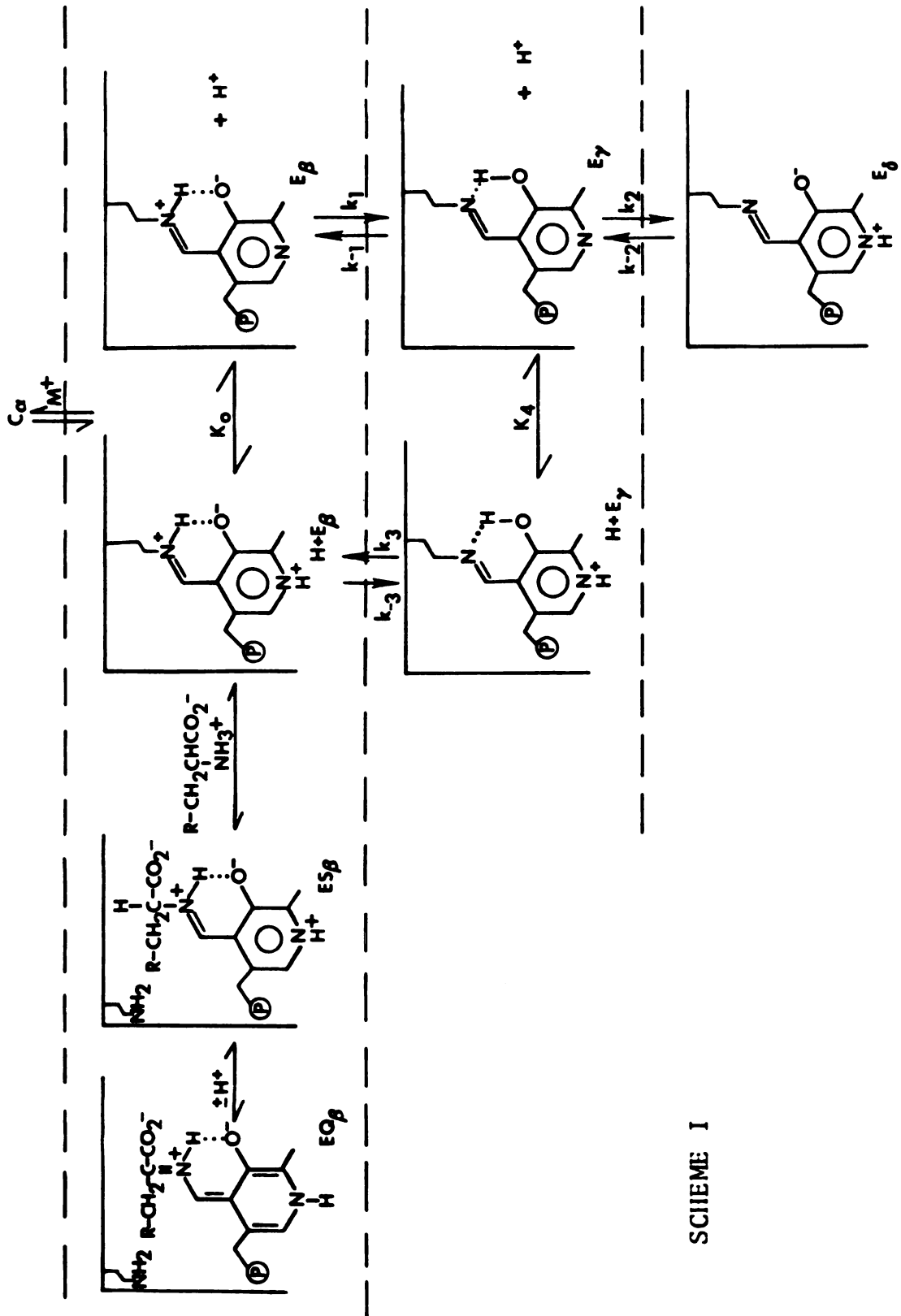


FIGURE 8

DISCUSSION

The results presented in this paper are consistent with a model of tryptophanase catalysis based on previous equilibrium and stopped flow studies on the effects of pH and monovalent cations on the spectral and catalytic properties of the enzyme. Scheme I is a representation of this model which involves four enzyme conformations, α , β , γ , and δ defined previously.

Ethionine and alanine were shown to interact with tryptophanase to form quinonoid derivatives absorbing at approximately 500 nm (Figures 1 and 2). The appearance of quinonoid as a function of time for the first six to eight seconds of the reaction was composed of a fast and a slow first order process with rates represented by k_1' and k_2' , respectively. The relative amplitudes of each phase at pH 8 were approximately equal with both ethionine and alanine (Tables I and II), although in the case of ethionine it appears as if a slightly greater percentage of the absorbance change in the two phases of quinonoid growth occurs in the fast phase. Examination of data presented earlier (Section 2, Table III) reveals that at pH 8.0 approximately 56 percent of the enzyme, in the absence of substrate or inhibitor, is in the β conformation while approximately 45 percent is in the γ conformation.



SCHEME I

The results presented in this paper for the biphasic formation of quinonoid at pH 8.0 are consistent with Scheme I where inhibitor interacts with the β conformation to rapidly form the quinonoid derivative with an apparent rate, k_1' . According to this interpretation, the slower phase, k_2' , represents the conversion of conformation γ to the β conformation. Enzyme in the β conformation, which is assumed to represent the active form of the enzyme, could thus rapidly form additional quinonoid with an apparent rate, k_2' , dictated by the rate of the conformational change.

This suggestion is supported by the fact that k_2' is essentially unaffected by inhibitor concentration (Figure 4) or the nature of the inhibitor which is consistent with a change in enzyme conformation. In addition, the average values of k_2' of $0.51 \pm 0.14 \text{ sec}^{-1}$ and 0.47 ± 0.15 obtained with ethionine (Table I) and alanine (Table II), respectively agree closely with the value for the rate of conversion of conformation γ to conformation β following a rapid decrease from pH 8.70 to 8.25 of $0.52 \pm 0.02 \text{ sec}^{-1}$ (Section II, Table I).

The changes in absorbance at 337 nm and 420 nm which occur when ethionine is mixed with tryptophanase are also consistent with Scheme I. The rapid disappearance of 420 nm absorbance coincides with the fast phase of quinonoid formation and suggests that the β conformation, containing species

of coenzyme which absorb at approximately 420 nm, is the active form of the enzyme. The disappearance of 337 nm absorbance occurs with essentially the same rate as the second phase of quinonoid growth. This implies that the γ conformation or 337 nm form of tryptophanase cannot form quinonoid directly but must first be converted to the β conformation before the α -proton can be removed from the inhibitor.

Although interpretation of the data for the growth of quinonoid at pH 7.2, 8.0 and 8.7 is complicated by the fact that the dissociation constant for ethionine increases as the pH is decreased, the variations in the rates and amplitudes of the three phases of quinonoid growth are again consistent with Scheme I. At lower pH values where the enzyme exists primarily in the β conformation (Section 2, Table III) relatively more quinonoid is produced in the fast phase (Table IV), which supports the suggestion that this is the active form of the enzyme. The second and third phases correspond to the slow conversion of conformation γ and δ , respectively, to conformation β , with subsequent rapid quinonoid formation accompanying the establishment of a new equilibrium between conformations in the presence of ethionine. The observation that the second and third phases of quinonoid growth account for a greater percentage of the total absorbance change at 508 nm as the pH is

increased follows from the fact that more of the enzyme is in the γ and δ conformations at higher pH values. Within experimental error, only the rate of the first phase, that is the formation of quinonoid, EQ_{β} from H^+E_{β} , is affected by pH, increasing from $8.7 \pm 0.28 \text{ sec}^{-1}$ at pH 7.2 to $19. \pm 2.3 \text{ sec}^{-1}$ at pH 8.7. The rates of the second and third phases appear to be constant with pH which again is consistent with the proposed conformational changes in Scheme I.

In the absence of activating cations, tryptophanase is inactive and absorbs at 420 nm (3). We have assumed that monovalent cations act at or near the catalytic site in close proximity to the coenzyme (9) and that in the absence of cations the coenzyme is held in a slightly different conformation in relation to enzyme functional groups required for catalytic activity. We have designated this inactive, 420 nm absorbing form of the coenzyme conformation α . Scheme I shows conformation α (C_{α}) capable of being converted to the conformations β , γ , and δ by monovalent cations. In the absence of cations it is assumed that ethionine forms a Schiff's base with conformation α (9) (not shown in Scheme I), but nothing else is known about this complex. In an attempt to obtain information on this interaction and possibly determine the rate of conversion of C_{α} to C_{β} we pushed an enzyme-ethionine complex without activating cations against saturating concentrations of

NH_4Cl , KCl , RbCl and CsCl as described in Materials and Methods. The results presented in Table V and Figure 7 show that the extent of quinonoid formation was approximately the same in NH_4^+ , K^+ and Rb^+ but less in Cs^+ . These results are consistent with those of Suelter and Snell (9) who found that the amount of quinonoid formed at equilibrium at pH 8.0, was proportional to the effectiveness of the cation as an activator. As mentioned, the values of k_1' and k_2' , the apparent first order rate constants for the fast and slow phases of quinonoid growth with the various cations, appear to increase as the effectiveness of the activator decreases. Since this increase in rates also parallels an increase in ionic strength from 0.025 M in the case of NH_4^+ to 0.5 M in Cs^+ , a full explanation of the effect of cations on quinonoid formation must await further studies on the effects of ionic strength on this process. Likewise, although the value of k_1' may reflect the rate of conversion of C_α to C_β prior to rapid quinonoid formation from the C_β conformation, the unavoidably low specific activity of the enzyme which resulted from dialysis in the absence of activating cations makes firm conclusions difficult.

Finally, Figure 8 shows that the substitution of deuterium at the α -position of alanine causes a dramatic decrease in both the extent of quinonoid formation and the rate of the fast phase of the biphasic quinonoid growth. These results are consistent with Scheme I if it is assumed that the fast phase of quinonoid (EQ_{β}) formation occurs through ES_{β} from $H^{\dagger}E_{\beta}$. The observed kinetic isotope effect on k_1' , the apparent first order rate constant for the fast phase implies that proton abstraction is the rate-limiting step in quinonoid formation with alanine.

REFERENCES

1. Jenkins, W. T. (1961) J. Biol. Chem. 236, 1121-1125.
2. Schirch, L., and Jenkins, W. T. (1964) J. Biol. Chem. 239, 3801-3807.
3. Morino, Y., and Snell, E. E. (1967) J. Biol. Chem. 242, 2800-2809.
4. Fonda, M. L., and Johnson, R. J. (1970) J. Biol. Chem. 245, 2709-2716.
5. Ulevitch, R. J., and Kallen, R. G. (1977) Biochem. 16, 5350-5354.
6. Kumagai, H., and Yanada, H. (1970) J. Biol. Chem. 245, 1773-1777.
7. Walsh, C. (1979) Enzymatic Reaction Mechanisms, W. H. Freeman and Co., San Francisco, Chapter 24.
8. Watanabe, T. and Snell, E. E. (1977) J. Biochem. 82, 733-745.
9. Suelter, C. H. and Snell, E. E. (1977) J. Biol. Chem. 252, 1852-1857.
10. Suelter, C. H., Wang, J., and Snell, E. E. (1977) Anal. Biochem. 76, 221-232.
11. Suelter, C. H., Wang, J., and Snell, E. E. (1976) FEBS Lett. 66, 230-232.
12. Högberg-Raibaud, A., Raibaud, O., and Goldberg, M. E. (1975) J. Biol. Chem. 250, 3352-3358.
13. Coolen, R. B., Papadakis, N., Avery, J., Enke, C. G., and Dye, J. L. (1975) Anal. Chem. 47, 1649-1655.
14. Papadakis, N., Coolen, R. B., and Dye, J. L. (1975) Anal. Chem. 47, 1644-1649.
15. Suelter, C. H., Coolen, R. B., and Dye, J. L. (1975) Anal. Biochem. 69, 155-163.
16. June, D. S., Kennedy, B., Pierce, T. H., Elias, S. V., Halaka, F., Behbahani, Nejad, I., El-Bayoumi, A., Suelter, C. H., and Dye, J. L. (1979) J. Amer. Chem. Soc. 101, 2218-2219.

References - continued

17. Dye, J. L., and Nicely, V. A. (1971) J. Chem. Ed. 48, 443-448.
18. Wilkinson, G. N. (1961) Biochem. J. 80, 324-332.

APPENDICES

APPENDIX A

- A. Derivation of the expression for the rate of interconversion of the β and γ conformational manifolds following a rapid change in pH (refer to Section II, Scheme I for the mechanism).

The differential equation describing the disappearance of the γ conformational manifold following a rapid decrease in pH is

$$\frac{-d([H^+E_\gamma] + [E_\gamma])}{dt} = k_{-1}[E_\gamma] - k_1[E_\beta] + k_3[H^+E_\gamma] - k_{-3}[H^+E_\beta]$$

from equilibrium considerations,

$$[E_\beta] = \frac{K_0 [H^+E_\beta]}{[H^+]} \quad (2) \quad \text{and} \quad [E_\gamma] = \frac{K_4 [H^+E_\gamma]}{[H^+]} \quad (3)$$

therefore,

$$\begin{aligned} \frac{-d([H^+E_\gamma] + [E_\gamma])}{dt} &= - \left(1 + \frac{K_4}{[H^+]} \right) \frac{d[H^+E_\gamma]}{dt} \\ &= \left(\frac{k_{-1}K_4}{[H^+]} + k_3 \right) [H^+E_\gamma] - \left(k_{-3} + \frac{k_1K_0}{[H^+]} \right) [H^+E_\beta] \end{aligned}$$

(4)

from conservation conditions,

$$[H^+E_\beta] + [H_\beta] + [H^+E_\gamma] + [E_\gamma] = [E_0] \quad (5)$$

or,

$$[H^+E_\beta] \left(1 + \frac{K_0}{[H^+]}\right) + [H^+E_\gamma] \left(1 + \frac{K_4}{[H^+]}\right) = E_0 \quad (6)$$

solving for $[H^+E_\beta]$ in terms of $[E_0]$ and $[H^+E_\gamma]$ we obtain

$$[H^+E_\beta] = \frac{[E_0]}{\left(1 + \frac{K_0}{[H^+]}\right)} - [H^+E_\gamma] \left\{ \frac{\left(1 + \frac{K_4}{[H^+]}\right)}{\left(1 + \frac{K_0}{[H^+]}\right)} \right\} \quad (7)$$

substitution of this expression for $[H^+E_\beta]$ into (4) gives

$$-\left(1 + \frac{K_4}{[H^+]}\right) \frac{d[H^+E_\gamma]}{dt} - \left(\frac{k_{-1}K_4}{[H^+]} + k_3\right) [H^+E_\gamma] + \left(k_{-3} + \frac{k_1K_0}{[H^+]}\right) \times$$

$$\left\{ \frac{\left(1 + \frac{K_4}{[H^+]}\right)}{\left(1 + \frac{K_0}{[H^+]}\right)} \right\} [H^+E_\gamma] - \left\{ \frac{\left(k_{-3} + \frac{k_1K_0}{[H^+]}\right)}{\left(1 + \frac{K_0}{[H^+]}\right)} \right\} [E_0] \quad (8)$$

simplifying,

$$\frac{-d[H^+E_\gamma]}{dt} = \frac{\left(k_{-3} + \frac{k_1 K_0}{[H^+]}\right) [E_0]}{\underbrace{\left(\frac{1 + K_4}{[H^+]}\right) \left(\frac{1 + K_0}{[H^+]}\right)}_a} + \frac{\left(\frac{k_{-1} K_4}{[H^+]} + k_3\right) \left(\frac{k_{-3} + k_1 K_0}{[H^+]}\right) [H^+ E_\gamma]}{\underbrace{\left(\frac{1 + K_4}{[H^+]}\right) \left(\frac{1 + K_0}{[H^+]}\right)}_b}$$

(9)

Equation 9 has the form,

$$\frac{d[H^+E_\gamma]}{dt} = a - b[H^+E_\gamma] \quad (10)$$

let

$$y = a - b[H^+E_\gamma] = \frac{d[H^+E_\gamma]}{dt}$$

then,

$$\frac{dy}{dt} = -b \left(\frac{d[H^+E_\gamma]}{dt} \right)$$

therefore,

$$\frac{dy}{dt} = -bdt$$

integration gives

$$y = y_0 e^{-bt}$$

Therefore the apparent first order rate constant for the conversion of the γ to the β manifold is equal to the expression for b given in equation 9. The expression is the same for the conversion of the γ to the β manifold. The parameter k_{-3} , may be eliminated from the expression for b through the use of the thermodynamic loop constraint

$$k_{-3} = \left(\frac{K_0}{K_4} \right) \left(\frac{k_1}{k_{-1}} \right) k_3$$

- B. Derivation of the expression for the rate of appearance or disappearance of E_δ following a rapid change in pH (refer to Section II, Scheme I for mechanism). The differential equation for the disappearance of E_δ following a rapid decrease in pH is

$$-\frac{d[E_\delta]}{dt} = k_{-2}[E_\delta] - k_2[E_\delta] \quad (1)$$

The equilibrium conditions are

$$K_0 = \frac{[E_\beta][H^+]}{[H^+E_\beta]} ; \quad K_1 = \frac{[E_\gamma]}{[E_\beta]} ; \quad K_2 = \frac{[E_\delta]}{[E_\gamma]}$$

$$K_3 = \frac{[H^+E_\beta]}{[H^+E_\gamma]} ; \quad K_4 = \frac{[E_\gamma][H^+]}{[H^+E_\gamma]}$$

The enzyme conservation equation is

$$\begin{aligned} [E_0] &= [H^+E_\beta] + [E_\beta] + [H^+E_\gamma] + [E_\gamma] + [E_\delta] \\ &= [E_\gamma] \left(1 + \frac{1}{K_1} + \frac{[H^+]}{K_0K_1} + \frac{[H^+]}{K_0K_1K_3} \right) + [E_\delta] \end{aligned} \quad (2)$$

therefore,

$$[E_\gamma] = \frac{[E_0] - [E_\delta]}{\left(1 + \frac{1}{K_1} + \frac{[H^+]}{K_0K_1} + \frac{[H^+]}{K_0K_1K_3} \right)} \quad (3)$$

Let $\left(1 + \frac{1}{K_1} + \frac{[H^+]}{K_0K_1} + \frac{[H^+]}{K_0K_1K_3} \right)$ equal D, then

$$[E_\gamma] = \frac{[E_0]}{D} - \frac{[E_\delta]}{D} \quad (4)$$

Substituting this expression for $[E_\gamma]$ into equation 1 gives

$$\frac{d[E_\delta]}{dt} = \frac{k_2[E_0]}{D} - \left(\frac{k_2}{D} + k_{-2} \right) [E_\delta] \quad (5)$$

Let

$$y = \frac{k_2[E_0]}{D} - \left(\frac{k_2}{D} + k_{-2} \right) [E_\delta]$$

then,

$$\frac{dy}{dt} = - \left(\frac{k_2}{D} + k_{-2} \right) \frac{d[E_\delta]}{dt} \quad (6)$$

or

$$\frac{dy}{y} = - \left(\frac{k_2}{D} + k_{-2} \right) dt \quad (7)$$

integration of equation 7 gives

$$y = y_0 e^{-\left(\frac{k_2}{D} + k_{-2}\right)t}$$

thus,

$$\frac{k_2}{D} + k_{-2}$$

is the expression for the apparent first order rate constant for the disappearance of E_δ following a sudden decrease in pH. This is also the expression for the appearance of E_δ following a rapid increase in pH.

APPENDIX B

DOCUMENTATION OF PROGRAM MPLOT.

MPLOT was developed in response to the need for the inexpensive construction of graphs of publishable quality.

The program enables the user to plot from one to five curves comprised of pairs of X, Y coordinates on a single set of axes using the MSU CalComp Plotter. In addition to the plotting of conventional X-Y data, MPLOT has the capability of calculating and plotting theoretical curves through selected data curves.

Usage:

A. Construction of conventional X-Y plots

The program MPLOT is maintained as a permanent file on the MSU CDC 6500 computer. It can be accessed via the subroutine THEQN as described below. For this application THEQN is a dummy subroutine and its contents will be ignored by MPLOT. The appropriate data cards are simply appended to the THEQN deck and the job is ready to be submitted.

B. Drawing theoretical curves through data

The major difference between this and the previous application is that a theoretical equation, describing the theoretical curve to be drawn, must be included in the subroutine THEQN. MPLOT will then use this equation along with the values of XMINTH(I) and XMAXTH(I) to calculate and ultimately construct the theoretical curve(s).

Deck Structure for the Use of MPLOT:

```
PNC
JOB CARD
PW =
ATTACH (MPLOT,MPLOT)
FTN.
LOAD, LGO.
MPLOT.
(789)
THEQN DECK
(789)
DATA CARDS
(6789)
```

Data Cards:

1. ITITLE (8A10)

ITITLE

A comment card. This comment will appear on the printout, not on the graph.

2. LABELX (A26)

LABELX

The label which will appear on the x-axis. Note: Center the label in the 26 character field.

3. LABELY (A26)

LABELY

The label which will appear on the y-axis. Note: Center the label in the 26 character field.

4. NCURVS, IQUEUE, LINTYP, XAXLENG, YAXLENG, FACT, IBORDER, ISET (315, 3E10.4, 215)

NCURVS

The number of data curves on the graph.

IQUEUE

The QUEUE to which the plot is submitted. Possible values of IQUEUE are 0,1,2,5,6, and 10. [see CDC 6500 User's Manual, Vol. VII].

LINTYP

If LINTYP = 1, the data points for each data curve will be connected by straight line segments. If LINTYP \neq 1, no straight lines will be drawn (Default = -1).

XAXLENG

The length of the x-axis in inches (Default = 3.0 inches).

YAXLENG

The length of the y-axis in inches (Default = 3.0 inches).

FACT

Alters the size of the entire graph. For example, a value of 2.0 for FACT would produce a graph 6 inches square using the default values of XAXLENG and YAXLENG (Default = 1.0) [see CDC User's Manual, Vol. VII under "Factor"].

IBORDER

If IBORDER = 1, a border will be drawn around the graph. If IBORDER \neq 1, no border will be drawn.

MICHIGAN STATE UNIV. LIBRARIES



31293100632649